FRACTURE IN METALS

by

S. O'HARA, B.Sc., A.R.C.S.T.

ProQuest LLC.
789 East Eisenhower Parkway
P.O. Box 1346
Ann Arbor, MI 48106 – 1346

THESIS

presented to

THE UNIVERSITY OF GLASGOW

for the

Degree of

FRACTURE IN METALS

DOCTOR OF PHILOSOPHY

by

Sydney O'Hara, B.Sc., A.R.T.C.S.T.

March, 1950.

T H E S I S

presented to

THE UNIVERSITY OF GLASGOW

for the

Degree of

DOCTOR OF PHILOSOPHY

by

Sydney O'Hara, B.Sc., A.R.C.S.T.

October, 1959.

ACKNOWLEDGEMENTS

The author wishes to thank his supervisor, Professor R. Hay, for his advice and encouragement while this work was being carried out, and Professor E.C. Ellwood for the interest he has shown. He also wishes to acknowledge the generous co-operation of Mr. J. W. Sharp of the Department of Natural Philosophy with all electron microscope studies.

The work for this thesis was carried out in the Departments of Metallurgy and Mechanical Engineering and the author would also like to express his gratitude for the facilities provided by the members of these departments.

CONTENTS

C O N T E N T S (cont'd)

INTRODUCTION

Damping measurements are very sensitive to small changes in the internal structure of metals even on an atomic scale. The original terms of reference for the work described in this thesis were to study the onset of fracture or the pre-fracture conditions in metals. Before the work was started it was thought that cracks and macroscopic internal defects would almost certainly be reflected in damping measurements made at kilocycle frequencies. It was also thought that the formation of a non-coherent precipitate might behave as an incipient or actual crack.

In order to deform metal specimens to the extent of crack initiation without altering their shape and size and thus their suitability for damping measurements, it was necessary to use fatigue as the means of producing damage.

The formation and growth of non-coherent precipitates can be obtained by the readily controlled process of internal oxidation. That means was therefore chosen to investigate the effect of precipitates on damping.

For simplicity it was decided to carry out the investigations on copper and aluminium, both of which have a face centred cubic structure. Two metals were chosen so that inter comparison of results would be possible.

When the experimental work was underway it was found that the effects due to cracks, internal defects and precipitates were insignificant compared with those due to

dislocation damping. The work therefore naturally resolved itself into determining the effect of fatigue and precipitation on dislocation behaviour as measured by damping. In the former case recovery measurements proved the most useful.

Within the department there was no experience of damping capacity measurements. It was, however, intended that the work should extend beyond that envisaged in the present thesis and so a large amount of time was spent on developing and calibrating the apparatus and investigating the effect of variables in technique which might in turn affect the accuracy of the damping measurements. This thesis describes these preliminary investigations in some detail.

It was found necessary to aid the investigations of damping on crack initiation with optical microscope observations. These were extended to optical and electron microscope studies of the surface structure arising during fatigue.

From the effect of fatigue on the damping capacity of the metals investigated combined with the information obtained from electron microscope studies and published work a general picture of metal fracture by fatigue is developed.

CHAPTER I

Section 1.

Fatigue of non-ferrous metals.

Section 2.

Precipitation by internal oxidation and associated effects on metallic properties

Section 3.

Dislocation damping and theories proposed to account for this phenomenon.

SECTION 1. THE FRACTURE OF NON-FERROUS METALS BY FATIGUE

Early theories of fatigue were based on insufficient experimental data. The application of new techniques along with an improved knowledge of the structure of metals have aided investigators in the past few years to arrive finally at what must be a near approximation to the mechanisms of fatigue.

Early Theories of Fatigue

The attrition theory of Ewing and Humfrey[1], which assumes that debris is built up in the slip bands, and the amorphous layer theory of Beilby[2] and further developed by Rosenheim and Ewing[3], are based on ideas which are not consistent with present knowledge of atomic structure.

Gough and Hanson[4] based the following theory on the formation of local plastic regions during fatigue. As fatigue proceeded deformation in these plastic regions was assumed to increase but at a decreasing rate because of strain hardening. It was then proposed that if the applied stress was less than the fatigue limit then plastic deformation would cease; for stresses above the safe range local strain hardening was thought to exceed the limit which the metal could undergo without forming a crack. Recent work by Wood and Segall[5], which shows that plastic strain and slip band development can continue without work hardening even at very low stresses, does not support the above ideas.

The quantitative theory developed by Orowan[6] and based on the ideas of Gough and Hanson[4] is also therefore based on an assumption that a coefficient of strain hardening existed for the plastic regions, and is not supported by experimental evidence.

In the past ten years experimental observations using the microscope, the electron microscope, stored energy measurements, X-ray diffraction observations and low temperature fatigue experiments have helped to elucidate fatigue mechanisms.

The most notable aspect of room temperature fatigue is the broad coarse slip bands which develop from initially fine slip traces during a test. This aspect of fatigue has been noted as early as 1903 by Ewing and Humfrey[1] and subsequently by many later workers such as Gough and Hanson[4], Rosenhein,[7] Thomson and Wadsworth,[8] Forsyth[9] and Wood[10] and is now recognised as a characteristic feature of fatigue. Wood[11] and others have shown that slip in these bands is of the order of a few lattice spacings giving a movement of approximately 10^{-7} cms. These broad bands can start and stop well within a grain; this in itself indicates that the slip movement in the individual lines of the band is fine since, as Wood points out, it is difficult to see how the metal structure could accommodate a coarse slip step away from a grain boundary. As the temperature is lowered these bands tend to

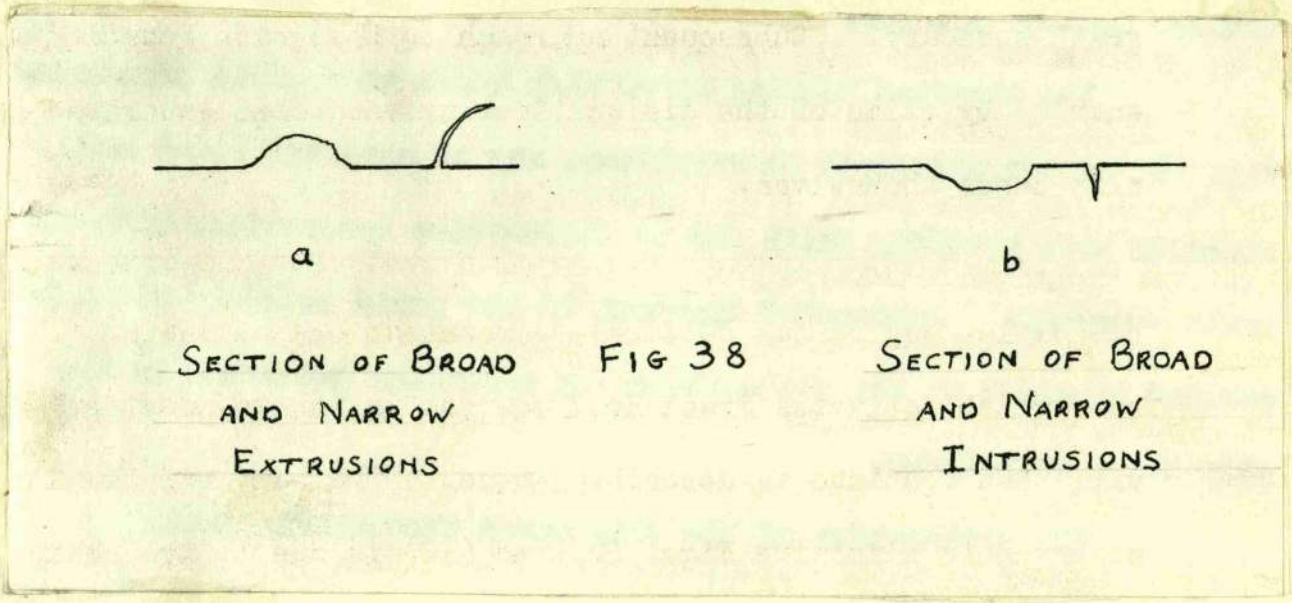

SECTION OF BROAD AND NARROW EXTRUSIONS

FIG 38

SECTION OF BROAD AND NARROW INTRUSIONS

become finer and more similar to bands arising from pure tensile stresses.

This development or coarsening of slip bands at room temperature can take place without continued work hardening of the metal as shown by Wood and Segall;[5] it can also occur giving rise to very little asterism in x-ray diffraction photographs[5, 12, 13]. Recovery measurements by Clareborough et al[14] have shown that the structure arising from this type of fatigue is removed at comparatively high temperatures; in this case a temperature of 400°C was required. This was 100°C higher than the normal recovery temperature of specimens which had been deformed by pure compression. These facts indicate that the dislocation configurations in the fatigued metal are extremely stable and that no agglomeration of dislocations of any one sign exist.

Mott[15] has proposed a model for the development of broad fatigue bands based on Seeger's[16] theory of cross slip and work softening. It is suggested that numerous short slip lines, Fig. 1a, are first formed which are terminated at some barrier. It is further suggested that during fatigue continual movement backwards and forwards of dislocations along AB Fig. 1b past slip line CD eventually lead to cross slip and subsequent annihilation of the dislocations. Such a process would permit source S and other nearby sources to generate more dislocations.

This theory will be discussed further in the conclusions of this thesis.

The use of high stresses in fatigue tests gives rise to vastly different effects from those described above. As the cyclic stress is increased asterism in back reflection x-ray photographs increases[5,12,13]. The slip bands tend to be restricted to much smaller regions i.e. they are no longer composed of multiple numbers of slip lines, and as shown by Kemsley[13] a smaller fraction of the grains contain slip lines. Hardness measurements made by Kemsley[13] show that the hardness in annealed specimens of copper fatigued at $\pm$ 16000 lbs in.^{2} falls off slowly during subsequent annealing between 450°C and 900°C without recrystallisation taking place. At $\pm$ 25000 lbs in.^{2} fatigue gives rise to behaviour which is more comparable with cold worked material: recrystallisation takes place between 350°C and 600°C. The fracture of annealed copper fatigued at high stresses is intercrystalline while at low stresses transcrystalline.[17] Apart from this last characteristic it can be seen that fatigue at high stresses gives rise to a structure which is more similar in properties to metals deformed by non-cyclic stressing.

Point Defects in Fatigued Metals

Only in recent years with the advent of irradiation damage, has the effect of point defects on the plastic properties of metals been appreciated. From the great

bulk of experimental work subsequently carried out on electrical resistivity measurements made on quenched gold, copper and aluminium, much quantitative information has been gathered[18,19,20]. The results obtained for gold and copper give the energy of formation of a vacancy E_F as being approximately 1·0 ev while the energy of migration E_M has repeatedly been found to be 0·7 ev. The sum $E_M + E_F$ should be the same as that for the activation energy for self diffusion E_D which has been reported as approximately 1·8 ev from diffusion experiments. The agreement between the two sets of results is considered satisfactory. The above experimental values of E_F in particular are in good agreement with theoretical estimates. Experimental values for E_D for aluminium vary between 0·9 and 1·4 ev; this is also in good agreement with the lower values obtained for E_F and E_M for aluminium which have been found to be 0·76 and 0·44 ev respectively. The significance of the above information is that recovery due to vacancy migration should occur at lower temperatures in aluminium than in copper.

The value of 0·7 ev for E_M in copper is associated with recovery effects which take place between 250°K and 350°K. Other types of recovery measurements which include damping, yield strength, and density measurements all show pronounced effects occurring in the region of room temperature after point defects have been introduced by either quenching, irradiation or

deformation. This recovery in copper is now attributed with confidence to the movement of vacancies[19].

Interstitial atoms do not appear to play anything like such a large part during recovery as do vacancies in deformed metals, although the experiments of McCammon and Rosenberg[21] suggest that their immobility at about 40°K increases the fatigue strength of the metal in that temperature region. Other types of defects such as divacancies and vacancy clusters are also thought to exist; the low E_M value of a divacancy in copper is thought to account for recovery phenomena after deformation and irradiation noted in the region of 170°K[19].

Mechanisms which have been proposed to explain the formation of point defects during deformation have been summarised by Mason[22], Mott[23], Seitz[24], and Cottrell[18]. Cottrell[18] has suggested a mechanism which would be particularly productive of point defects during deformation by fatigue.

By comparing many of the results and observations obtained from fatigue experiments, with the above information the impression is obtained that point defects are created in abundance during fatigue and play a large part in the process of fatigue.

The low fatigue resistance of age hardened alloys as demonstrated by Hanstock[25,26,27] using damping experiments, has been reported as being due to overageing. This would

require that diffusion during fatigue was much more rapid than during static deformation. Forsyth and Stubbington[28] have suggested that the formation of extrusions in fatigued Al - 4% copper is due to the confinement of slip to soft narrow over-aged regions, this effect being suppressed at -90°C.

Broom, Molineux and Whittaker[29] give the ratio of fatigue strength to U.T.S. for fully hardened D.T.D 683 alloy fatigued at 18°C and -183°C; in the former case the ratio is 0·48 while in the latter it is 0·67. Broom et al[29] suggested that precipitation and overageing had occurred at room temperature.

By increasing the rate of room temperature diffusion, the presence of large numbers of vacancies in fatigued metal would account readily for all the above observations.

Broom and Ham[30] have found that work hardened copper can be softened by fatigue at 293°K whereas no softening occurs at 90°K. This suggests that vacant lattice sites are produced in such numbers as to give dislocation climb and local rearrangement akin to polygonisation. X-ray back reflection photographs also showed improvement in the resolution of the copper K_{α_1} and K_{α_2} doublet in the specimen fatigued at 293°K.

The conclusion that work softening during fatigue is due to point defects is partly supported by work softening which has been shown to occur during the irradiation

of work-hardened metals[31].

Work softening has also been shown to take place in hard worked materials during fatigue by Polakowski and Palchoudhuri[32], Kemsley[13], Ludwic and Scheu[33] and Kenyon[34]. Forsyth[28] has stated that recrystallisation takes place at room temperature along slip striations during the fatigue of work hardened aluminium.

It has recently been suggested that hardening of annealed metal by fatigue is more similar to irradiation hardening than to work hardening. By comparing the ratios of $(\frac{\sigma}{\mu})_T$ for unidirectionally worked copper, with copper fatigue hardened at 90°K and 293°K and also with irradiated copper, Broom and Ham have shown that, with respect to hardening, room temperature fatigue compares with irradiation and low temperature fatigue compares with unidirectional deformation, σ_T is the flow stress at temperature T and μ is the elastic constant. Broom and Ham[36] have subsequently shown clearly that hardening takes place in the regions between the slip bands of single crystals of copper fatigued at room temperature and that the resulting tensile curve obtained after fatigue shows a yield drop and is very similar to that obtained by irradiation. The authors concluded that point defects can make a large contribution to hardening during fatigue.

Finally high densities of dislocation loops have been observed by Segall and Partridge[37] in F.C.C. metals fatigued and examined by transmission electron microscopy. These are taken to arrive from large numbers of point defects.

The above survey shows the importance of point defects in fatigue at room temperature. Several recent theories[23, 38] of fatigue have been based on the effects of these point defects. Mott[23] for example has proposed that plates of defects are formed in the slip bands and can not diffuse away before recrystallisation takes place. After 10^4 to 10^5 cycles it is further suggested that the atomic planes round the active slip planes are completely disordered and the crystal expands. During recrystallisation, which is assumed to take place because of these stresses, contraction occurs and cracks are thus formed in the regions of the slip bands.

METALLOGRAPHIC OBSERVATIONS SHOWING THE RELATIONSHIP BETWEEN FATIGUE CRACKS AND FATIGUE SLIP BANDS.

As early as 1903 Ewing and Humfrey[1] noted that cracks developed in slip bands formed by fatigue in Swedish iron; these cracks were shown up by subsequent polishing and etching of the metal. Slip bands formed during fatigue have since been the object of most metallographic observations made on fatigued metals.

Thomson[38] has recently described a series of observations made on annealed copper and nickel by fatiguing the metal in push pull at about 1000 c/s, electrolytically polishing, then re-fatiguing and so on until fracture occurred. The part played by slip bands in crack initiation is shown clearly by these experiments. Thomson et al have found that after as little as 5% of the fatigue life of the specimen some of the slip bands are not polished away as are the majority; he has called these persistent slip bands. On subsequent application of a tensile stress to the fatigued material, persistent bands which were greater than one grain long were observed to open up into large cavities showing these bands to be cracks. The final fracture was always caused by the propagation of these persistent markings. Similar results have been noted on nickel by Thomson[38] and in aluminium by Smith[39]. In the latter case however, a similar effect was noted to occur at the grain boundaries at room temperature .

Forsyth[28] has observed holes in the slip bands of fatigued and polished aluminium and aluminium alloys. These rows of holes were stated to form the path along which the active crack eventually propagated. Similar observations were made by Smith[39] on aluminium fatigued at low stress, i.e. at stress amplitudes of the order of

one-half the 10^7 endurance limit. Smith noted that these dots joined up to give the usual type of persistent markings when the specimen was fatigued at a higher stress.

Extrusion of crystalline material from the slip bands of fatigued aluminium -4% copper has been observed by Forsyth and Stubbington[28]. On subsequent polishing and etching with 10% NaOH crevices were observed adjacent to the position of the original extrusion. Subsequent tensile stress applied to the metal gave rise to elliptical cracks forming in the regions from which extrusion had taken place. Forsyth[9] did not observe this type of surface structure in fatigued 99·99% pure aluminium, but rather the surface of the pure metal was deformed by grooves and ridges. Hull has fatigued O.F.H.C. copper at 4°K and has observed extrusions and intrusions along the slip bands on the surface of the metal. The formation of intrusions and extrusions is therefore not suppressed at low temperatures in copper.

All the above metallographic and electron microscope studies show that the operating slip bands play a major role in the initiation of fatigue cracks. The deep crevices produced in these slip bands during fatigue have been suggested by several workers to act as stress raisers in a manner similar to a crack or that the crevices

are in fact incipient cracks. This is substantiated by the work of Thomson and Wadsworth[8] who found that if the deep slip bands were repeatedly removed when they extended only over one grain, then the life of the specimen appeared to be prolonged indefinitely. The development of permanent slip bands was found by Thomson and Wadsworth to be considerably decreased by testing in pure nitrogen. It is notable that Gough and Sopwith[41] obtained a marked increase in the fatigue life of copper, 70/30 brass and lead during tests made at a pressure of 10^{-2} m.m. Similar improvements have been noted recently at Farnborough in Al-Zn-Mg-Cu alloys and also in iron when fatigue was carried out at an air pressure of 10^{-5} mm. Hg. Thomson[38] et al have suggested that the presence of gaseous atoms, oxygen in particular, would assist in the process of permanent slip band formation by preventing the two sides of the bands from joining together once formed. the above results would appear to support this.

When the present work was started, the relative part played by point defects as compared with the simple notch effect produced by intrusions was not known.

SECTION II. THE EFFECT OF PRECIPITATES ON THE DEFORMATION AND FRACTURE OF METALS.

The process of growing a precipitate in a solid lattice is usually accompanied by an increase in the hardness of the lattice. This is particularly so when the precipitate is small and evenly dispersed throughout the metal. The great bulk of work on age hardening in certain alloy systems bears this out. Another method of introducing a growing precipitate is by internal oxidation, which may be defined as the oxidising and precipitating out of one or more of the minor and less noble elements in an alloy system.

Internal Oxidation

In the present work precipitation by internal oxidation was studied.

A general survey of the literature up to 1953 has been given by Cupp[43].

Internal oxidation of an alloy may be carried out when the free energy of formation of the solute oxide is greater than the solvent oxide. A second necessity is that oxygen must dissolve and diffuse in and through the solvent metal at a greater rate than the solute. Actual formation of the dispersed oxide takes place by oxygen firstly diffusing through the solvent then combining with the solute. The particles may extend from the completely

unoxidised surface of the solvent right into the interior of the specimen. An unoxidised solute may be obtained by maintaining the partial pressure of the oxidising atmosphere just below that required to form the solvent oxide. in the case of copper alloys this is usually done by annealing the copper alloys in the atmosphere obtained from an equal mixture of copper and cuprous oxide powders[71]. The time required to completely oxidise a piece of metal and the type of dispersed phase obtained varies with temperature of formation, oxygen partial pressure, the relative heats of formation of solute and solvent oxide and the relative diffusion rates of the solute metal outwards compared with oxygen inwards. Rhines[44] and Mijering and Druyvesteyn[45] have outlined the ways in which the above variables effect the particle size, distribution and rate of formation. Rhines[44] has also shown that internal oxidation in copper alloy occurs between 750°C and 1000°C as a relatively simple diffusion process, which can be described mathematically. The simplified relation derived is

$$\log \frac{x^2 C_m}{t} = \frac{a'}{T} + b' \text{ ----------(1)}$$

where a' and b' are constants, t is the time in seconds and T is the absolute temperature, C_m is the concentration of solute. This expression is valid only when the solute content is between 0·1 and 1%.

The accuracy is given as approximately 5%.

Effect of Internal Oxidation on the Physical properties of alloys.

Hardness and Tensile Strength

As would be expected a dispersed fine oxide phase hardens the metal. This is most noticeable in the cases of fine precipitates obtained from very stable phases such as Al_2O_3 in copper. A large number of fine particles will block slip in more glide planes than will a smaller number of coarse particles. This was demonstrated by Smith and Dewhirst[46] who took hardness measurements from the outside to the inside of a specimen. In the copper 0·6% aluminium alloy the hardness at the outside was 110 v.p.n. The inner zone containing larger particles had a hardness of 80 v.p.n. A similar specimen annealed in nitrogen had a hardness of 50 v.p.n.

Intercrystalline embrittlement also takes place in the case of polycrystalline alloys especially where large hardness increases have been obtained, elongation often being reduced to as little as 1 to 2%.

Gregory and Smith[47] using Ag-Si and Ag-Al alloys have reported greatly increased room temperature tensile properties with reduced ductility after internal oxidation of these alloys.

Creep.

De Jong[48] first realised that internal oxidation

could improve the creep strength of a metal. Martin and Smith[49] concluded that improvement in creep resistance took place at 200°C after internally oxidising Cu-Si and Cu-Al alloys; the greater creep resistance was shown by specimens containing the finer dispersions.

Fatigue. The only work on this aspect of the subject appears to have been carried out by Martin and Smith[50] who noted that internal oxidation of copper silicon and copper aluminium alloys resulted in a diminished fatigue life in polycrystalline specimens and an increased fatigue life in the case of single crystals. It was concluded that in polycrystalline specimens the grain interiors were at least as strong as the unoxidised specimens but cracks formed and propagated much more readily from the weakened or embrittled grain boundaries.

Effect of Internal Oxidation on Damping.

Granato and Lucke[51] have stated that removal of impurities by internal oxidation increases the damping. This was taken as proof that impurities which were not in solid solution did not pin down dislocation lines. Hanstock[26] has also shown that the amplitude dependent damping of age-hardening alloys increases rapidly when overageing takes place. Again this was interpreted by Granato and Lucke[51] as being due to the removal of the alloying elements from solid solution.

SECTION 3. DISLOCATION DAMPING OF METALS

Glossary of Terms used in Chapter

The meaning of the term is as stated below unless specifically mentioned otherwise in the text.

A - effective mass per unit length of dislocation = $\pi \rho b^2$

a - lattice parameter

B - damping constant

b - Burgers vector of a dislocation

C - line tension in a bowed out dislocation $\approx \mu b^2$

c - concentration of impurity atoms on a dislocation line

c_0 - concentration of impurity atoms in lattice

C_p - specific heat - constant pressure

C_v - specific heat - constant volume

D - diffusion coefficient $= D_0 e^{-\frac{Q}{RT}}$

D_{TH} - thermal diffusivity

E - Young's modulus

f - frequency of vibration

K - (Granato and Lucke theory) - a parameter dependent on orientation and anisotrophy, probably given by $\frac{\mu}{4\pi E}$ where R is the resolved shear stress factor.

K - Gas constant

k - Boltzman constant

L_N - dislocation network length

L_c - dislocation length between impurity pinning points.

L - (Granato and Lucke) - the average loop length = $\frac{LN \cdot Lc}{LN + Lc}$

r - $\delta\Delta / \delta \frac{\Delta E}{E}$

T - temperature in degrees absolute

t - time

Δ_I - amplitude independent decrement

Δ_H - amplitude dependent decrement

$\frac{\Delta E}{E}$ - modulus defect accompanying either Δ_I or Δ_H

ω - angular frequency of vibration

τ - relaxation time

Δ_0 - relaxation strength

Δ - $\Delta_I + \Delta_H$

ε_0 - strain amplitude of measurement

ε - fractional difference in the size of solute and solvent atoms

Λ - dislocation density

λ - average wavelength of stress field of impurity atom

μ - shear modulus

σ - applied stress

σ_M - average value of stress field of impurity

Ω - orientation factor accounting for difference in resolved shear stress on the slip planes and applied longitudinal stress.

ζ - Cottrell misfit parameter measuring the magnitude of the lattice dislocation at a point defect.

ρ - density

ν - Poissons ratio

Measures of Internal Friction

There are several measures of internal friction and these are all related as follows:

The logarithmic decrement Δ is given by the fractional decrease in vibration amplitude per cycle. From the shape of the resonant curve the decrement is given directly by $\frac{\pi}{3} \frac{V_2 - V_1}{V_r}$ where V_2 and V_1 are the half amplitude frequencies and V_r the resonant frequency. The term damping capacity per cent used by engineers is related to the decrement Δ by 200Δ. Also if δW is the vibrational energy dissipated per cycle and W is the total vibrational energy of the resonant specimen then $\Delta = \frac{\delta W}{2W}$

The attenuation of ultrasonic waves in a material is related to its damping by the following, $\Delta = \frac{AV}{f}$ where A is the attenuation, V the velocity of the propagating wave and f its frequency. The relationship between these various measurements and $\frac{I}{Q}$ the damping capacity is therefore

$$\Delta = \frac{\pi}{\sqrt{3}} \frac{\sqrt{2}-\sqrt{1}}{\sqrt{r}} = \frac{\delta W}{2W} = \frac{AV}{f} = \frac{\text{DAMPING CAPACITY } \%}{200} = \frac{\pi}{Q}$$

Foster[52] Zener[53] Nowick[54] and Mason[22] have all summarised the various types of apparatus for determining the above measures of damping in solids.

Dislocation Damping

The damping in metals which is ascribed to dislocation motion is made up from two distinct contributions. Fig. (1)

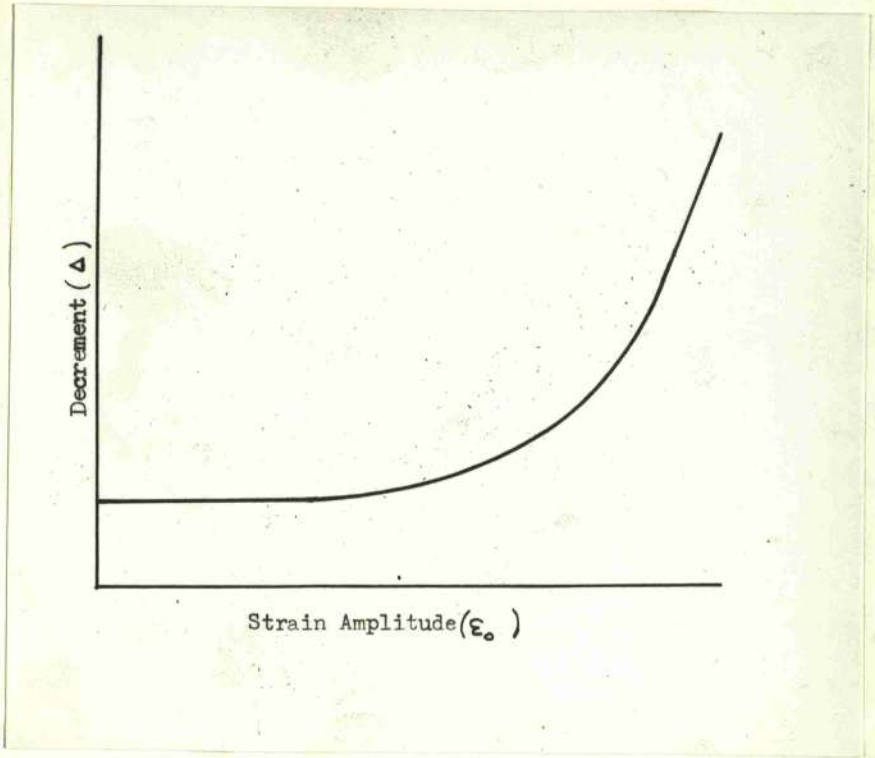

FIG. 1.

shows typical damping measurements as a function of measuring strain amplitude. The curve is seen to be made up of a low amplitude region in which the damping is amplitude independent. In the second region the damping increases rapidly with measuring amplitude of vibration. These two components will hereafter be signified by Δ_1 and Δ_H respectively. The latter type of damping was first demonstrated by Read[55] in zinc single crystals. The rate of increase of this damping depended very strongly on orientation of the crystal being greatest when the specimen axis-hexagonal axis was about 60°. These experiments of Read were the first to signify that the component of stress resolved along the slip plane was important, and the damping of the metal was associated with slip and dislocation motion. The form of the damping-amplitude measurement curve has subsequently been shown to apply to copper, silver, aluminium, lead and germanium. In cubic metals the orientation dependence of Fig. (1) was found by Read to be slight compared with hexagonal metals; this must be a direct result of the many more possible slip planes in cubic metals.

Both Δ_1 and Δ_H measurements are affected by impurity content of the metal, state of anneal, temperature of measurement, pre-straining and in the former case frequency. The ways which these variables affect the two damping components are qualitatively

similar. Variations in Young's modulus $\frac{\Delta E}{E}$ are usually associated with changes in Δ_I and Δ_H. As Δ increases E decreases, and in the case of amplitude dependent measurements, the parameter $r = \frac{\delta \Delta_H}{\delta \Delta E/E}$ is usually between 1 and 4, and, as shown by Nowick[96], appears to be independent of temperature and frequency. Read[55] has provided exceptional results to this. In zinc single crystals r_4 was found to vary from 0·5 to 11 with the orientation of the crystal.

Changes in E are usually followed by changes in the resonant frequency of the vibrating specimen, a parameter to which E is intimately related. The modulus effect arises from the strain in a stressed metal being made up of two components, namely, ε_E and ε_o where ε_ϵ is the elastic strain and ε_D the strain due to dislocations. If a dislocation bows out, the out of phase component of ε_D contributes to the damping loss and the in phase component of ε_o contributes to the modulus defect $\frac{\Delta E}{E}$.

Effect of Impurity on Δ_I, Δ_H and E Measurements.

The damping of pure metals in the kilocycle per second frequency range is greatly reduced by added impurity and a corresponding increase in Young's modulus is associated with this. The exact amount of this reduction is modified by the state of anneal of the metal. Weertman and Salkovitz[56] have demonstrated the reduction in damping which occurs when impurities are added to lead while Takahashi[57] and Weinig and Machlin[58] have shown the same

effect by adding impurities to copper. In the case of Δ_I measurements, the value of Δ_I decreases as the impurity content increases, whereas in the case of Δ_H measurements the stress amplitude at which the damping increases is moved to the right in Fig. (1).

More recently it has been found that effects similar to those of impurities are obtained by quenching or irradiation. The effect of quenching or irradiation, however, is not immediate, and a time interval exists between the treatment and the final attainment of the low damping; this time interval is very temperature dependent. Levy and Metzger[59] have demonstrated the effect of water quenching aluminium; in this case Δ_H almost disappeared Rosewall and Nowick[60] have reported large decreases in the internal friction of gold which was cooled in air from 900°C. Duckamp and Sosin[61] reduced the damping and increased the Young's modulus of polycrystalline copper by means of electron bombardment at -180°C plus a room temperature anneal. Neutron and gamma irradiation of copper single crystals has the same effect as shown by Thomson, Holmes and Blewitt[62] and Thomson and Holmes[63], Barnes, Hancock and Silk[64] have found that the effects of gamma and neutron irradiation and quenching are practically the same provided the treatments introduce similar numbers of vacancies into the metal.

The presence of impurity atoms and point defects therefore

lowers Δ and these imperfections are more effective if annealing has allowed them to diffuse to the dislocations.

There are observed exceptions to the above effects, for example, Read[65], using 99.999% pure zinc obtained damping measurements which were an order of magnitude less than those obtained by Swift and Richardson[66], who used zinc with a minimum impurity of 10^{-2}. The reason for this is not at all clear. Weertman and Salkovitz[56] also report exceptions to the above generality in some of their lead-bismuth specimens, although the authors have not commented on it. Weertman and Salkovitz have concluded that actual pinning of the dislocations does not take place at room temperature in their lead alloys. They arrive at this conclusion because of the calculated low binding energies of bismuth, tin and cadmium to the dislocations.

Effect of Temperature of Measurement

Both Δ_I and Δ_{II} depend very much on the temperature of measurement. In copper Δ_I measurements at low temperatures have shown that between two and four peaks occur in the range 20 - 130°K in annealed copper[67], while recently the single peak, which has been noted[68, 22, 69] to occur at about 100°K in worked copper and named the Bordoni peak, has been shown by Thomson and Holmes[67] to consist of many superimposed peaks. Niblitt and Wilks[69] and Thomson and Holmes[67] have shown that apart from these peaks there exists a

background Δ_i loss which increases with increasing temperature of measurement between 0°K and 250°K. The results of the former gave an almost linear rise in Δ_I with temperature between 150°K. and 290°K. The latter workers have stated that this background rise may be subdivided into two ranges, i.e. between 40°K. and 180°K and from 180°K upwards. Between 180°K. and room temperature Thomson and Holmes fitted the rise in Δ_I against a T^2 curve. Further work is necessary to establish the exact nature of the relationship between Δ_I and temperature. A modulus change was always found to be associated with each damping process observed between 20°K. and room temperature. This dependence of the modulus on temperature is important as a measure of the validity of some of the proposed mechanisms.

Bimbaum and Levy[70] reported a relaxation peak in aluminium however only after straining and rapid cooling to 72°K. The relaxation peak occurred at 100°K. Apart from this peak the decrement Δ_I of deformed crystals exhibited only a slight dependence on temperature in the range 77°K to 350°K.

Very little work has been done on the temperature dependence of Δ_H. Niblett and Wilks[71] have found that in copper the amplitude dependent damping varies almost linearly between 15 and 300°K, larger variations being obtained with higher measuring amplitudes. Weertman and Salkovitz[56] have also found a rise in Δ_H with temperature

in dilute lead-tin alloys.

Effect of Frequency.

Δ_I Measurements - These are divided into two ranges, namely, the kilocycle range and the megacycle range.

In the first case comparison of measurements made on even the same specimen at different frequencies are complicated due to the structure sensitivity of the measurements, since at different harmonics different parts of the specimen are excited. Small differences in dislocation densities or impurity contents over the length of a specimen will therefore give rise to misleading results. Results of Marx obtained from 10^{-5} impurity copper and published by Weertman[75] show that Δ_I increases less than 50% at room temperature between 40 and 260 Kc/sec. Measurements made by Weinig and Machlin[58] at 1 cycle/sec, and mentioned earlier in connection with impurities, show a range of Δ_I values comparable with those obtained from kilocycle measurements.

It is impossible to say precisely at present in which manner Δ_I varies at lower frequencies.

In the megacycle range ultrasonic attenuation measurements have been made by Granato et al[72] on germanium and the attenuation A was found to be equal to a constant x f^n where f is the frequency and n approximately equal to 2.

Hikato and Truell[73] have found that the damping values

of aluminium measured at 10 megacycles per sec. after plastic deformation were twice that obtained when measured at 5 megacycles per sec. The measured modulus was the same at both frequencies. Since the attenuation $= f\Delta$, the above two sets of results show that in the megacycle range Δ_I is proportional to frequency.

Δ_μ Measurements - Nowick found that a scatter exists for damping measurements made on copper single crystals in the kilocycle range. The scatter was about a frequency independent line. As with Δ_I measurements in the kilocycle range comparison of results are difficult due to different parts of the specimen being excited at different harmonics. Zener, Clark and Smith[74] have reported frequency independent values for cold worked materials. It is generally accepted that Δ_μ values are independent of frequency. The mechanism is amplitude dependent and is characteristic of a static hysteresis loss which in turn is quite independent of frequency.

Effect of Prestressing

The damping capacity of pure annealed metals is altered drastically by even small stresses such as involved in handling. Swift and Richardson[86] have shown that handling annealed zinc could increase the damping by ten times. Other striking examples of the susceptibility of the damping properties of single crystals have been reported by Read,[55] Found,[76] and Lawson.[77]

Investigations on the effect of low stresses on annealed 99.999% copper were made by Read[55], who demonstrated that the damping systematically increased with increasing pre-strain between 60 and 150 lb/in^2. Nowick[78] has published results similar to those of Read for pre-stresses between 70 and 170 lb/in^2. In the latter case no change in length of specimen was observed. For larger prestresses many workers[74,77,79,115] have shown that the internal friction goes through a maximum when plotted against degree of cold work. The results of Weertman and Koehler[80] are informative in this respect; for copper crystals of 10^{-5} impurity, it is shown that the position of the maximum increases as the measuring stress amplitude decreases; it is also shown that heavily worked crystals have little amplitude dependent damping. In general the maxima in the damping-pre-strain curves are observed in the range between 1 and 10% elongation[74,77,79]. The temperature at which deformation is carried out affects the resulting maxima. Thus, Lawson found that the lower the temperature of deformation the higher the maximum. The time between deformation and making measurements is also of importance. Boulanger[81], established that whether or not a maximum occurred with a deformed nickel-chrome alloy depended on how long the specimen had rested at room temperature. This was not found to be the case with aluminium, however, as the results of Granato et al Fig.(4) show. Here a maximum was observed while deformation was taking place. The time allowed before taking measurements also affects the size of the

maximum; thus Zener, Clark and Smith[74] reported only a very small maximum at about 5% elongation in polycrystalline brass after the specimen had rested for two weeks. Some investigators have found no peak. Koster obtained a continuous increase in damping with cold work of iron[82] and aluminium[83]. Darling has determined that the internal friction 24 hours after straining of tough pitch copper as a function of pre-strain depends markedly on the state of anneal of the metal. The higher the prior anneal the greater the maximum; all curves exhibited a maximum to a greater or lesser degree. The size of the maximum also depended on the period of time between straining and measuring. For tough pitch copper the maximum was always greater for the shortest periods of time, while for high purity copper the magnitude of the maximum varied in a complex manner with time; this latter variation was due to an increase in damping with time after deformation by small pre-strains and a decrease in damping with time after large pre-strains. Mima[85] has observed two peaks after working aluminium. These occurred for 15% and 55% reduction of area. Again, the size of the peaks diminished greatly with time after the pre-strain.

When simultaneous observations are made on modulus changes occurring with the damping changes caused by pre-straining these generally show an increase, i.e., the natural frequency of a resonating specimen increases.

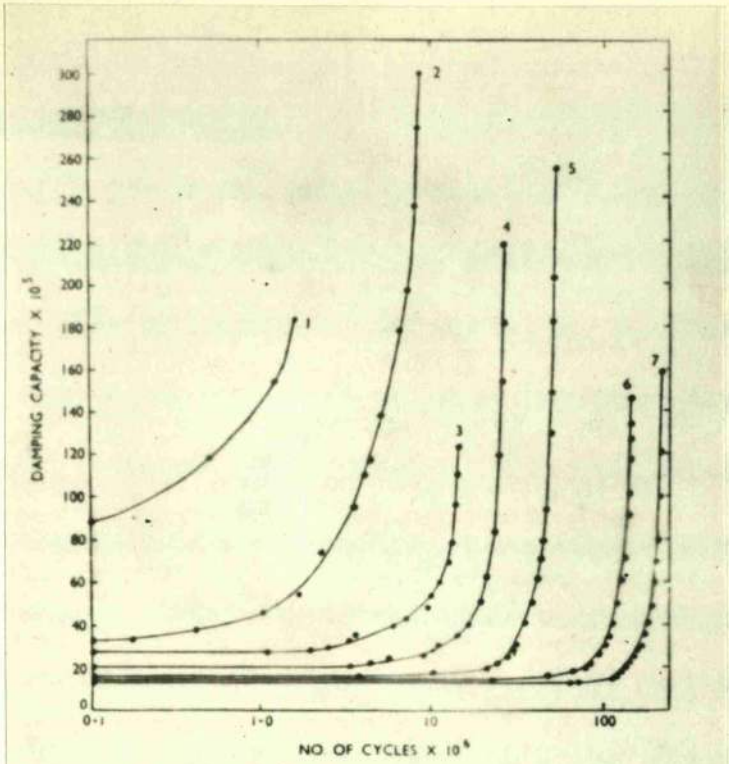

FIG. 2.—Changes in Damping of L65 During Vibration at Constant Strain.

KEY.

1. Strain = 48·2 × 10^{-6}.
2. Strain = 45·0 × 10^{-6}.
3. Strain = 42·5 × 10^{-6}.
4. Strain = 40·0 × 10^{-6}.
5. Strain = 37·5 × 10^{-6}.
6. Strain = 35·0 × 10^{-6}.
7. Strain = 32·5 × 10^{-6}.

FIG 2

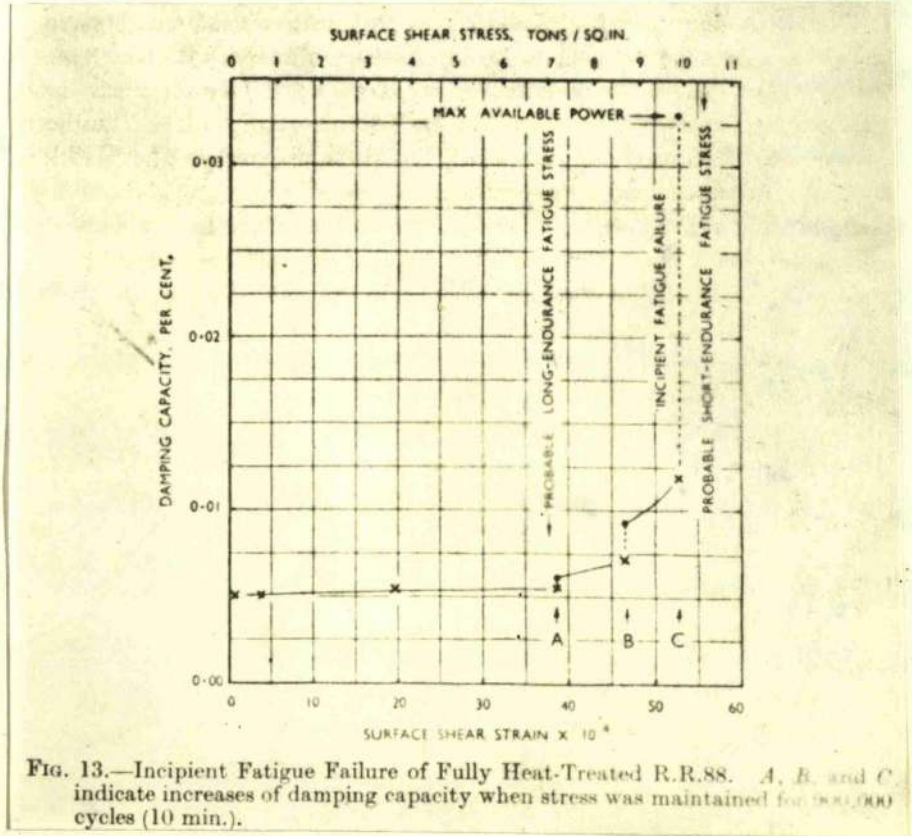

FIG. 13.—Incipient Fatigue Failure of Fully Heat-Treated R.R.88. *A*, *B* and *C* indicate increases of damping capacity when stress was maintained for (000,000) cycles (10 min.).

FIG. 3.

Effect of Fatigue on Damping

Fig.(2) gives the damping results obtained by Hanstock[26,27] during fatigue of a fully heat-treated aluminium alloy at the shown stress levels. The end point of curves 1, 3, 4, 6 and 7 represent the number of cycles at which a fatigue crack appeared. No fatigue crack, however, was formed at the end points of curves 2 and 5. The results show that the value of Δ shows an increase after a much smaller number of stress cycles when higher alternating strains are used. Fig. (3) taken from Hanstock and Murray[25] shows that after a critical amplitude of vibration the damping rises with continued vibration. The actual rise in damping after 900,000 cycles for specific amplitudes is shown at points A, B and C. It should be noted that these results are also for a fully heat-treated alloy, and the results in Fig. (3) can be related to those in Fig. (2). Truel and Hikato[87] found that continued fatigue of various aluminium alloys generally resulted in a gradual increase in the ultrasonic attenuation. Failure of the metal by fatigue was preceded by large increases in attenuation. The warning period of increasing attenuation decreased as the stress level was increased, from several minutes to one minute.

In pure aluminium the damping measurements themselves can alter the damping of the metal. This gives rise to the retention of the high amplitude Δ after the stress amplitude

has been reduced to lower values. This effect has also been observed in aluminium by Wert[88], in zinc by Swift and Richardson[66], and has been discussed by Birbaum[89], who also noted the effect in salt. The result is a double valued decrement behaviour. Read[55] first noted this behaviour in zinc. In copper the effect has not been noted until recently; Beshers[90], has observed an increase in the decrement of copper and copper-gold crystals, while vibrating at strain amplitudes of $2{\cdot}4 \times 10^{-5}$ and $1{\cdot}08 \times 10^{-4}$ respectively. The increase slowed down or stopped after a while. This residual damping is therefore very similar to the double valued decrement behaviour of aluminium and zinc. It occurs, however, at higher strain amplitudes.

Pre-straining or fatiguing a metal is seen to increase the damping of annealed metals; the amount of the increase depends greatly on the static or alternating strain, the time between straining and measuring, and the state of prior anneal of the metal.

Recovery of Damping at Low Temperatures after Deformation

The damping capacity of a metal after handling or stressing can change markedly at room temperature. In most cases this change is a reduction. Changes in the modulus of elasticity are always associated with these changes in damping. This type of recovery cannot be related to the softening behaviour associated with the

onset of normal recovery and recrystallisation, for no reduction in tensile strength occurs during annealing at room temperature, and no reductions are observed in X-ray line breadth. In view of the large changes in damping which can occur at room temperature it has been felt that this type of recovery must therefore be associated with some mechanism other than that which gives rise to self diffusion.

Forster and Koster[91] first demonstrated this low temperature annealing in deformed brass and low-carbon steel. Nowick[54] has summarised most of the earlier observations on low temperature recovery of damping after deformation. These consistently show that complete recovery of damping can take place at room temperature in tens of hours or in minutes at 100°C. This applies to deformed brass[92,93] and iron[82]. In the case of aluminium Koster[83] has found that recovery was not complete below recrystallisation temperatures. More recently Weertman and Salkovitz[56] reported recovery of the increased damping of lead caused by handling. This recovery took place at room temperature. Fusfield[93] obtained an activation energy of less than 10,000 cals/mol, i.e. ·435 e v for the recovery of cold worked brass.

Koster and Stolte[94] have made recovery measurements on alpha brass with and without a load on the specimen. Their first experiments showed that recovery took place after loading whether

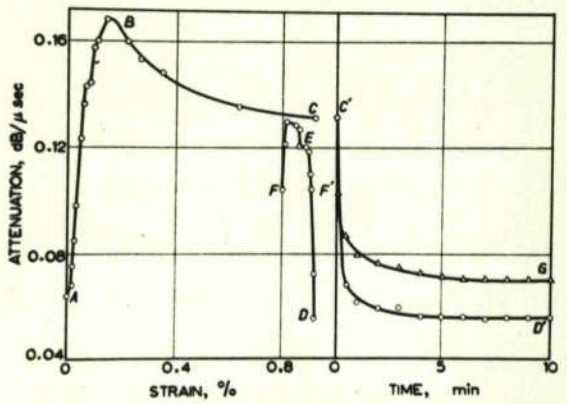

FIG. 3. Attenuation as a function of strain. As the load is increased (A–B) the attenuation increases, passing through a maximum. At point C, the strain is held constant, and the attenuation decreases (C'D') with time. When the load is now decreased, the attenuation again increases, passes through a maximum and decreases (D–E–F). With the load completely off, the remaining attenuation now decreases again with time (F'G), but at a slower rate.

FIG. 4.

the load was removed immediately or kept on. In other experiments it was found that if the load was removed after some recovery had taken place, then a new increase in internal friction was produced. This increase also recovered with time. The rate at which this second recovery took place depended on the duration of the first recovery, even if the damping during the first recovery had reached a steady state. Granato, Hikato and Lucke[95] have published results similar in nature to the above. These were obtained from ultrasonic attenuation measurements made during loading and unloading of aluminium. The results are shown in Fig. (4) and are equivalent to those obtained by Koster and Stolte. Gordon and Nowick[97] have made modulus and damping recovery measurements on NaCl crystals and found that if two deformed crystals were allowed to recover to different extents after straining, subsequent X-ray irradiation immediately completed the recovery process. The sum total recovery due to both deformation and irradiation was the same for both crystals although the individual amounts due to deformation and irradiation differed. Mima[85] has measured the rate of recovery of damping of aluminium at room temperature after reduction of areas of 15%, 65·4% and 72·3%. In the first case the decrease in damping followed a $t^{2/3}$ law, but this rate of decrease was not found to apply in the other two cases. Smith[98] has measured the modulus increase of O.F.H.C. copper after 1% and 8%

deformation, from a mechanism based on dislocation interaction. Smith obtained two activation energies for the recovery process after 1% extension and 8% extension, namely, 25,000 cals/mole ± 10% and 21,500 cals/mole ± 5%. In the recovery experiments made by Darling[84] on annealed tough pitch copper and high purity copper, the tough pitch copper always showed a decrease of damping after stressing. In the case of high purity copper a rise in damping with time was observed after small pre-stresses and a fall after higher pre-stresses for material previously annealed at 400°C. A rise followed by a fall, however, was obtained in specimens previously annealed at 600°C. Modulus measurements showed an increase in all cases. Such effects so far have not been found by other investigators. Darling's measurements were made at approximately 1 cycle/sec.

Room temperature recovery of the increase in damping caused by measurements, and mentioned previously, can take place in a manner similar to the recovery of damping after deformation. Swift and Richardson[66] showed that the hysteresis effect in zinc annealed out after a few minutes at room temperature following a sudden reduction of oscillating amplitude. Beshers[90] found that the recovery of his measurement-induced increase in pure copper followed a $t^{2/3}$ law, when subsequent measurements were made at lower amplitudes. Valluri[99] has observed the recovery of internal friction during periods of rest in high purity aluminium specimens

after being subjected to fatigue stresses in torsion. A dislocation rearrangement mechanism gave an effective activation energy of 10,000 calories or less per gram molecule for the process.

Similar types of low temperature damping recovery behaviour have been noted with irradiation or quenched copper and aluminium. Barnes, Hancock and Silk[64] measured a gradual decrease in the initially high damping of pure annealed copper after gamma irradiation, neutron irradiation and quenching. This decrease was almost complete after 8 hours at room temperature. Levy and Metzger[100] obtained complete recovery of quenched aluminium in less than 40 mins, the final value being $3 \cdot 7 \times 10^{-5}$. Slow rates of cooling to 350°C followed by quenching gave much higher damping values and slower recovery.

Proposed Theories to Account for Dislocation Damping

Until very recently quantitative models put forward to account for the internal friction results just described have been restricted in the temperature and frequency ranges which they cover. It will be shown that even now there is still no comprehensive model which will account quantitatively for the frequency variation and temperature variation of the existing experimental results.

Read[55] suggested that dislocations moving under an applied oscillatory stress might be the cause of the damping observed in his own experiments. This was the first reference to dislocation

damping. Read postulated a type of work-hardening process occurring each cycle. This gave rise to a hysteresis loss during dislocation motion. Read and Tyndall[101] subsequently abandoned this elementary idea, since it was observed that the damping could remain constant for oscillatory stresses above the elastic limit. To explain the increase that could occur in the damping with increasing strain amplitude Swift and Richardson[66] suggested that the dislocations were torn away from pinning points at higher amplitudes, and did not rejoin them immediately the strain amplitude was reduced. A hysteresis loop therefore resulted giving rise to an increase in the damping.

Recent theories can be divided mainly into three groups. Those which depend on a static hysteresis model, those based on potential well models, and, finally, models based on the string-wise vibration of dislocations.

In the first type of mechanism the dislocation is thought of as giving rise to a strain contribution which is in phase with the applied stress while the stress is increasing. During the decreasing stress part of the cycle, a similar type of in phase dislocation strain will occur, of a different value however from that contributed during loading. A hysteresis loop is therefore formed giving rise to an energy loss for each cycle of stress. This energy loss will be independent of frequency since the

dislocation strain contribution occurs instantaneously without a time derivative; hence the term static hysteresis has been applied to this type of damping. The different ways in which this hysteresis is applied to dislocation motion gives rise to the various mechanisms proposed.

Models based on the string-wise vibration of a dislocation in contrast to the above all have a time derivative in the stress-strain equation, i.e., the process is of a relaxation nature and should give rise to a relaxation peak in the plot of damping against temperature or frequency. The hysteresis arises from the inclusion of a damping constant in the equation of motion of the dislocation, which is pictured as vibrating string-wise between pinning points.

Most mechanisms which depend on the dislocation being held in energy wells also fall into the strain relaxation or anelastic category. In this case the dislocation is pictured as lying in a potential trough, and an applied stress can then move part of whole of the dislocation into an adjacent trough. The well between troughs is generally taken to be Pierl's stress. Such a process would also be thermally activated. When the stress is periodic the strain has an out of phase component which gives rise to an anelastic hysteresis loop. In this last treatment the damping is characterised by the relationship $\Delta = \Delta_0 \frac{\omega \tau}{\omega^2 \tau^2 + 1}$ where Δ_0 is the relaxation strength and τ the relaxation time. τ in this case obeys the Arrhenius type equation $\tau = \tau_0 e^{H/KT}$

Static Hysteresis Models

Nowick[54] proposed that dislocation damping may be accounted for by a process of static hysteresis. His proposed theory was purely qualitative. He pictured the dislocations as being torn loose from small barriers for each increment of stress $\delta\varepsilon$, a step-like stress strain loop thus results. Hysteresis occurs because the dislocation once pulled loose would not return to its original position unless a reverse stress was applied. The model as such would account qualitatively for the amplitude dependent damping noted in the kilocycle range. Weertman[75] and Weertman and Salkovitz[56] used Nowick's idea for the basis of a more quantitative theory to account for the amplitude independent damping observed in their experiments on impure lead and measured in the kilocycle range. The dislocations are postulated as moving backwards and forwards over the stress fields of impurity atoms. The theory requires that the dislocation lines are not actually pinned by the impurities which are in turn more or less randomly distributed throughout the lattice. Weertman and Salkovitz[56] carried out calculations to show that these requirements are fulfilled in the case of impure lead where $\xi \approx 0{\cdot}1$. The decrement Δ_I has been calculated and is given by

$$\Delta_I = \frac{0{\cdot}02\,\Lambda\,\lambda b/\mu}{\sigma_M} \qquad \ldots\ldots\ldots\ldots\ldots(2)$$

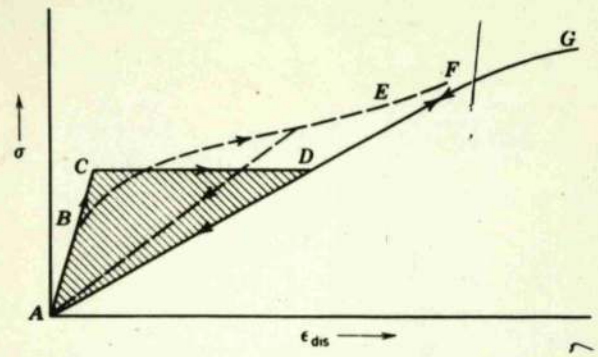

Fig. 8. The solid line shows the stress-strain law that results for the model shown in Fig. 7. The elastic strain has been subtracted out so that only the dislocation strain is shown. The path *ABCDEF* is followed for increasing stress; the path *FA* is followed for decreasing stress. The dashed line is that which would result if not all of the loops had the same length, but there was a distribution of lengths L_c (ref. 4). (Courtesy *Journal of Applied Physics.*)

FIG. 5

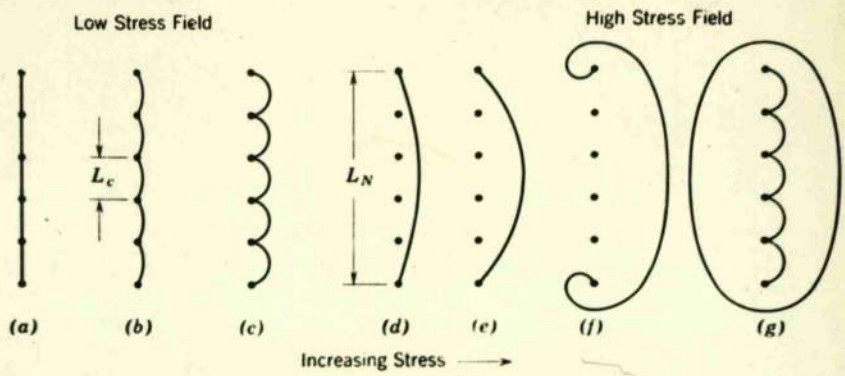

Fig. 7. The successive drawings indicate schematically the bowing out of a pinned dislocation line by an increasing applied stress. The length of loop determined by impurity pinning is denoted by L_c, and that determined by the network by L_N. As the stress increases, the loops L_c bow out until breakaway occurs. For very large stresses, the dislocations multiply according to the Frank-Read mechanism (Ref. 4). (Courtesy *Journal of Applied Physics.*)

FIG. 6.

Weertman and Salkovtiz used the theory of Mott and Nabarro for determining σ_M and this is given by

$$\sigma_M = (2\pi)^{-\frac{1}{3}} \mu \varepsilon^{4/3} c^{11/9} \left[\ln \frac{1}{c}\right]^{4/3} \qquad \ldots\ldots\ldots\ldots (3)$$

The modulus change $\frac{\Delta E}{E}$ was found to be Equal to Δ_I ; thus the ratio $r_I = 1$. This is the major fault of the above theory since Thomson and Holmes[63] and Gordon and Nowick[97] have obtained values of r_I which approximate to one tenth. Furthermore, Thomson and Holmes have shown rather conclusively that $\Delta_I \propto \frac{1}{c^4}$ and $\frac{\Delta E}{E} \propto \frac{1}{c^2}$; this does not agree at all with the above theory.

Weertman and Salkovitz proposed that the large increase in damping observed at higher strain amplitudes takes place when $\varepsilon_0 > \sigma_M$ and presumably is also of a static hysteresis nature.

Granato and Lucke[103, 104, 51] also used the static hysteresis mechanism to account for the amplitude dependent, frequency independent damping. The stress-dislocation strain curve for a half oscillation is postulated to be of the form shown in Fig.(5). This stress-strain curve arises directly from a breakaway mechanism of the dislocation from impurity pinning points, as shown in Fig. (6). When the dislocation breaks from one impurity pinning point the process is catastrophic along the length L_N . A rather complex mathematical treatment gives

$$\Delta_H = A_1 e^{-A_2/L} \qquad \ldots\ldots\ldots\ldots (4)$$

where

$$A_1 = \frac{2.5 \pi \Lambda L N^3}{\pi^2 L} \cdot \frac{K^2 a}{L \varepsilon_0} \; ; \qquad A_2 = \frac{K^2 a}{\varepsilon_0}$$

This relationship is slightly more complex for frequencies nearing dislocation resonant frequencies.

Granato and Lucke[104] have tested the theory fairly rigorously, and there is little doubt that this mechanism can account for a great deal of the present amplitude dependent results. The theory predicts that a plot of log Δ_H against $\frac{1}{\varepsilon_0}$ for any one specimen will give a straight line. Such plots however do not give straight lines over a large range of stress amplitudes. This is particularly so when the extensive results of Niblett and Wilkes[71] and Takahaski[106] are so plotted. Niblett and Wilkes[71] have suggested that Granato and Lucke's theory is correct in nature and that the above deviation from a straight line may be due to increases in Δ_L during the breakaway process; the corrected Δ_H values may then give a linear plot. Mason[22] has suggested that the plot is not linear due to some other damping mechanism interfering at higher amplitudes. The temperature dependence of the Granato and Lucke model depends purely on the variation of L which varies according to the Cottrell[197] relation

$$\frac{a}{L_c} = C = e_0 e^{Q/KT} \qquad \text{.....(5)}$$

Thus from measurements at various temperatures, Q the binding energy between impurity and dislocation can be obtained. When this is done the values obtained appear to be high in comparison with other estimates[56]. Equation (4) predicts a levelling off at high strain amplitudes, This is not found generally in practice.

However, it is quite probable that some other damping mechanism is predominating at higher stress amplitudes. Mason[22] has proposed a specific mechanism. The model is also probably not applicable to the results of Weertman and Salkovitz since, as these authors have shown, the dislocations are not pinned by the impurities in lead; the calculated binding-energies showed that little segregation would occur at all. This may account for the discrepancy in the value of Q obtained by Granato and Lucke[51].

The modulus change occurring with the dislocation breakaway in the above theory is shown to be the same as equation (4). Thus, the ratio $r_\mu = 1$ is in agreement with experimental results[55, 96]. The above model and treatment however are the most extensive so far given to account for amplitude dependent damping. Beshers quite independently obtained the empirical relationship

$$\Delta_H = Be^{-A/\varepsilon_0} \qquad \text{.....(6)}$$

where A + B are constants for a particular curve, from his amplitude dependent damping results. This was taken as confirmation of the Granato and Lucke theory for impure metals.

Models Based on Visco-elastic Relaxation

Koehler has applied Rayleigh's[109] equation of motion of a stretched string to a bowing dislocation held between two pinning points, thus Koehler takes as the basic equation of motion of the dislocation

$$A\frac{\delta^2 x}{\delta t^2} + B\frac{\delta x}{\delta t} - C\frac{\delta^2 x}{\delta y^2} = b\sigma \qquad \text{.....(7)}$$

The meanings of the constants A, B and C are given in the glossary of terms used.

Koehler solved the above equation of motion for kilocycle frequencies only. Weertman[75] pointed out that the bowing mechanism should also give rise to large losses at megacycle frequencies of measurements. At these higher frequencies Weertman suggested that the hysteresis model proposed by Weertman and Salkovitz[56] would not have time to operate. The dislocations would however be able to osciallate backwards and forwards between impurities which would effectively pin the dislocation at these higher frequencies.

Equations for the damping factor B have been given by Eshelby[110] and Leibfreid[111]. In the latter case Nabarro[112] has corrected an apparent error and has shown that the estimate was of the correct form and magnitude but numerically too high. Granato and Lucke have tabulated the results obtained using the above two theories for lead, copper, aluminium, zinc and germanium. The results obtained from Leibreid's theory are two orders of magnitude higher than those obtained from Eshelby's treatment. Leibfreid treated the damping constant B as arising from the interaction of moving dislocations with thermally excited sound waves while Eshelby thought of the damping as arising from irreversible heat flow occurring in the neighbourhood of the oscillating dislocation.

The latest and fullest solution to the equation (7) has

being given by Granato and Lucke[103]. This analysis of Granato and Lucke was aimed at explaining Δ_I damping. Their model is shown in Fig. (6) and pictures the dislocation oscillating between Cottrell pinning points. At higher stresses the dislocation breaks away and gives the static hysteresis loss already described. At low stresses where no breakaway occurs the dislocation motion is opposed by some damping mechanism (const. B equation 7), which gives rise to a phase lag for an oscillating stress and hence damping and modulus effects. At low frequencies (below 10 Kc/sec) Granato and Lucke have pointed out that their theory does not apply. Their solution to equation (7) for kilocycle frequencies gives[95]

$$\Delta_I = A_3 L^4 \quad \ldots\ldots\ldots (8) \qquad \left(\frac{\Delta E}{E}\right)_I = A_4 L^2 \quad \ldots\ldots\ldots (9)$$

where $A_3 = \frac{120\,\Omega\,\Lambda\,B\omega}{\pi^3 C}$ and $A_4 = \frac{6\,\Omega\,\Lambda}{\pi^2}$

for megacycle frequencies the solution takes into account the fact that the measuring frequencies are nearing the dislocation resonant frequency.

The megacycle results described under the heading "Effect of Frequency" are in agreement with the above expression for Δ_I and $\left(\frac{\Delta E}{E}\right)_I$. The dependence of Δ_I and $\left(\frac{\Delta E}{E}\right)_I$ on L^4 and L^2 respectively has been verified by Thomson and Holmes[62] with irradiation experiments. This agreement on the effect of loop length bears considerable weight in favour of the theory, since $\frac{a}{L} = c$ the damping is proportional to the fourth power while

the modulus varies with the second power. A consequence of this theory is that the dislocations bow out approximately 80 lattice diameters for L_N values of 2×10^{-3} cms at strains of 10^{-7}.

The temperature dependence of the decrement depends on the parameters B and L while the modulus is temperature independent. In this respect the theory is invalid since Thomson and Holmes[63] have found the modulus to vary intimately with the decrement. Also at temperatures where impurities are immobile, variations in B will not account for the temperature dependence of Δ_I. The treatment is otherwise sufficiently rigorous to enable determinations of L_N, L_c, Λ and B to be made; the value obtained for B is in agreement with the Leibfreid-Nabarro theory[112].

Thomson and Holmes[67] have also used the dislocation bowing model to explain the temperature dependent Δ_I damping in the second temperature range of the background loss. This range is from 180°K. upwards. The decrement and modulus changes are derived as

$$\Delta_I = 5\Lambda B \Lambda L^4 \quad \ldots\ldots\ldots(10) \qquad \left(\frac{\Delta E}{E}\right)_I = \frac{B^2 \Lambda L^2 E_E}{\pi} \quad \ldots\ldots\ldots(11)$$

These are essentially similar to Granato and Lucke's values without the frequency term in the Δ_I expression. E_E is the elastic Young's modulus. Using Leibfreid's suggestion that the average unpinned length of dislocation increases with temperature combined with this equation for the force of a pinning point due to thermally induced oscillation, Thomson and Holmes have obtained

an expression for the number of effective pinning points per unit length; neglecting network pinning points this is

$$C_{eff} = cf\left(\frac{A}{T^{\frac{1}{2}}}\right) \qquad \text{where } A = \frac{F_0}{2\left(\frac{ck}{a}\right)^{\frac{1}{2}}}$$

Since $L_e = \frac{1}{C_{eff}}$ equations (10) and (11) become

$$\Delta_I = \frac{51\beta^2 l}{c^4\left[f\left(\frac{A}{T^{\frac{1}{2}}}\right)\right]^4} \quad \ldots\ldots\ldots(12) \qquad \left(\frac{\Delta E}{E}\right)_I = \frac{\beta^2 l\left(\frac{F_E}{l}\right)}{c^2\left[f\left(\frac{A}{T^{\frac{1}{2}}}\right)\right]^2} \quad \ldots\ldots\ldots(13)$$

where β^2 is an orientation factor and F_0 is the force which must be exceeded if the dislocation is to be effectively free from its pinning point. For high enough temperatures, i.e. above approximately 170°K for the results of Thomson and Holmes

$$f\left(\frac{A}{T^{\frac{1}{2}}}\right) \sim \frac{A}{T^{\frac{1}{2}}}$$

Thus $\Delta_I \propto T^2$ and $\frac{\Delta E}{E} \propto T$. This relationship gives good agreement with the temperature dependence of their own results. The theory appears to be satisfactory for frequencies of measurement made in the kilocycle range where damping has no marked frequency dependence. The omission of a frequency term arises because Thomson and Holmes did not use equation (7) but simply calculated the dislocation modulus defect from a loop length distribution function. They then used this relationship as a basis for the damping loss. The fourth and second power terms of the loop length for the decrement and modulus defects respectively were determined experimentally.

Potential Well Models

Mason[113], Seeger[114], and Thomson and Holmes[67] have all used

potential well models with some success to account for the low temperature damping peaks originally observed by Bordoni[68]. Thomson and Holmes[67] based their model on Seeger's ideas. Their interpretation has the advantage over others in that their own recent experimental results and those of Niblett and Wilkes[69] have thrown a great deal of light on the problem. This aspect of damping and the background rise in Δ_I associated with these peaks, i.e. Δ_I rise between 15°K. to 150°K, will not be discussed further since the mechanism involved is not relevant to the present work.

Eshelby[110] has obtained an expression for Δ_I by assuming the dislocations to be held in potential wells; the nature of these wells is not specified. It is assumed that the dislocation is completely free to vibrate in the well. During vibration the dislocation is pictured as oscillating in the well. Since the stress field of the dislocation will accompany it and cause a fluctuating temperature distribution in the material the process gives rise to Zener type thermoelastic damping. The macroscopic effect of thermo-elastic damping is described fully later. The expression derived for Δ by Eshelby[110] is

$$\Delta = \frac{\omega a^2}{10 D_{TH}} \cdot \frac{C_p - C_v}{C_p} \cdot \text{Log} \frac{D_{TH}}{\omega l^2} \left(\frac{\mu}{2\pi\sigma_2}\right)^2 \Lambda \quad \ldots\ldots\ldots (14)$$

In equation (14) l is the "cut-off" length below which the homogeneous elastic solution of the dislocation stress field equation does not

apply and is approximately equal to b. The well energy is taken as having a wave length λ and σ_L is the limiting shear stress. This expression for Δ_r does not have the temperature dependence that experimental results require. The dependence of Δ_r on the fourth power of loop length is not present. Indeed, the effect of impurity is not accounted for at all. The model would appear to be too hypothetical to be applied practically.

Comparison of Theories

Amplitude Independent Damping

The theory of Granato and Lucke as applied to room temperature damping measurements appears to give a reasonable interpretation of Δ_r. As will be shown, however, and contrary to their own specificiation, the theory appears to apply to measurements made well below 10 Kc/sec. The temperature dependence analysis used by Thomson and Holmes in equations (12) and (13) could readily be incorporated into the Granato and Lucke theory. The resulting expression for Δ_I will not account for the low temperature peaks. It is however not necessary that one mechanism in itself should account for all the observed results.

Amplitude Dependent Damping

Of the theories to account for amplitude dependent damping, the expression derived by Granato and Lucke has received the most rigorous test and appears, so far, to be the most satisfactory.

Without stating why, Niblitt and Wilkes[71] suggested that Δ_I might increase as the loop length increases due to breakaway. This seems reasonable since during parts C - D and D - A of fig. (5) the increased length of dislocation L_N will now be moving. Granato and Lucke have taken this motion to be completely elastic. It does seem that to assume the non-existence of any type of damping factor during these parts of the cycle is rather drastic. This may account for the non-linear plots of $\log \Delta_H/\epsilon_0$ which have already been mentioned.

No satisfactory treatment has yet been given to account for the temperature dependence of Δ_H quoted by Niblitt and Wilkes[71]. As these workers pointed out the concentration of impurities on the dislocation lines would not be expected to change much during the few hours when the specimens were cooled below room temperature during their experiments. A temperature analysis of Δ_H similar to that used by Thomson and Holmes for Δ_I is therefore still required for the amplitude dependent decrement.

Theories Proposed to Account for the Relationship between Damping and Pre-Strain

The relationship between damping and pre-strain has been explained qualitatively by Nowick[54] and Hikato[115] et al as follows. When a stress is applied to an annealed metal the dislocations can break away from their impurity pinning points. This gives rise to longer free dislocation loops L which can now vibrate more

readily and thus give rise to an increase in damping. As the stress is increased long Frank-Reid sources start to operate giving rise to an increase in the dislocation density. These newly created dislocations will also give rise to an increase in the damping of the metal, with little if any shortening of L. This can all occur in what appears to be the linear elastic part of the stress strain curve[115]. For continued stressing a stage will be reached when the addition of more dislocations to the lattice will result in dislocation interaction. This in turn will decrease L and the ability of the dislocations to oscillate. The above sequence will give rise to a maximum in the damping-pre-strain curve. Such a picture seems quite reasonable.

The results obtained by Hanstock[26,27] from damping measurements made during fatigue can best be interpreted as arising from an overageing process. The high surface shear strains used by Hanstock for fatigue and damping measurements will give rise to gross plastic deformation and precipitation as already discussed in the section on fatigue. As precipitation proceeds the damping will increase due to the greater amount of slip which can take place. Hanstock's earlier theory assumed that the increase of damping was due to crack formation in the specimen; however, the results of Fig.(2) show that cracks are not necessary for a large increase in damping to occur during cyclic stressing.

Theories Proposed to Account for the Recovery of Damping after Stressing

These fall into three classes.

The Annihilation Theory

Smith[98] proposed that the increase in modulus observed after 1% and 8% elongation could only be accounted for by some dislocation mechanism; he suggested annihilation by the cross slip of screw components of dislocation loops. Using a modulus decay rate based on an exponential function of time Smith obtained two different activation energies (already mentioned) for specimens elongated by two different amounts. For either deformation the activation energy obtained was not unique but distributed about a mean. in a Gaussian manner. Smith therefore concluded that the decay was due to dislocation motion rather than to some mechanism which would depend on a unique activation energy, e.g. point defect migration. It should be noted however that the two differing elongations would give rise to two vastly different concentrations of point defects, and it will be shown that this difference between the two sets of specimens unless taken into account would give rise to two activation energies instead of one. The above theory could not explain the results shown in Fig. (4).

Dislocation Rearrangement Theory

In both the models to be described it is assumed that the dislocations in deformed metal are in two forms, namely, those

tightly bound in the subgrain structure, and those which are relatively free to move within the subgrains. The process of recovery is visualised as rearrangement of these dislocations within the subgrains. The above ideas were first suggested and developed by Nowick[116, 97, 117]. Nowick has not proposed any specific rearrangement mechanism but simply a reduction in the effective number of free dislocations. In accordance with this theory Nowick has shown semi-quantitatively that the reduction in damping of Nacl deformed by 2% in compression is due to a reduction in relative free dislocation numbers and not due to a shortening of loop length. The above results were obtained from a mathematical analysis of modulus recovery and irradiation recovery results. It is difficult to visualise how the dislocations can rearrange themselves in such a fashion that the decrement decreases and yet the loop length remains constant.

Valluri[99] has proposed that during deformation, dislocations inside the subgrains giving rise to a term Δ_2 are piled up and that during recovery the back stress of these "pile-ups" causes the dislocations to move to stable positions in the subgrain boundaries where they are temporarily immobilised. The remaining damping is caused by these dislocations in the subgrain boundaries. Valluri has simply proposed that

$$\frac{d\Delta}{dt} = \frac{dh}{dt} = K_1 e^{-(Q - K_2 A)} \qquad \text{.....(15)}$$

where $\Delta = \Delta_I + \Delta_2$, Δ_I is assumed to remain constant. K_1 and K_2 are constants, η is the number of relatively free dislocations piled up in the subgrains. For fatigued aluminium the effective heat of activation of the recovery process $(Q - K_2\Delta)$ is found to be 9,980 cals/gm mole. Why the dislocations should move to the subgrain boundaries is not at all clear, although this is an essential assumption of the theory.

Point Defect Pinning Theory

Granato and Hikato and Lucke[95] have proposed that recovery of Δ_I, Δ_H and $\frac{\Delta E}{E}$ after deformation is due to the migration of point defects, created during deformation, to the dislocation lines. Since the only variation of Δ_I, Δ_H and $\frac{\Delta E}{E}$ with time is in L, the Cottrell-Beilby relation

$$\eta_1(t) = \eta_{10} \alpha \Lambda \left(\frac{AD}{KT}t\right)^{2/3} \quad \ldots\ldots\ldots\ldots\ldots(16)$$

or $$C_1(t) = C_{10}\frac{4\alpha}{a^2}\left(\frac{AD}{KT}t\right)^{2/3} \quad \ldots\ldots\ldots\ldots\ldots(17)$$

has simply been incorporated into equations (4), (8) and (9) through equation (5) to give

$$\Delta_H \chi \left(\frac{\Delta E}{E}\right) = A_1 e^{-\frac{A_2}{a}(C_{10}+C_{20})(1+\beta t^{2/3})} \quad \ldots\ldots\ldots\ldots\ldots(18)$$

$$\Delta_I = \frac{A_2 a^4}{(C_{10}+C_{20})^4}\left[\frac{1}{1+\beta t^{2/3}}\right]^4 \quad \ldots\ldots\ldots\ldots\ldots(19)$$

$$\left(\frac{\Delta E}{E}\right)_I = \frac{A_4 a^2}{(C_{10}+C_{20})^2}\left[\frac{1}{1+\beta t^{2/3}}\right]^2 \quad \ldots\ldots\ldots\ldots\ldots(20]$$

where $\beta = \frac{C_{10}}{C_{10}+C_{20}} \cdot \frac{4\alpha}{a^2} \cdot \left(\frac{AD}{KT}\right)^{2/3}$

where A_1, A_2, A_3 and A_4 have the meaning previously ascribed to them.

$\zeta_1(t)$ is the number of mobile defects which have diffused to the dislocations in time t

ζ_{10} is the number of defects of the above type in the lattice

c_1 (t) and C_{10} are $\zeta_1(t)$ and ζ_{10} expressed as concentrations,

α is a constant $\simeq 3$. A is a measure of the strength of the Cottrell attraction between defect and dislocation. C_{20} is the concentration of immobile point defects, i.e. impurities.

If the rate of recovery of Δ_H, Δ_Γ and $\frac{\Delta E}{E}$ is made at more than one temperature after deformation and c_{10} has the same initial value, then the activation energy for the process can readily be calculated.

Granato and Lucke[95] have tested their theory rigorously using the published results on salt by Gordon and Nowick[97], deformed copper by Smith, aluminium by Hikato et al and Koester, and on zinc by Alers. Apart from the last case where the amount deformation was very small, -0·5%, the agreement between theory and experimental results is excellent. Granato and Lucke have estimated the activation energy for recovery in salt as being about 23 kcal/mole and have suggested that this is due to negative ion vacancies. From the results on copper by Smith, Granato and Lucke have obtained an activation energy of 24 kcal/mole, i.e. just slightly greater than 1 e.v. Again it is suggested that vacancies produced by deformation cause the pinning of dislocations. Application of the

theory to the results of Gordon and Nowick gives all the parameters in equations (18), (19) and (20) and reasonable results were obtained. Since it is assumed that the deformation is sufficiently large to produce point defects and yet small enough so that dislocation interaction does not occur, the mechanism is valid for deformation between approximately 0·5 to 5%.

As stated earlier a consequence of the constants in the terms A_3 and A_4 in equations (8) and (9) is that the theory for Δ_r does not apply below 10 kc/sec. Granato and Lucke have pointed out however that should lower frequency measurements be found to apply, then only A_3 and A_4 of equations (8) and (9) will require alteration. Granato et al [95] without knowing the frequency of measurements have shown that the results of Smith for 1% deformation fit their theory very well. These results however were obtained from measurements made at 900 cycles/sec [86], well below the lower limit for the above theory. It must be concluded therefore that Granato and Lucke's theory for Δ_r requires revising. Beshers has found empirically that the rate of decrease of the rise in damping caused by the high amplitude damping measurements in pure copper could be represented by

$$\Delta_H = Ke^{-\beta t^{2/3}} \qquad \text{.....(21)}$$

Beshers has used Harper's evaluation of β which is given by

$$\beta = \alpha - \Lambda \left(\frac{AD}{KT}\right)^{2/3} \qquad \text{.....(22)}$$

where K is a constant and α and A are as for Granato and Lucke's equations. The combination of equations (21) and (22) gives rise to an expression very similar to equation (18) obtained theoretically by Granato and Lucke. The equation of the latter workers is more complete and takes into account varying values of C_{10} formed by different amounts of deformation. It also takes into account the effect of impurities.

Both Granato and Lucke's theory and Beshers' equation are based on the $t^{2/3}$ law derived by Cottrell and Beilby. Since in the derivation of the Cottrell-Beilby expression, it is assumed that the concentration C_{10} of mobile point defects does not change, the above equations can only be used to describe the early stages of recovery. For longer periods of time it would be necessary to modify the equations according to Harper[102]. Using equation (21) Beshers[90] has obtained an activation energy in the region of 15 k.cals/mole. This is taken as evidence that the recovery is due to the migration of point defects to the dislocation lines.

Mima[85] has shown that his damping recovery result obtained after 15% reduction of area follow at $t^{2/3}$ law and this is taken as meaning the recovery process is due to diffusion of point defects to the dislocation lines. This law was not obeyed for 65·4 and 72·3% reductions of area and it was assumed that dislocation interaction was also playing a part in the recovery

process for these larger amounts of deformation.

In favour of a point pinning mechanism are the results of Koster and Stolte, and Granato, Hikato and Lucke discussed earlier. It would be very difficult to explain their results by any mechanism other than one based on dislocation pinning by point defects.

The damping recovery results caused by quenching and irradiation also favour the above theory since point defects are created in abundance during the processes while the dislocation density is altered very little or not at all.

It would seem reasonable to suggest that the recovery results noted by Valluri are also due to point defect pinning since as has already been shown point defects appear to be created in abundance during fatigue.

Nowick[117] has pointed out that the results of Gordon and Nowick[97] which show that $\sim\Lambda$ decreases during Δ and $\frac{\Delta E}{E}$ recovery of deformed salt contradict the above theory. They admit however that their conclusions are drawn from only one set of results on Na ℓ. In favour of the pinning theory are all the results just described. For deformation greater than about 5% dislocation interaction may occur and modify the theory.

CHAPTER 2

Construction of apparatus to measure damping capacity, calibration and investigation of the effect of certain variables on measurements of damping.

CONSTRUCTION OF APPARATUS FOR MEASURING INTERNAL FRICTION

The aim of the present work was to use damping measurements as an aid to investigating fracture of metals. A method of measuring damping was sought which would not entail the construction of elaborate amplifiers or tuning circuits. Measurements made in the kilocycle range are attractive because large strain amplitudes can be obtained, and in some cases these have been made large enough to fatigue specimens[25].

Fatigue was chosen as the method of introducing fracture since it is possible to deform the metal to the extent of crack initiation without altering the shape of the specimen; it was further decided to do this on a separate apparatus. Because the damping capacity of a bar varies immediately after deformation, rapid insertion of the specimen and taking of initial measurements is of importance. Furthermore ability to incorporate the specimen in the apparatus without straining is necessary. Measurements made at more than one temperature are also valuable for giving information on activation energies.

The apparatus which seemed most suitable to fulfil these requirements was that initially developed by Forster[52]. In this method the bar vibrates transversely in free free motion and the damping capacity is measured from the width of the resonant peak at half amplitude.

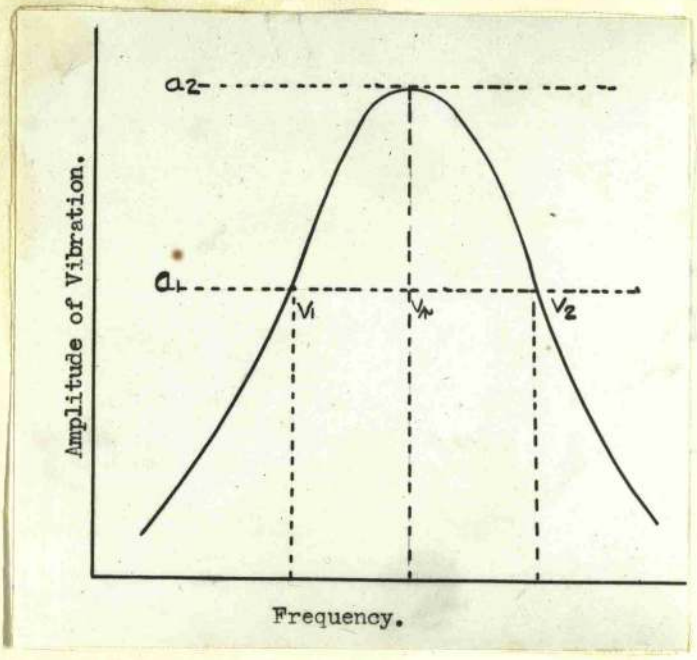

FIGURE I

Fig. 1 shows a typical vibration amplitude versus frequency curve for a material of amplitude independent damping, where V_r is the resonant frequency of the bar and $a_2 = 2a_1$. The damping capacity is given by

$$\Delta = \frac{V_2 - V_1}{V_r} = \frac{\pi}{\sqrt{3}} \quad \ldots\ldots\ldots\ldots (1)$$

The specimen is supported at short distances from the nodes by wire or cotton threads and these two supports can be used to vibrate and detect vibration of the bar. From the many types of vibrators and transducers available, Rochelle salt piezo electro crystals were chosen as a means of converting alternating voltages into mechanical vibrations and vice-versa. Any standard type oscillator which can supply alternating voltages at any kilocycle frequency is suitable for feeding the crystals. The voltage generated in the output crystal is fed into an amplifier and oscilloscope; the output from the amplifier in turn is fed into a valve voltmeter which then gives a reading

directly proportional to the voltage generated in the crystal. Fig. 2 shows schematically the general arrangement of the apparatus.

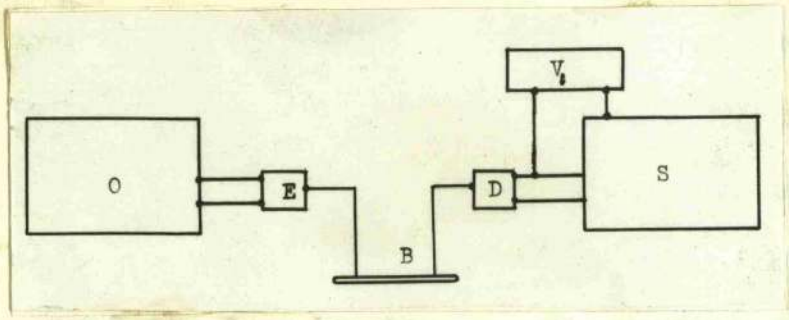

FIG. 2.

D - Decade Oscillator

E and D - Exciting and Detecting Crystals

B - Test specimen supported by threads approximately 7" long

S - oscilloscope with gain of x 900

V - valve voltmeter

Electrical Apparatus

Muirhead Wigan Decade Oscillator. This instrument has a continuously variable frequency range of 1 - 11,000 cycles per second and 10 - 111,100 cycles per second. The hourly stability of the frequency is specified as ± 0·02% . This was verified from actual measurements made over a period of one day; however, when making damping capacity measurements at low stress amplitudes it was necessary to use the feed-back control and this accelerated frequency drift. Although the frequency accuracy is ± 0·2% or ± 0·5% (whichever is the greater), a high degree of accuracy is not necessary since the damping measurements depend only on the first power of the frequency. The above frequency accuracy is obtained after 15 minutes warming up period for the frequency range 1 - 10,000 c/s.

Exciter and detector piezo electric crystals.- These units consist of Rochelle salt parallel bender crystals and for present purposes are best employed by clamping at one end between thin pads of stiff rubber, i.e. giving a cantilever mounting. The dimensions of both crystals are $1'' \times \frac{1}{4}'' \times 0.060''$ and they possess a resonant frequency given by $f = \frac{23T}{L^2}$ kc/s where T = thickness of the crystal and L its free length. The crystals were clamped midway which gave them a resonant frequency of 23 kc/s. This frequency is well removed from the resonant frequencies of the transversely vibrating specimens used.

The makers gave the following relation between displacement applied voltage and crystal dimensions $\frac{D}{V} = 219 \ 10^{-12} \ (\frac{L}{T})^2$ where D is in meters, V in volts and L and T in inches.

A maximum input voltage of up to 50 V r.m.s. may be used at 1000 c s.

At one stage of the work a Goodman vibrator was substituted for the driver crystal in an attempt to obtain higher amplitudes of vibration. For this purpose the power from the oscillator was amplified. The results, however, were no more satisfactory than those obtained from the crystal and were some bars actually poorer.

Amplifier and Oscilloscope - This instrument is a Cossor Double Beam Oscillograph. It was decided to use the actual amplifier in the oscilloscope for amplifying purposes and this amplified voltage was taken directly from the cathode ray tube plates via external terminals provided for this purpose. The maximum gain obtainable is x 900 from the main amplifier and is stable up to frequencies of 20,000 c/s. The second beam and amplifier, gain x 30, can be used to follow the voltage supplied to the driver crystal. The two beams are also useful for determining frequency stabilities by means of lisadiew figures. Phase differences, as measured on this instrument, between input and output voltages cannot be used as an indication of damping beacuse of the intervening capacitance present in the exciter and driver crystals.

Valve voltmeters V.- Marconi vacuum tube voltmeter Type TF 1300. This instrument has an impedance of 6 megohms at frequencies of up to 20 kc/s and when connected to the output of the oscilloscope no visible loading is observable on the oscilloscope trace. The accuracy of measurement is ± 3% of full scale deflection ± 0·02 volts.

During part of the period over which this work was carried out a different instrument was used from that described above. This was a Model 26 Laboratory Valve

Voltmeter, the accuracy of which was given by the makers as being better than ± 1% full scale. This instrument was supposed to comply with BSS. No. B.S. 89 for First Grade moving coil meters. Stability is given as being better than 0·75% in twenty-four hours. Acceptance of the accuracy of ± 1% gave rise to large errors in damping capacity measurements as will be described later.

The suspension system.

Fig. 3 shows the frame-work and suspension system while Fig. 4 is a photograph of the general assembly. The bar is suspended in cotton threads which in turn are fixed to the piezo electric crystals by means of small aluminium clips. The crystals are clamped between fine pads of rubber on to the steel weights. These steel weights are isolated from vibration in the room by suspending them on bronze springs which have a low resonant frequency, approximately $\frac{1}{2}$ cycle per second. These springs prevent all but severe vibrations from reaching the crystals. The frame-work rests on a steel plate which in turn lies on a heavy slate bench. Because vibrations from the exciting crystal are transmitted directly to the receiver crystal by the air between them it was found necessary to shield the receiver crystal completely in an aluminium can. Voltage is fed to and taken from the crystal by means of

SUSPENSION SYSTEM

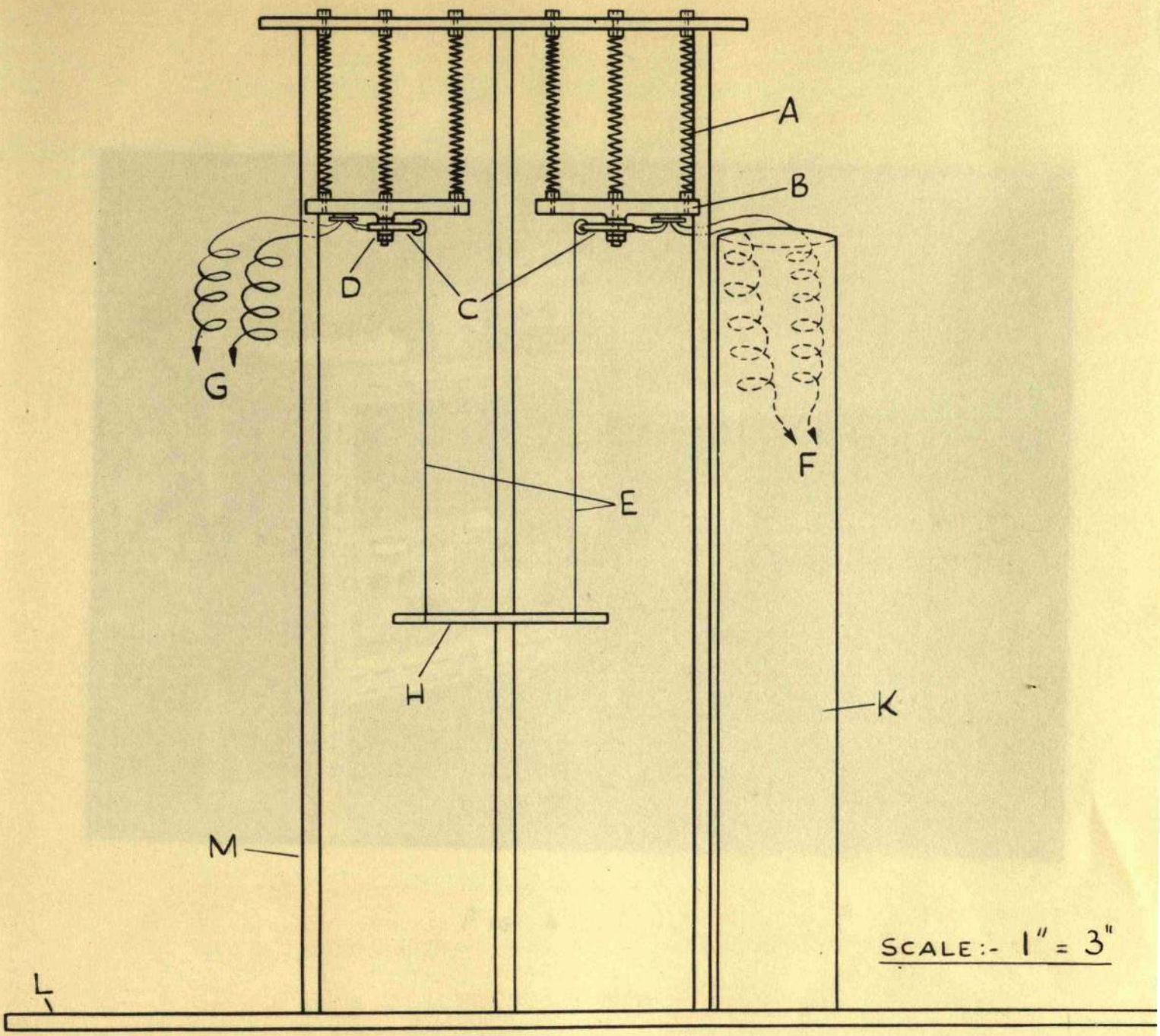

A - SUSPENSION SPRINGS
B - STEEL WEIGHTS
C - PIEZO ELECTRIC CRYSTALS WITH ALUMINIUM CAPS
D - RUBBER BETWEEN METAL CLAMPS
E - COTTON THREADS
F - TO OSCILLATOR
G - TO OSCILLOSCOPE
H - SPECIMEN
K - EARTHED IRON CYLINDRICAL SHIELD
L - EARTHED IRON BASE PLATE
M - EARTHED METAL FRAME

FIG. 3.

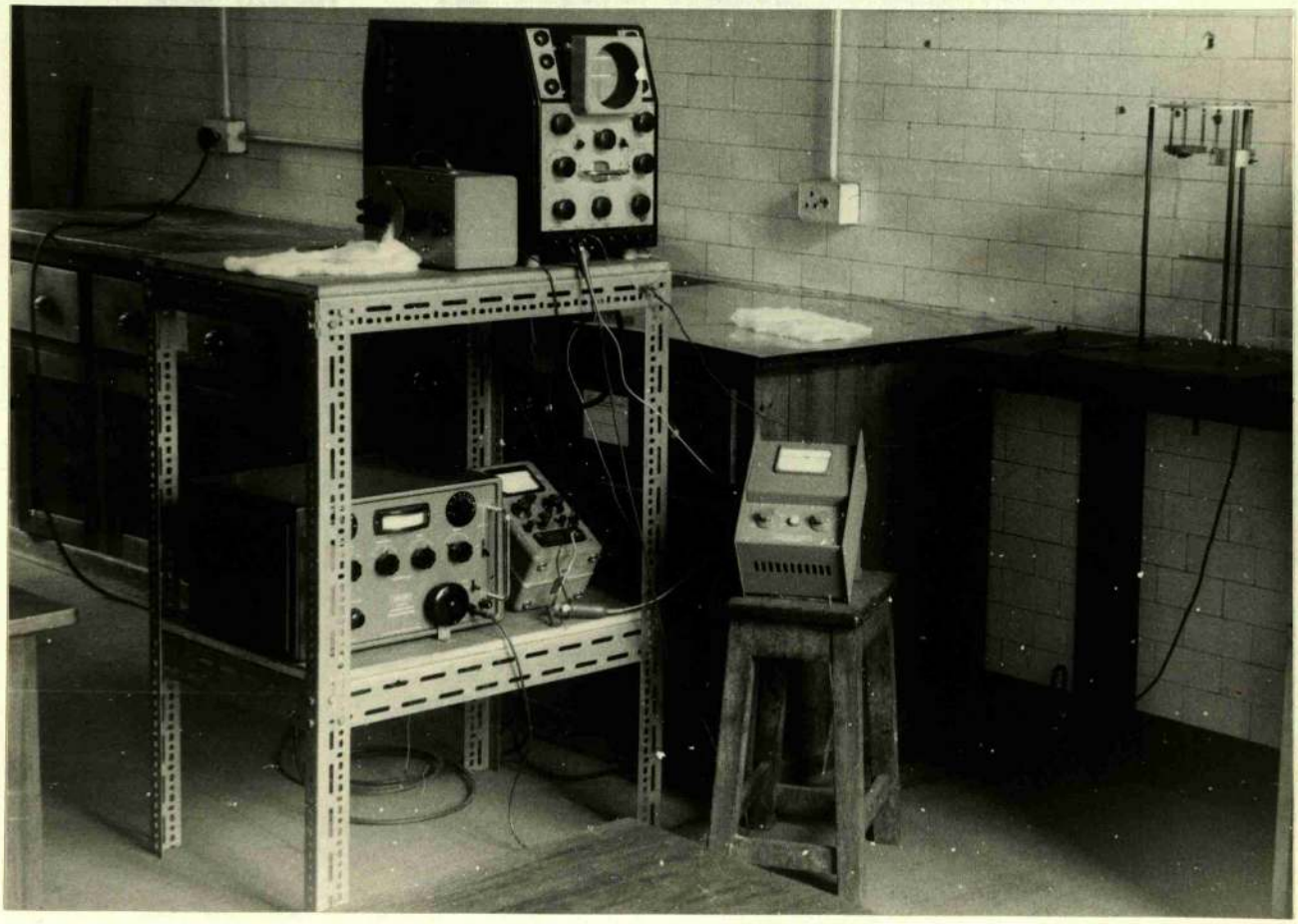

FIG. 4.

light flexible springs via vacuum tight terminals on the base plate. The complete assembly as shown in Fig. 3 is designed to operate under vacuum.

Difficulty was at first encountered due to mains interference. This was finally reduced to 0·5 millivolts by earthing the table framework, base plate and suspension system and surrounding the detector voltage carrying springs by an earthed steel shield.

Free-Free transverse vibrations of a stiff bar.

The equation of motion of a stiff bar is

$$\frac{d^2y}{dt^2} + k^2c^2\frac{d^4y}{dx^2} = 0 \quad \text{.....(2)}$$

where $C = \sqrt{\frac{E}{\rho}}$; C is the velocity of a longitudinal wave in the bar for longitudinal vibrations; E is Young's Modulus; ρ is the density of the material. The transverse vibrations $k^2 = \frac{a^2}{4}$ where for a round bar a is the radius; for a rectangular bar of thickness in the plane of vibration, $k = \frac{t^2}{12}$. When the wavelength of vibration λ is large compared with k, then the natural frequency of vibration of the stiff rod of length l in transverse motion is obtained from the solution of equation (2) and is given by

$$N = \frac{\pi}{8}\cdot(4S-1)^2\frac{K}{l^2}\sqrt{\frac{E}{\rho}} \quad \text{.....(3)}$$

For the fundamental frequency, $(4S - 1)$ should be replaced by 3·0112. From (3) it can be seen that N is approximately proportional to $(4S - 1)^2$ where $S = 1, 2, 3 \ldots$. The overtones are therefore not harmonious as in the case of a vibrating string but are proportional to $3^2, 7^2, 11^2 \ldots\ldots$. The asymmetric modes of vibration have frequencies proportional to $(4S + 1)^2$ i.e. $5^2, 7^2, 13^2 \ldots\ldots$.

For symmetric and asymmetric vibration therefore $N \propto (\frac{3}{3})^2, (\frac{5}{5})^2, (\frac{7}{3})^2 \ldots\ldots$ where the respective number of nodes are 2, 3, 4, ... Table 1 gives the position of the nodes and relative frequencies.

Table 1

No. of tone	No. of nodes	Distance of nodes from end expressed as $\frac{x}{\ell}$ of length of bar			Relative Frequencies	Frequencies as a ratio for N.
1	2	0·2242	0·7758		$3·011^2$	1
2	3	0·1321	0·5	0·8679	5^2	2·756
3	4	0·0944	0·3588 0·9056	0·6442	7^2	5·409
4	5	0·0734	0·277 0·9266	0·5 0·723	9^2	8·933

From equation (2) Raleigh[109] has shown that

$$\frac{y}{y_0} = \frac{1·018(\cosh 4·73\,x/\ell - \cos 4·73\,x/\ell) - \sinh 4·73\,x/\ell + \sin 4·73\,x/\ell}{2·036} \quad \ldots\ldots(4)$$

where y is the vertical displacement of any point distance x from one end of the bar and y_0 is the vertical displacement

FORM ADOPTED BY A TRANSVERSELY VIBRATING BAR OF LENGTH 1 UNIT.

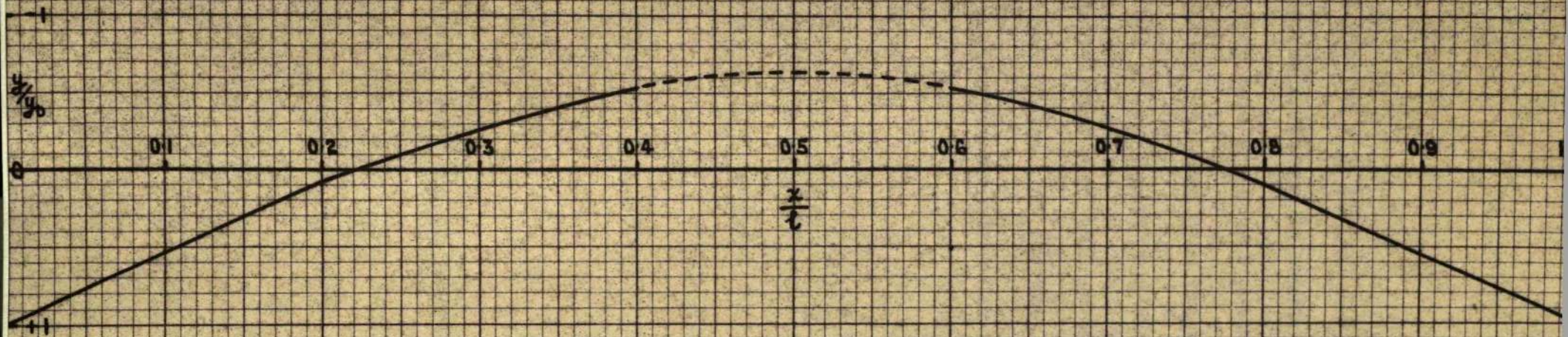

FIG. 5.

of the end. A plot of y/y_0 against x/l for a fully deflected bar can be drawn and is shown in Fig. 5.

It can be seen from this graph that practically no damping contribution will come from the specimen for distances up to 0·2 of its length from each end, since the bar is practically linear over this portion and is therefore virtually free from strain. The main damping contribution comes from the region between the nodes and in particular the centre.

INITIAL OBSERVATIONS ON TRANSVERSELY VIBRATING BARS

The Resonant Frequency

Exploratory work with the apparatus was carried out on cold worked and machined copper bars. These were 10 cms. long and $\frac{3}{16}$ inch in diameter. All subsequent work except where specifically stated, was carried out on bars of these dimensions. The first observation to be noted was that most of these bars had two fundamental resonant frequencies. The difference between these frequencies varied from 1 - 100 c/s.; where the resonants were close, e.g. 1 c/s apart, measurements of damping could not be made because the peak of one resonant interfered with the half amplitude frequency of the other. Where the peaks had a large separation it was possible to rotate the bar until one of these almost or completely disappeared. Examination of equation (3) shows that the two resonants can best be accounted for by the presence of a maximum and minimum diameter in the bar.

Modulation

With certain bars vibrating at higher amplitudes, exceedingly high voltages were sometimes generated quite suddenly. The oscilloscope trace showed that this was due to the bar frequency being modulated on to some high amplitude low frequency. This modulation effect was traced to the threads supporting the bar, which were

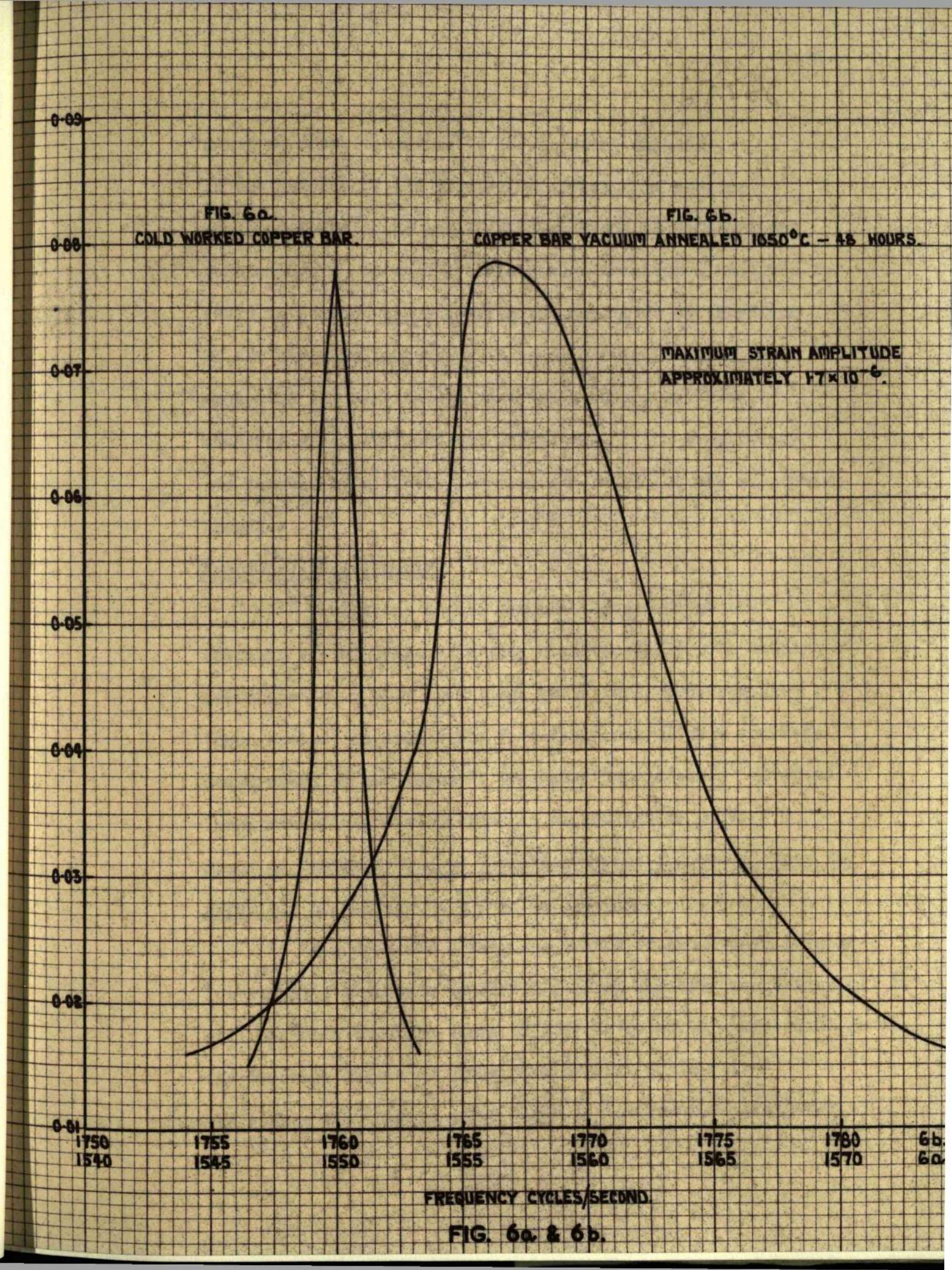
FIG. 6a.
COLD WORKED COPPER BAR.
FIG. 6b.
COPPER BAR VACUUM ANNEALED 1050°C – 48 HOURS.
MAXIMUM STRAIN AMPLITUDE APPROXIMATELY 1·7 × 10⁻⁶.
0·09
0·08
0·07
0·06
0·05
0·04
0·03
0·02
0·01
1750
1540
1755
1545
1760
1550
1765
1555
1770
1560
1775
1565
1780
1570
6b.
6a.
FREQUENCY CYCLES/SECOND.

FIG. 6a. & 6b.

noted on these occasions to be vibrating markedly. In the absence of the modulation effect, the threads appeared to be quite still although known to be vibrating vertically. On most occasions when modulation occurred it could be removed by decreasing the amplitude of vibration of the bar then increasing it again slowly. When the apparatus was originally constructed this modulation occurred frequently and was persistent. The persistency was removed by slightly altering the length of the supporting threads.

Frequency measurements.

Variations in the resonant frequency of the specimen are of value when made simultaneously with damping measurements. Only when large variations occurred are these quoted, as use of the feed back control made accurate measurement of the resonant frequency impossible. Even so large variations must be treated as indicative only.

Shape of the Amplitude of Vibration versus frequency curve for materials of low and high damping capacity.

Fig.s.6a and b show the graphs of two copper bars of low and high amplitude dependent damping capacity respectively. It will be noted that the curve of Fig. 6a is quite symmetrical about the resonant frequency while that of Fig. 6b is not. The reason for this is quite clear. The resonant frequency

of the bar in Fig. 6b increases as the amplitude of vibration decreases; this is caused by the reduced amplitude dependent damping and a corresponding increase in Young's Modulus. Therefore, as the bar is off-tuned to the high frequency side of the curve, the resonant frequency of the bar will no longer be 1766.2 (Fig. 6b) but will be some value higher than this; therefore the bar must be off-tuned still further to reach the half amplitude frequency. In opposition to this the half amplitude will be reached early on the low frequency side of the curve. These two effects therefore tend to cancel each other out and a relatively correct indication of the amplitude dependent damping is given. Nowick[54] has pointed out that these curves can actually bend back on themselves in extreme cases and thus cause a discontinuity in the frequency amplitude plot.

Initial measurements of the amplitude dependent damping of an annealed copper bar.

Before calibration, measurements of damping at different amplitudes were made as follows. The bar was tuned to one of its resonant frequencies then rotated in the supports until the second resonant frequency almost or completely disappeared. This procedure also permitted the bar to be excited to higher amplitudes. The input to the driver crystal was adjusted until the output voltage reached some desired value; the internal friction was then

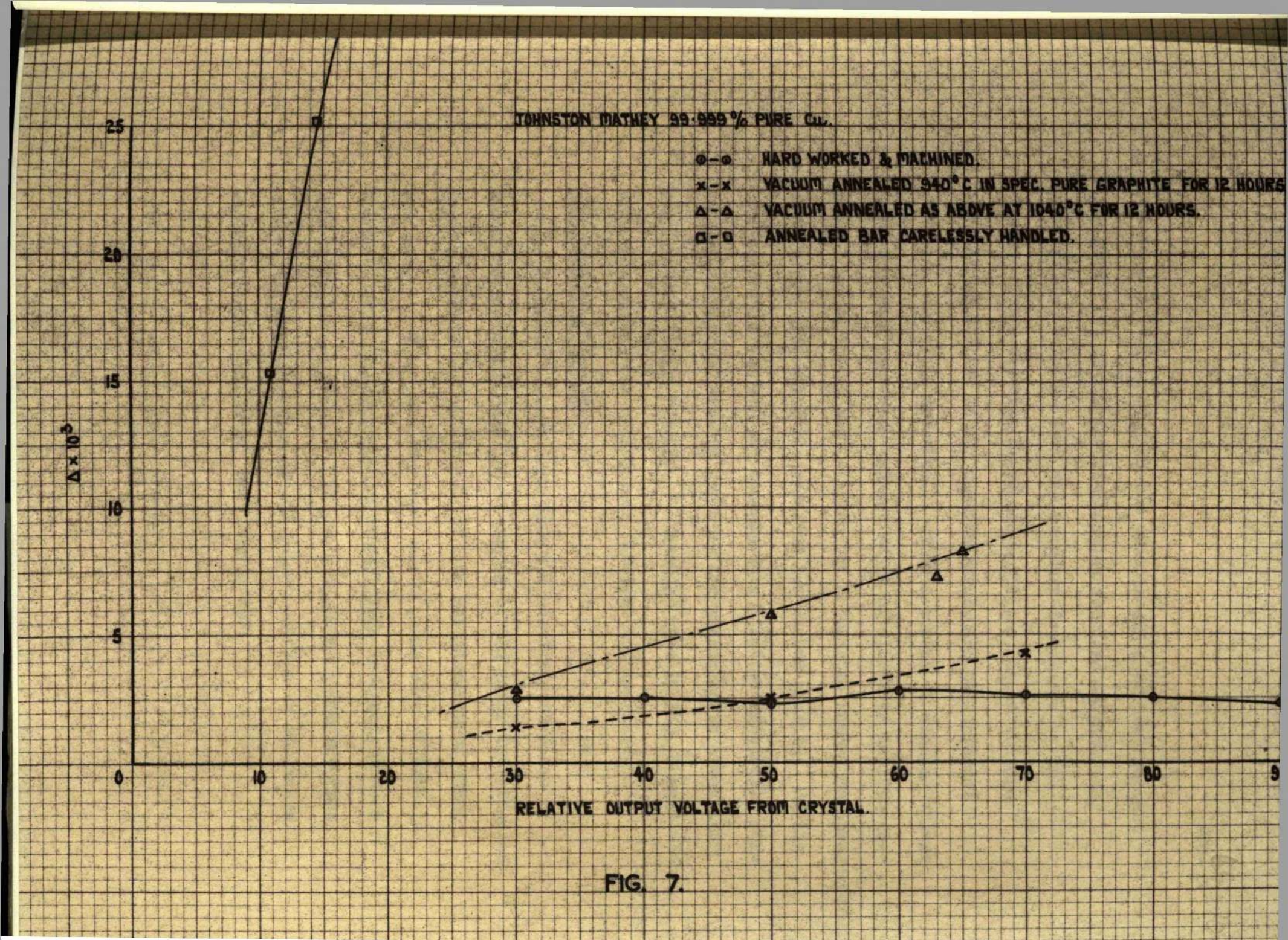
JOHNSTON MATHEY 99·999 % PURE Cu.
●–● HARD WORKED & MACHINED.
×–× VACUUM ANNEALED 940° C IN SPEC. PURE GRAPHITE FOR 12 HOURS
△–△ VACUUM ANNEALED AS ABOVE AT 1040° C FOR 12 HOURS.
□–□ ANNEALED BAR CARELESSLY HANDLED.
Δ x 10³
25
20
15
10
5
0
10
20
30
40
50
60
70
80
RELATIVE OUTPUT VOLTAGE FROM CRYSTAL.

FIG. 7.

measured by off-tuning the bar on both sides of the resonant frequency and noting the frequencies required to give half the voltage obtained from the resonant frequency. The input voltage was then increased until the output voltage reached some other higher desired value, and the internal friction was again measured. Thus a series of damping values were obtained over some unknown range of vibration amplitudes. Fig. 7 shows the values obtained for a Johnston Mathey spectroscopical pure copper bar which has received two vacuum anneals; during these anneals the bar was contained in a spectroscopically pure graphite case. The top curve is for measurements after the bar was carelessly handled. Included also in Fig. 7 are measurements of the material as received and machined.

Discussion of Results

These results show that the heavily worked and machined bar has a peak in the middle of the range investigated. Such a peak is not in accordance with the findings of other workers. This peak was observed in other bars of annealed copper - 0·2% Si which should be amplitude independent over the range investigated. It was concluded therefore that either the amplification of the output voltage or the valve voltmeter scale, or both, were non-linear.

It is felt that the increase in damping shown in Fig. 7 is caused by annealing since this specimen was handled with great care. The results obtained are in accordance with those obtained by Barnes, Hancock and Silk[64], who suggested the rise in damping with annealing temperature was due to agglomeration of the impurities into aggregates on the dislocation lines thus giving rise to longer free lengths of dislocations. Whether or not this explanation is correct is not known.

The effect of careless handling of annealed copper was demonstrated clearly by Read. The large increase is known to be caused by the generation of the new and therefore unpinned dislocations and also increased free lengths on previously pinned dislocations. The effect has been explained in a quantitative manner by Granato and Lucke[104] who showed that the active dislocation length/cm.^{3} of pure copper single crystals increased systematically from 3×10^{-6} to 12×10^{-6} after compressive loads varying from 0 to 150 p.s.i. Such a theory accounts readily for the curve obtained after careless handling of the specimen.

Preliminary work also established that the apparatus was capable of detecting recovery in the metal after fatigue. Unfortunately, however, these results are now known to be inexact because of the non-linear scale on

the valve voltmeter.

Conclusions

The apparatus demonstrated its ability to measure internal friction qualitatively and detect the effect of deformation and recovery after deformation. The measurements, however, were not exact and complete calibration of the electrical apparatus used has been shown to be necessary irrespective of the instrument makers claims.

CALIBRATION OF APPARATUS

Electrical apparatus. - Amplifier and valve voltmeter.

Fig. 8 shows the assembly used to calibrate the combination of the amplifier and valve voltmeter.

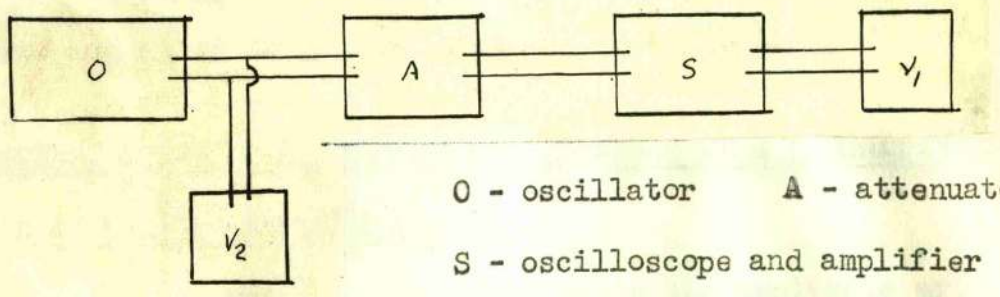

O - oscillator A - attenuator

S - oscilloscope and amplifier

V_1 - valve voltmeter used for damping measurements

V_2 - similar valve voltmeter used for determining input voltage to attenuat

Fig. 8.

A fixed voltage of 6 volts output from the oscillator was fed directly into a standard Marconi attenuator. The output voltage from the attenuator was then fed into the input of the oscilloscope and the final amplified voltage was measured on the valve voltmeter V_1. Since altering the attenuation in turn altered the loading on the oscillator, a valve voltmeter was required to measure the output voltage from the oscillator. It was possible therefore to supply an absolutely constant voltage to the attenuator. The above procedure gives a very accurate micro voltage supply. Using the 6 volt input as a standard the measurements on the instrument V_1 were plotted against input for all combinations of oscilloscope and voltmeter scales used Fig. 16 (see appendix). This standardisation in turn permitted true voltage measurement to be made from the receiver crystal.

DETERMINATION OF AMPLITUDE OF VIBRATION OF A RESONATING BAR AT VARYING AMPLITUDES.

Several methods of measuring the amplitude of vibration of a flexing bar are available e.g. (a) the combination of stroboscopic lighting and a microscope (b) by proximity meter methods and (c) direct observation of reflected light from the bar. Method (c) was used.

The nodes and centre of the bar were spotted with black cellulose and then dusted with 700 mesh carborundum powder. A microscope giving x 700 magnification was focused on a suitably small piece of carborundum. The width of the particle on the graticule was noted. The bar was then vibrated at its resonant frequency and the width of the particle again noted along with the output voltage on the valve voltmeter. This was done throughout the amplitude range used in this work. At off resonant frequencies and at the nodes during resonance, the particles were sharp and easily defined. At the centre of the bar and during resonance, however, the particles appeared as white lines of reflected light. These observations show that the bar was not being deflected up and down in a non-flexural manner by the crystals and that the measurements being made were caused purely by transverse vibrations of the bar. The microscope was standardised against a millimeter scale which was subdivided into hundredths. The bar was prevented from swinging backwards and forwards by bringing the stage of the microscope up to and just touching the bar. This diminished the output from the bar by only 3%.

The voltage generated by the output crystal was found to vary with clamping pressure. The clamping pressure

was therefore adjusted until the observed vertical amplitude of the bar corresponded approximately to some standard output voltage. The clamping pressure then required approximately two days to settle down, after which the calibration was determined. The curves of vertical amplitude against voltage generated are plotted in Fig.17 (see appendix to this chapter).

Fig.16 (see appendix) shows the various calibration curves for the electrical apparatus over a period of many months. These plots demonstrate the stability and linearity of the amplifier and Marconi valve voltmeter.

The strain in a flexing bar varies from zero at the neutral axes to a maximum at the surface; there is also a variation in strain along the length of the bar. The strain amplitude is therefore best quoted for some reference position in the bar; the strain amplitude at the middle is derived in the appendix, and all quoted strain amplitudes are for this position.

Combination of the above two calibrations enabled damping measurements to be plotted as a function of strain amplitude.

Vacuum Measurements

Although the apparatus was designed to work under vacuum conditions, consistent results could not be obtained

with vacuum measurements or measurements made afterwards in air. Since the only part of the apparatus which could be affected by evacuation is the crystals, it was concluded that these behaved abnormally when under vacuum. It was later determined that Rochelle salt crystals decomposed in the region of room temperature when under low pressure: this supports the above conclusion. Air damping losses, therefore, could not be determined by making measurements under vacuum.

Other spurious losses include losses due to the supports, rubber clampings and losses in the piezo electric crystals themselves; the impedance of these was measured and found to be 0·8 mΩ. As will be shown later experimentally the total of all these losses is negligible compared to the damping measurements obtained throughout this work.

Effect of position of supports on measured damping capacity

A true measurement of the damping capacity is not obtained when the bar is supported at any position other than the nodes.

This effect has been investigated both theoretically and practically by Watchman and Tefft[105] for materials of very low damping capacity, i.e. between 1-2 x 10^{-5}. Using the relationship

$$\Delta_M = \frac{1}{2} \frac{\Delta E_S + E_A}{E_S + E_A} \qquad \text{.....(5)}$$

where $E_a = k_a y^2$ and $E = k y_o^2$, direct substitution gives

$$\Delta_M = \frac{\Delta_s + k \Delta_A (y/y_o)^2}{1 + k (y/y_o)^2} \qquad \text{.....(6)}$$

where Δ_M is the measured internal friction. Δ_S is the true internal friction of the specimen. ΔE_A and ΔE_S are the energy losses in the apparatus and specimen respectively; k_a and k are constants for a given suspension and specimen; $k = k_a/k_s$; y is the vertical displacement of the suspension point from equilibrium and y_o is the displacement of the end of the specimen. The relationship between y and y_o is given in equation (4). By obtaining Δ_M for three different support positions it is possible to obtain Δ_S, $k \Delta_A$ and k from equation (6). Watchman and Tefft obtained an excellent fit between equation (6) and a complete series of Δ_M values at various support positions. The specimens used were cermets which presumably have practically no amplitude dependent damping.

In the present work no difficulty was encountered in investigating this effect for bars having a low amplitude independent internal friction, such as those specimens used for determining the effect of grain size. However, for bars with high dislocation damping capacities and hence having large amplitude dependence it became increasingly

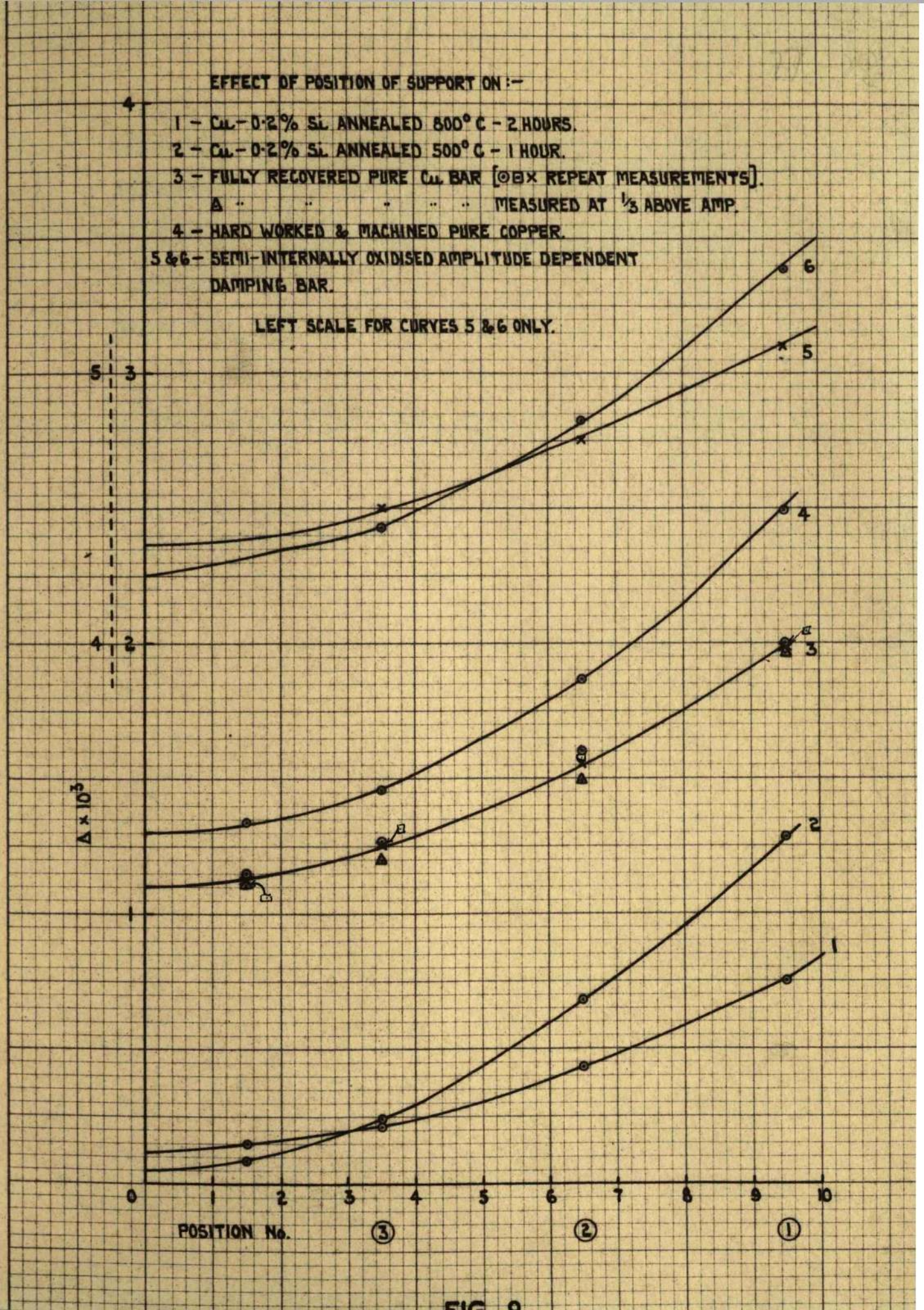
EFFECT OF POSITION OF SUPPORT ON :-
1 - Cu. - 0·2 % Si. ANNEALED 800° C - 2 HOURS.
2 - Cu. - 0·2 % Si. ANNEALED 500° C - 1 HOUR.
3 - FULLY RECOVERED PURE Cu. BAR [⊙⊡× REPEAT MEASUREMENTS].
△ " " " " " MEASURED AT 1/3 ABOVE AMP.
4 - HARD WORKED & MACHINED PURE COPPER.
5 &6 - SEMI-INTERNALLY OXIDISED AMPLITUDE DEPENDENT DAMPING BAR.
LEFT SCALE FOR CURVES 5 &6 ONLY.
Δ x 10³
POSITION No.
1
2
3
4
5
6

FIG. 9.

difficult to measure the effect of the position of the supports. This difficulty arose because it was not possible to vibrate the bar at an absolutely constant amplitude with each shift of the supports. The theoretical voltage which should be drawn from the receiver crystal to give a constant amplitude of vibration can readily be calculated for each support position. However, unless the supports are exactly positioned the bar vibrates at some other amplitude; the amplitude dependent dislocation contribution will therefore alter and this can obscure the effect of the support position. Figure 9 shows the variation of damping with support position for five bars, the lower four of which have amplitude independent damping. The upper curve is at the best an estimate since its damping is amplitude dependent and the inconsistency of the measurements is demonstrated by the two curves which are for the same bar. The fully recovered fatigued bar (curve 3) however, is shown measured three times at one amplitude and a fourth time at an amplitude approximately $\frac{1}{3}$ that of the other three: these measurements are seen to be quite consistent.

The values of three of the measured points from each curve were substituted in equation (6) and values for Δ_I, $k\Delta_A$ and k were obtained in each case. These are

shown below in Table 2. Table 3 shown the positions chosen and the respective values of $(y/y_o)^2$ obtained from equation (4).

TABLE 2

Bar.No.	Δ_S	$k\Delta_A$	k	Comments
1	$1{\cdot}27 \times 10^{-4}$	$4{\cdot}4 \times 10^{-3}$	0·75	Calculated Q_s^{-1}
2	5×10^{-5}	$9{\cdot}44 \times 10^{-3}$	0·152	fits well Q_s^{-1}
3	$1{\cdot}12 \times 10^{-3}$	$7{\cdot}82 \times 10^{-3}$	1·3	Estimated
4	$1{\cdot}25 \times 10^{-3}$	$10{\cdot}2 \times 10^{-3}$	1·1	from drawn curv
5-6	$4{\cdot}317 \times 10^{-3}$	$10{\cdot}47 \times 10^{-3}$	0·91	results not reliable

TABLE 3

Position No.	$x \not\in 1$	y / y_o	$(y / y_o)^2$
1	0·129	0·405	0·164
2	0·159	0·272	0·074
3	0·189	0·1443	0·0208

The differences between Δ_S and Δ_M at position (2), the one used throughout this work, are shown [Fig. 10] below, plotted against the measured damping Δ_M at position (2)

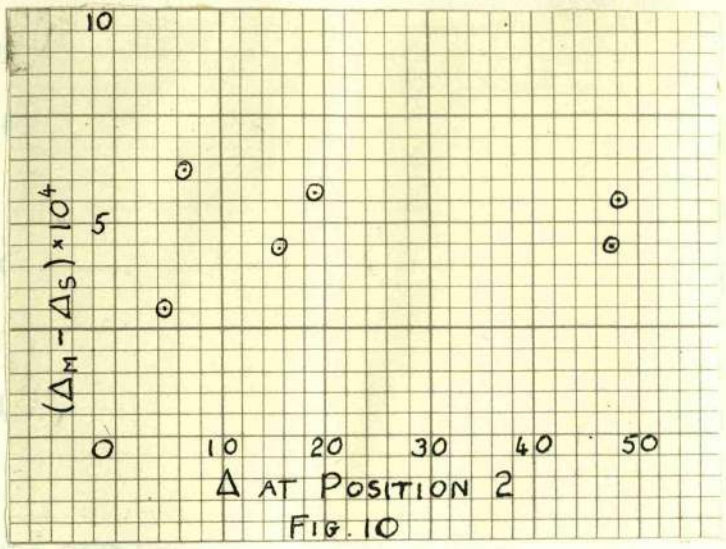

FIG. 10

For bars having an amplitude independent internal friction all values of Δ_M were amplitude independent for the supports kept at any one position.

Discussion of Results

The calculated values of Δ_S fit the extrapolated curves drawn through the Δ_M values in Fig. 9 very well. These results therefore verify the validity of Watchman and Tefft's equation for higher values of damping capacity. The effect of support position is independent of amplitude of measurement; this is also in agreement with equation (6). The crossing of curves (1) and (2) can be seen to arise from the large value of the product

k Δ_A for bar No. 2. This crossing of the curves is also apparent in the results of Watchman and Tefft although these workers have not commented on it. In the other cases investigated the curves are almost parallel. Only for bars of low damping capacity will the support effect obscure the relative damping capacities, and this is noted in the work dealing with defective material.

The most important conclusion to be drawn from the above results is that the true Δ measurements made on bars having amplitude dependent internal friction can only be estimated. In chapter 4 dealing with the recovery of damping after fatigue, all the results include the support effect which is approximately $0{\cdot}5 \times 10^{-3}$. It can be seen from Fig. 10 that this factor is a fair average estimate of the additional damping due to the supports for damping values of Δ_M between 1 and 5×10^{-3}. The error is removed automatically from Δ_H values when Δ_I is subtracted from Δ_M.

In chapter 3, section 2 which deals with the effect of precipitates, no attempt has been made to correct the results obtained and these measurements can therefore only be considered as relative. Similarly it was only desired to make relative measurements on aluminium and no correction was made for aluminium specimens.

Measurements at Higher Harmonics.

With the present apparatus comparison of results is complicated by the position of the supports with respect to the nodes at different harmonics. Although the amplification system was sufficient to detect vibrations up to the fifth harmonic it was not possible to make damping measurements at frequencies above the second harmonic. Since little is gained by making measurements at different frequencies in the kilocycle range measurements were confined to frequencies associated with the fundamental mode of vibration.

DAMPING LOSSES DUE TO MACROSCOPIC AND MICROSCOPIC THERMAL DIFFUSION.

Theory. Macroscopic loss.

The above relaxation processes arise in a vibrating bar because the strain existing in the bar at any one time is never uniform. In the case of a transversely vibrating bar, at full deflection, one side of the bar is in tension while the other side is in compression. Since the application of a tensile stress gives rise to a reduction in temperature and application of a compressive stress yields a rise in temperature, heat will therefore flow across the specimen from the side in compression to the side in tension and will thus give rise

to a certain amount of strain relaxation. At very low frequencies of vibration this heat flow will have time to proceed to completion and the relaxation process will be in phase with the applied stress; this system will be isothermal within itself. At very high frequencies the process will not have time to take place and the vibration will be adiabatic.

Zener[128] has shown theoretically that the frequency at which the above effect is a maximum for circular specimens vibrating transversely is given by

$$f_o = \frac{0.539}{rad^2} D_{th} \quad \ldots\ldots\ldots\ldots\ldots\ldots (7)$$

where D_{th} is the thermal diffusivity of the metal. The magnitude of the effect was also calculated and the decrement is given by

$$\Delta = \pi \frac{E_u - E_R}{E_u} \cdot \frac{f \cdot f_o}{f^2 + f_o^2} \quad \ldots\ldots\ldots (8)$$

where E_u and E_R and the adiabatic and isothermal moduli of the metal respectively. Zener has derived values for $\frac{E_u - E_R}{E_u}$ for different metals. f_o is the resonant frequency as given above and f is the working frequency of the bar.

For copper $D_{th} = 1.2$ cms^2 sec. and $\frac{E_u - E_R}{E_u} = .003$.

For a copper bar of $\frac{3}{16}$" diameter and resonating at 1800 c s. Equation 7 and 8 give f_0 = 12·6 c/s and Δ = 6·5 x 10^{-5} respectively. The above theory of Zener was applied to the experimental results, by Bennewitz and Rotger[116] and gave excellent agreement.

Theory. Microscopic Loss or Intergrain Thermal Diffusion

In polycrystalline metals and non-cubic metals in particular a non-homogeneous strain will exist between neighbouring grains of different orientation. A thermal diffusion process similar to the effect described above will therefore take place across the grain boundary of the two grains; also as above, this thermal relaxation will give rise to an anelastic effect. Zener has shown that this effect is present even in cubic metals since it cannot be assumed that a uniform stress exists throughout the strained metal.

The resonant frequency of this effect is given by

$$f_0 = \frac{3\pi}{2} \cdot \frac{Dth}{g^2} \quad \text{.....(9)}$$

where g is the grain size as determined by any conventional method.

It is difficult to determine the magnitude of this effect theoretically and it is therefore normally obtained experimentally. To do this a number of specimens each with

Cu – 0·2 % Si ANNEALED 500° C – 1 HOUR
⊙ × – TWO SPECIMENS
Δ × 10³
1·4
1·2
1·0
0·8
0·6
0·4
0·2
0
1
2
3
4
5
6
7
8
9
10
POSITION OF SUPPORT IN M.M. FROM NODE.

FIG. 11.

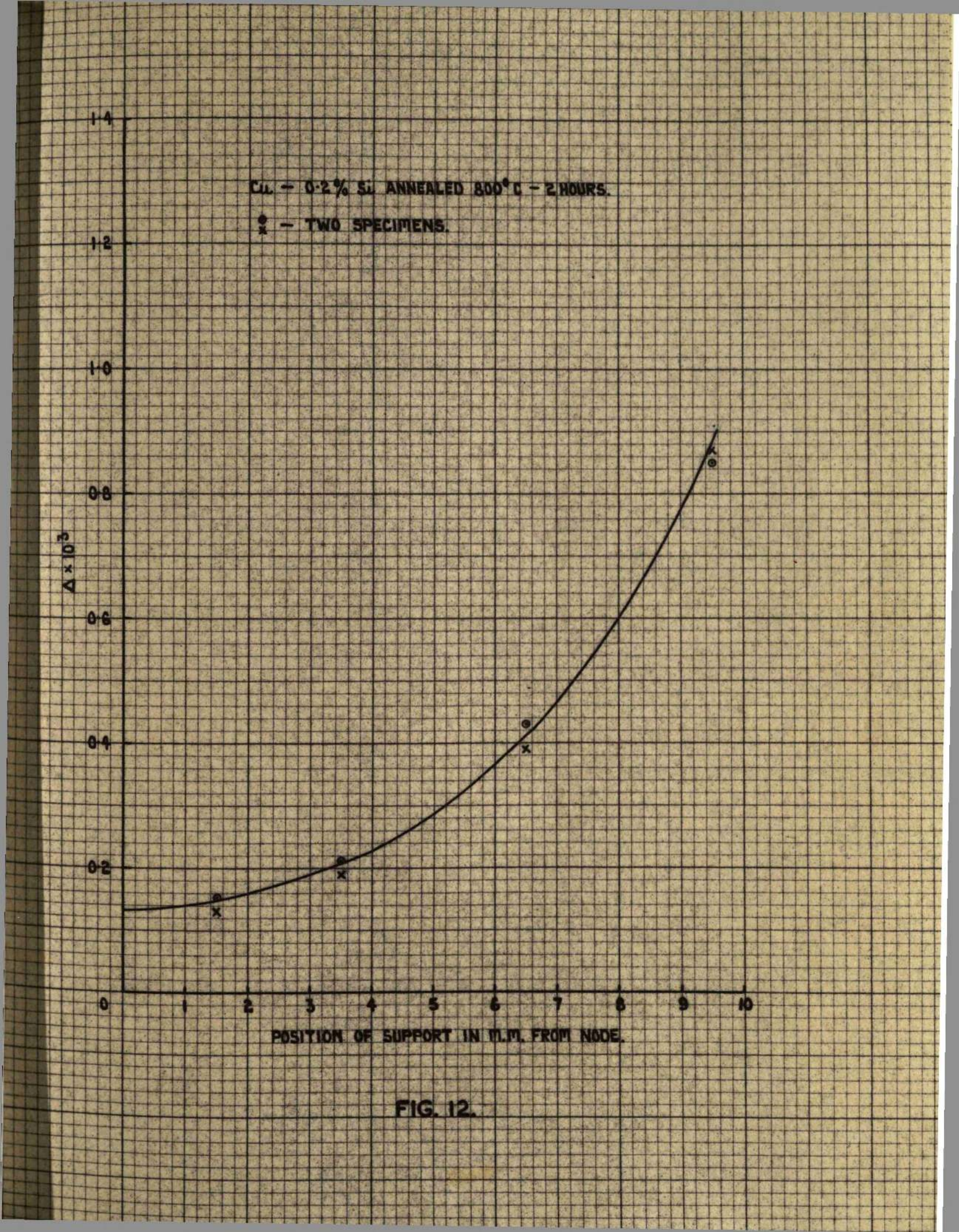
Cu. – 0·2% Si. ANNEALED 800° C – 2 HOURS.
⊙ – TWO SPECIMENS.
Δ × 10³
1·4
1·2
1·0
0·8
0·6
0·4
0·2
0
1
2
3
4
5
6
7
8
9
10
POSITION OF SUPPORT IN M.M. FROM NODE.

FIG. 12.

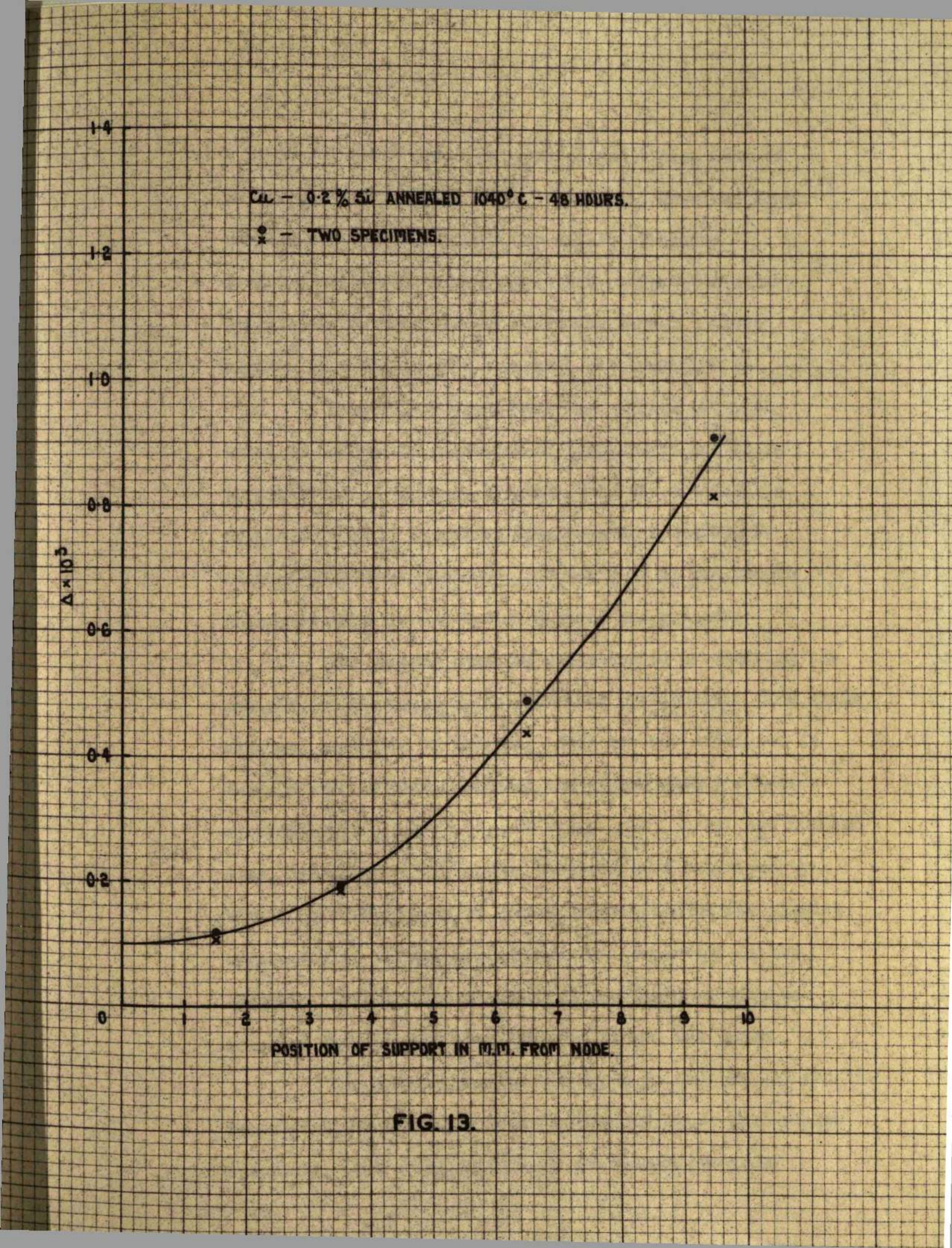
Cu – 0·2 % Si ANNEALED 1040° C – 48 HOURS.
● × – TWO SPECIMENS.
1·4
1·2
1·0
0·8
0·6
0·4
0·2
0
Δ × 10³
1
2
3
4
5
6
7
8
9
10
POSITION OF SUPPORT IN M.M. FROM NODE.

FIG. 13.

a different grain size are measured and a plot made of decrement against grain size. Randall, Rose and Zener[119] carried out this experiment for metals vibrating longitudinally and Entwhistle[120] has performed similar experiments on transversely vibrating bars. These results were all in good agreement with equation 9.

Since the present work was carried out with annealed copper the magnitude of this effect had to be investigated. A range of grain size was obtained in copper 0·2% Si by annealing specimens at temperatures between 500°C and 1040°C. Copper 0·2% Si was chosen to ensure that no dislocation damping was present.

The damping capacity was measured by altering the position of the supports as described previously. The grain size was estimated as follows. Each bar was sectioned in three places mounted, polished and etched with a solution containing 40 c.c.s NH_4OH, 10 c.c.s H_2O, 2 ml. 5o KOH and 4 ml. 12% H_2O_2. The grains observed were estimated by taking half the number of grains intersected by the viewing eyepiece plus all the grains enclosed completely in the observed field. The diameter of the field of view was measured directly and thus the area viewed was known.

The damping results are shown in Fig. 11, 12 and 13. These give the estimated true damping for three sets of two specimens, each specimen of each set having received

identical treatment.

Discussion of Results.

The minimum damping observed was given by the copper 0·2% silicon bars annealed at 500°C for one hour Fig. 11, and the average true damping is approximately 6×10^{-5}. This loss includes air damping and all other spurious losses mentioned earlier. These specimens will have virtually no microscopic loss as will be shown. The calculated macroscopic loss has been shown to be $6{\cdot}5 \times 10^{-5}$. The overlap of $0{\cdot}5 \times 10^{-5}$ must be taken as experimental error and it must further be assumed that all extraneous losses in the apparatus are negligible. Watchman and Tefft[105] noted that air damping was only $1{\cdot}5 \times 10^{-5}$ for rectangular specimens much larger than those used in the present work.

The true variation of damping observed with varying grain size is seen to be of the order of 10^{-4}, in agreement with Entwhistle[120]. This variation, however, is obscured entirely by the effect of the supports when measurements are made at position 2. It is impossible, therefore, to justify any correction term for thermo-elastic damping. The results in Table 4 below show the grain size of the specimens; resonant frequency of the effect for the measured grain size and the resonant frequency of the bar.

It can be seen from this table that the bars annealed at 1040°C should show the highest damping. It is impossible, however, to distinguish between the results obtained for the specimens annealed at 800°C and those annealed at 1040°C. The specimens annealed at 500°C however are quite distinguishable and show the lowest damping as would be expected.

TABLE 4

Annealing Treatment	Grain size sq.cms.	Calculated resonant frequency of thermo-elastic damping	Resonant frequency of bars	Range of estimated values obtained from figs. (11) (12) (13)
500°C 1 hour	$7 \cdot 08 \times 10^{-5}$	79,380 c s	1568-1588	$(5\text{-}6) \times 10^{-5}$
800°C 2 hours	$1 \cdot 6 \times 10^{-3}$	4,485 c s	1808-1830	$(11\text{-}14) \times 10^{-5}$
1040°C 48 hours	$3 \cdot 3 \times 10^{-3}$	1,710 c s	1783-1872	$(9\text{-}15) \times 10^{-5}$

These results cast doubt on the experimental accuracy. The bars which were annealed at 800°C and 1040°C were given a second anneal at 500°C to ensure that no anomalous distribution of silicon was present due to different cooling rates. The bars were then remeasured and the results were similar to those obtained before the 500°C anneal. It must be assumed, therefore, that the

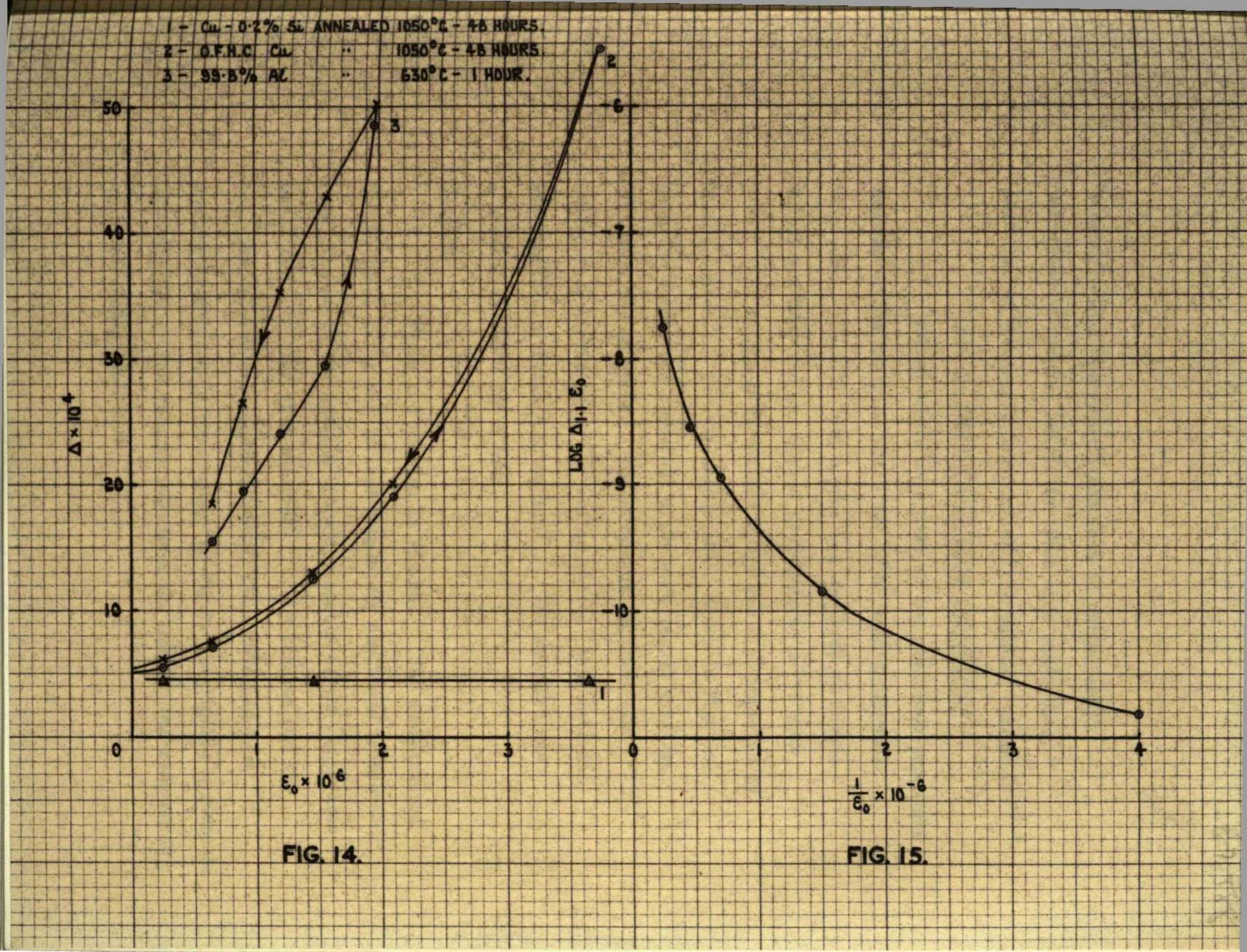
1 - Cu - 0·2% Si ANNEALED 1050°C - 48 HOURS.
2 - O.F.H.C. Cu " 1050°C - 48 HOURS.
3 - 99·8% Al " 630°C - 1 HOUR.
Δ x 10⁴
50
40
30
20
10
0
1
2
3
3
1
ε₀ x 10⁻⁶
LOG Δ₁₋₁ ε₀
2
-6
-7
-8
-9
-10
0
1
2
3
4
1/ε₀ x 10⁻⁶

FIG. 14.

FIG. 15.

damping values are correct and that an actual small variation of damping exists in these bars other than that due to transverse intercrystalline thermal currents.

INITIAL MEASUREMENTS AFTER CALIBRATION

Measurements were made on the amplitude dependent damping of the material which was to be used throughout this work. B.S.S. 1861 copper was supplied by Thomas Bolton and Sons and was stated by makers to be 99·996% pure. A copper 0·2% silicon alloy was also supplied by Thomas Bolton. For the measurements shown in Fig. 14 both the copper and copper-Si alloy were vacuum annealed at 1040°C for 48 hours. The aluminium specimen was milled from 99·80% pure $\frac{3}{16}$" rolled sheet; this material was supplied by British Aluminium. The specimen was annealed at 630°C for 1 hour.

Results

These are plotted in Fig.14. The measurements on the Cu-Si alloy are low and completely amplitude independent, remaining so to the maximum operating strain of the apparatus which is 10^{-5} for this material. The results for the B.S. 1861 copper are comparable with those obtained from the spectroscopically pure copper of Fig.7. Negligible hysteresis are observed at the strains used when the damping was remeasured with decreasing amplitude.

The aluminium showed a much larger amplitude dependent damping than copper and on re-measuring with decreasing amplitude a large hysteresis was noted, i.e. the high amplitude decrement was partially retained when the stress amplitude was reduced to lower values.

Discussion of Results.

The results obtained on aluminium are interesting and very important. It may be concluded that any measurements on the recovery of amplitude dependent damping in an aluminium bar after deformation will be affected by the measurements themselves; that is, one single bar cannot be used to give a complete recovery curve for amplitude dependent damping. This effect has already been noted and discussed in chapter 1. It is most likely that large movements of the dislocations are taking place during the high amplitude measurements of aluminium and these displaced dislocations are not returning to their original position.

The measurements obtained from the copper 0·2% silicon specimen are in agreement with the theory of impurity pinning of dislocation lines.

The amplitude dependent damping of the copper specimen appears to obey to some extent the exponential law derived by Granato and Lucke[103]. A plot was made of

$\log \Delta_H \varepsilon_0$ against $\frac{1}{\varepsilon_0}$ Fig. 15, which according to the theory should give a straight line. A straight line is not obtained and the results are very similar to those obtained recently by Niblett and Wilks[71]. These present results therefore add to the bulk already available to show that in fairly pure copper the rise in damping with measuring strain amplitude is more complicated than present theories assume.

GENERAL CONCLUSIONS

Apparatus for measuring internal friction has been constructed and calibrated. Various effects which might lead to erroneous results have been investigated fully. It is realised that the effect the support position has on the damping is a disadvantage of the apparatus. This can be virtually eliminated however by making measurements with the supports positioned at less than 2 mms. from the nodes. Such a modificiatioh, however, would require a much larger and tuneable output amplifier. Such an amplifier was not available for the present work and measurements therefore, had to be made in position 2 in order that reasonable voltages were generated in the output crystal. Measurements on annealed copper, copper - 0·2% Si and aluminium give results which are in agreement with results already published.

APPENDIX

Determination of maximum strain amplitude of a transversely vibrating bar.

The equation of motion of the bar is taken as

$$\frac{d^2y}{dt^2} + k^2c^2\frac{d^4y}{dx^4} = 0 \quad \text{.....(2)}$$

This assumes negligible rotary motion of the bar and a radius of curvature $R = \frac{1}{d^2y/dx^2}$. For a bar length l and taking x at the midpoint, then since the end conditions are $d^2y/dx^2 = 0$ at $x = \pm \frac{l}{2}$ the strain must vary from zero to a maximum at the centre of the bar. It is impossible therefore, to quote a true strain amplitude for a transversely vibrating bar and relative measurements are best given by the maximum strain amplitude i.e. at $x = 0$

A solution to the above equation is

$$y = (A \cosh mx + C \cos mx) \cos nt \quad \text{.....(10)}$$

By using a second end condition, i.e., that $d^3y/dx^3 = 0$ at $x = \pm \frac{l}{2}$ a solution is obtained for m which satisfies

$$\tan \tfrac{1}{2} ml = - \tanh \tfrac{1}{2} ml$$

For the fundamental mode it is necessary to plot $\tan \theta$ against $- \tanh \theta$ to obtain an accurate value for $\frac{ml}{2}$. This was done and gave $m = 0{\cdot}473 \text{ cms}^{-1}$

Using $y = 0$ at the nodes in equation 10 the ratio of A/C can be obtained and was found to be -.1324

For $x = 0$ at centre of the bar equation 10 can be written as

$$Y = C[-.1324 \cosh mx + \cos mx] = 0 \quad \text{.....(11)}$$

In the original derivation of equation (10) A and C are assumed constant. In order that equation 10 can be applied to the real case of bars vibrating at different amplitudes it will be assumed that A and C are constant only at any one amplitude. The various values for A and C for each amplitude are determined by inserting the measured values for Y at the midpoint in equation 10.

The radius of curvature R is obtained from the inverse of the second derivative of equation 10 and this is

$$R = \frac{1}{m^2(A - C)} \quad \text{.....(12)}$$

The strain amplitude is obtained by inserting the derived value of R in equations 13 or 14. For a transversely vibrating bar of circular cross section and radius r, the strain amplitude ε_o is given by

$$\varepsilon_o = \frac{4}{3} \cdot \frac{r}{\pi R} \quad \text{.....(13)}$$

For a bar of square cross section where b is half the thickness

$$\varepsilon_o = \frac{b}{2R} \quad \text{.....(14)}$$

Fig. (17) shows the relationship between the voltage generated by the output crystal and the observed amplitude of vibration Y and Fig. (18) gives the calculated relationship between Y and ε_o. The evaluation of ε_o is given

in Table 5.

Any Measurement of Y cms	C	A	Radius of Curvature R-Cms	Strain ε_o at X=0 for Circular Bar	Strain ε_o at X=0 for Square Bar
$3 \cdot 25 \times 10^{-5}$	$3 \cdot 76 \times 10^{-5}$	$-\cdot 496 \times 10^{-5}$	$1 \cdot 05 \times 10^{5}$	$9 \cdot 62 \times 10^{-7}$	$1 \cdot 13 \times 10^{-6}$
$7 \cdot 5 \times 10^{-5}$	$8 \cdot 64 \times 10^{-5}$	$-\cdot 114 \times 10^{-4}$	$4 \cdot 57 \times 10^{4}$	$2 \cdot 21 \times 10^{-6}$	$2 \cdot 59 \times 10^{-6}$
$1 \cdot 2 \times 10^{-4}$	$1 \cdot 38 \times 10^{-4}$	$-\cdot 132 \times 10^{-4}$	$2 \cdot 85 \times 10^{4}$	$3 \cdot 54 \times 10^{-6}$	$4 \cdot 18 \times 10^{-6}$
$1 \cdot 68 \times 10^{-4}$	$1 \cdot 94 \times 10^{-4}$	$-\cdot 256 \times 10^{-4}$	$2 \cdot 04 \times 10^{4}$	$4 \cdot 95 \times 10^{-6}$	$5 \cdot 84 \times 10^{-6}$
$2 \cdot 2 \times 10^{-4}$	$2 \cdot 54 \times 10^{-4}$	$-\cdot 336 \times 10^{-4}$	$1 \cdot 55 \times 10^{4}$	$6 \cdot 49 \times 10^{-6}$	$7 \cdot 64 \times 10^{-6}$
$2 \cdot 68 \times 10^{-4}$	$3 \cdot 08 \times 10^{-4}$	$-\cdot 408 \times 10^{-4}$	$1 \cdot 28 \times 10^{4}$	$7 \cdot 89 \times 10^{-6}$	$9 \cdot 3 \times 10^{-6}$

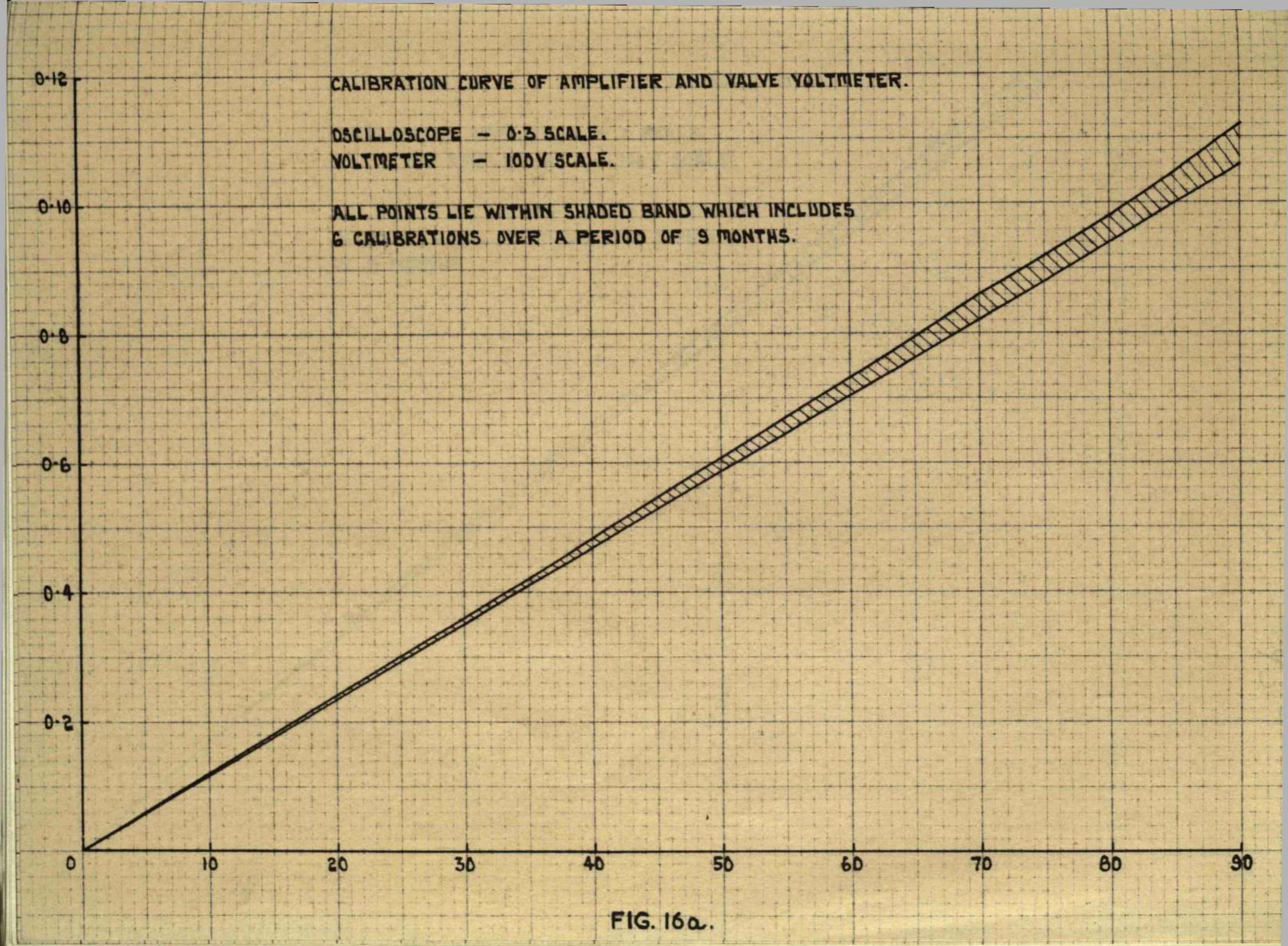
CALIBRATION CURVE OF AMPLIFIER AND VALVE VOLTMETER.
OSCILLOSCOPE – 0·3 SCALE.
VOLTMETER – 100V SCALE.
ALL POINTS LIE WITHIN SHADED BAND WHICH INCLUDES
6 CALIBRATIONS OVER A PERIOD OF 9 MONTHS.
0·12
0·10
0·8
0·6
0·4
0·2
0
10
20
30
40
50
60
70
80
90

FIG. 16a.

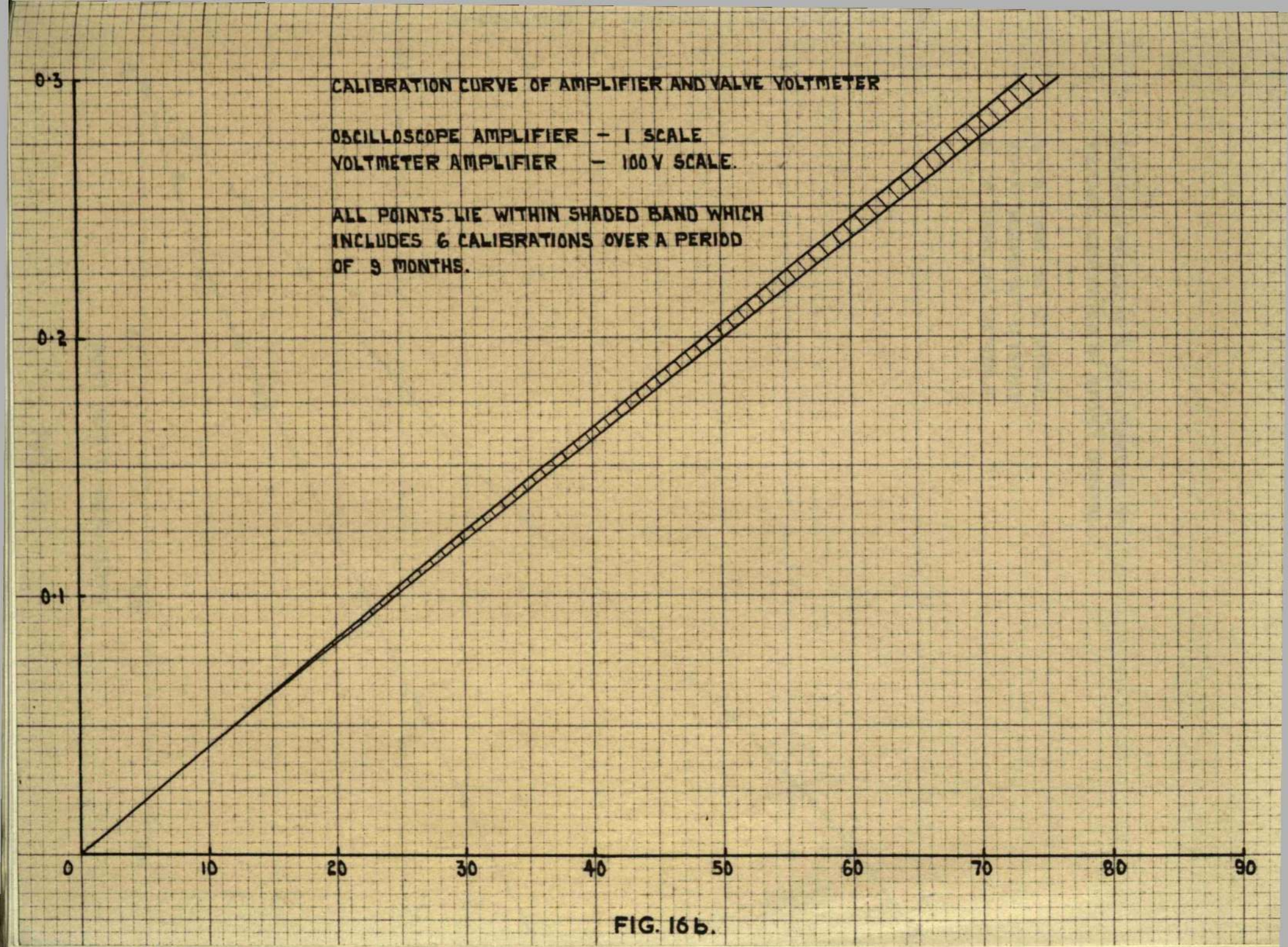
CALIBRATION CURVE OF AMPLIFIER AND VALVE VOLTMETER
OSCILLOSCOPE AMPLIFIER – 1 SCALE
VOLTMETER AMPLIFIER – 100 V SCALE.
ALL POINTS LIE WITHIN SHADED BAND WHICH INCLUDES 6 CALIBRATIONS OVER A PERIOD OF 9 MONTHS.
0·3
0·2
0·1
0
10
20
30
40
50
60
70
80
90

FIG. 16b.

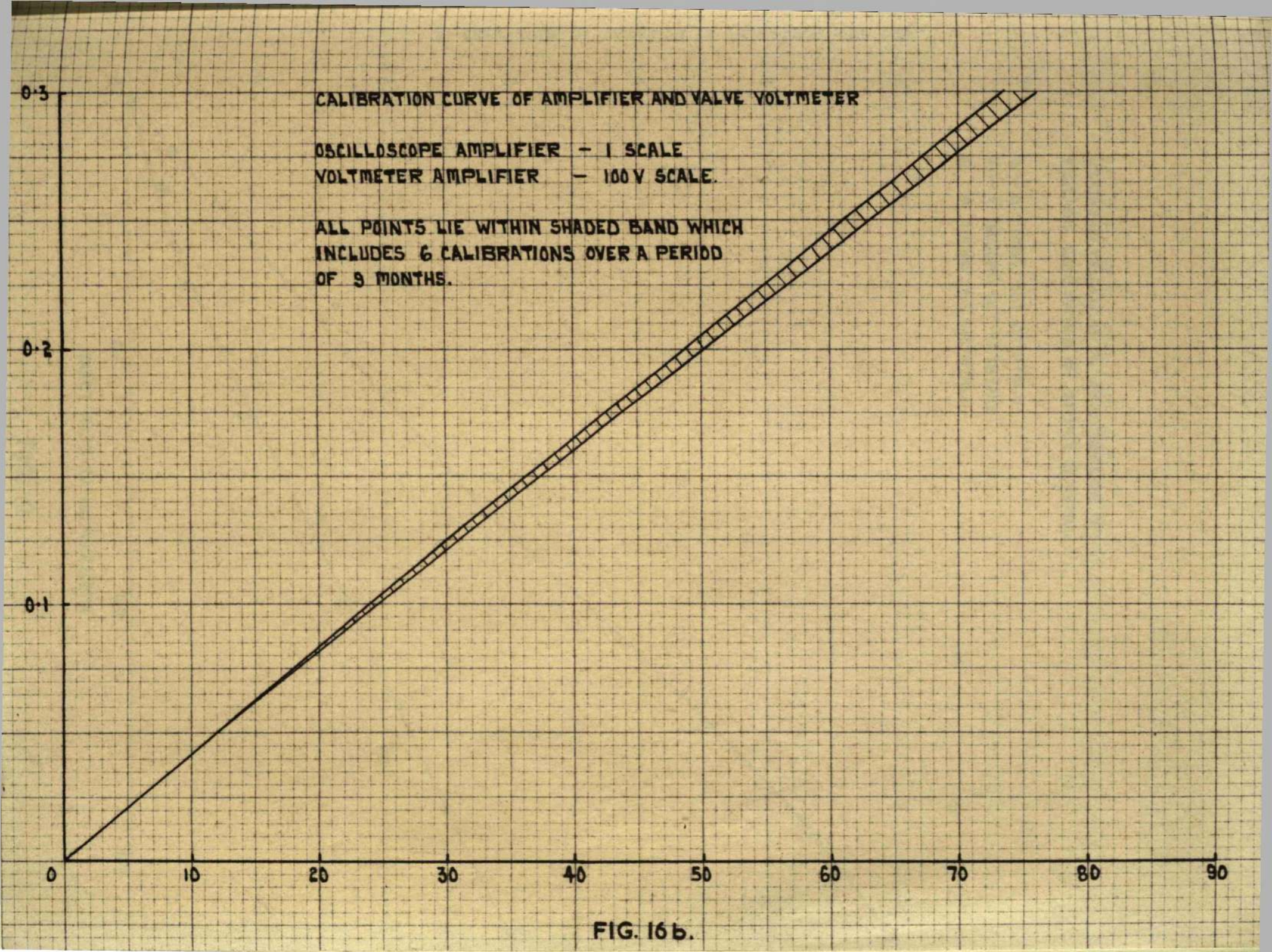
CALIBRATION CURVE OF AMPLIFIER AND VALVE VOLTMETER
OSCILLOSCOPE AMPLIFIER - 1 SCALE
VOLTMETER AMPLIFIER - 100 V SCALE.
ALL POINTS LIE WITHIN SHADED BAND WHICH INCLUDES 6 CALIBRATIONS OVER A PERIOD OF 9 MONTHS.
0·3
0·2
0·1
0
10
20
30
40
50
60
70
80
90

FIG. 16b.

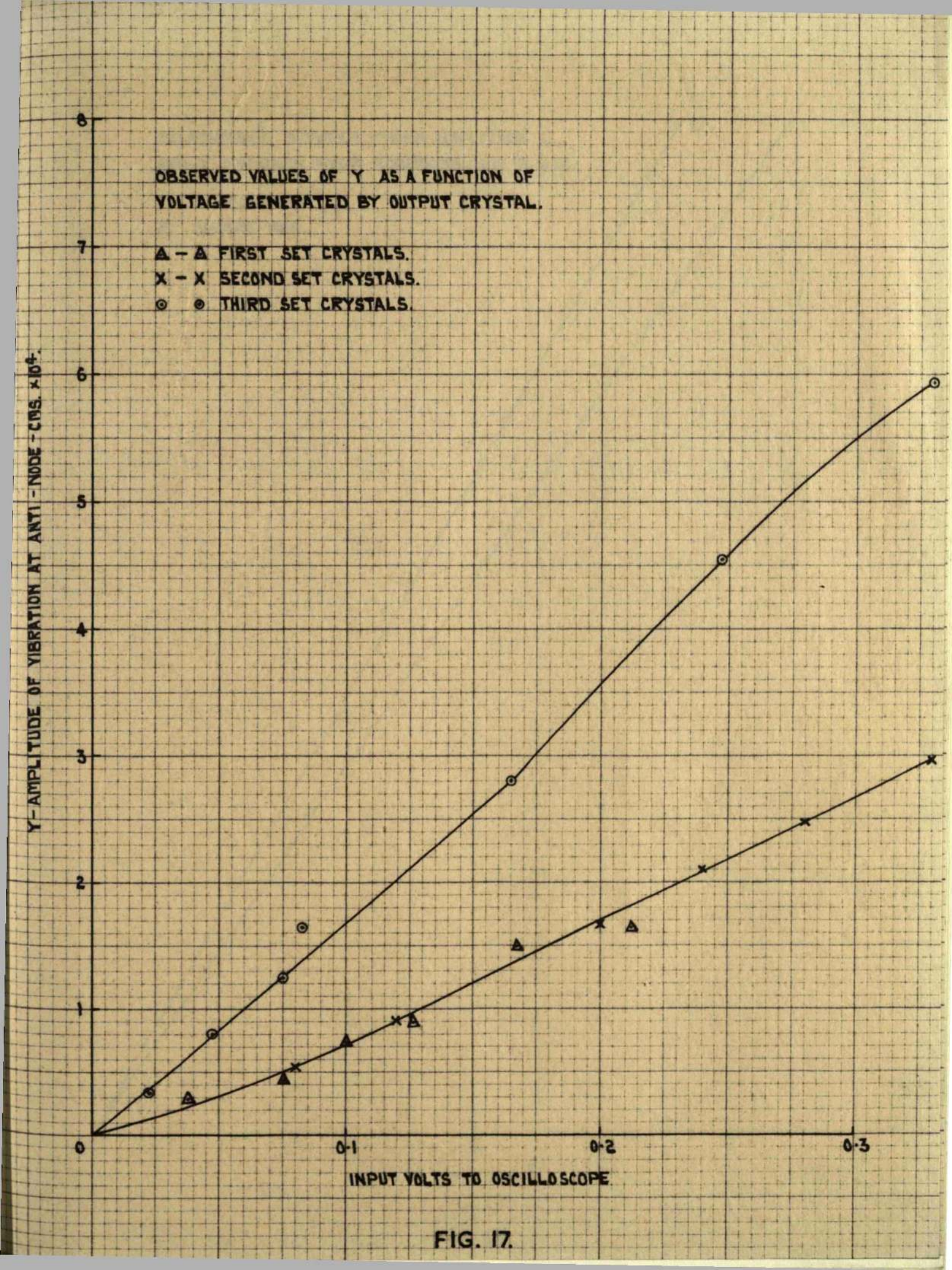
OBSERVED VALUES OF Y AS A FUNCTION OF
VOLTAGE GENERATED BY OUTPUT CRYSTAL.
△ - △ FIRST SET CRYSTALS.
X - X SECOND SET CRYSTALS.
⊙ ⊙ THIRD SET CRYSTALS.
Y - AMPLITUDE OF VIBRATION AT ANTI-NODE - CMS. ×10⁻⁴.
8
7
6
5
4
3
2
1
0
0·1
0·2
0·3
INPUT VOLTS TO OSCILLOSCOPE.

FIG. 17.

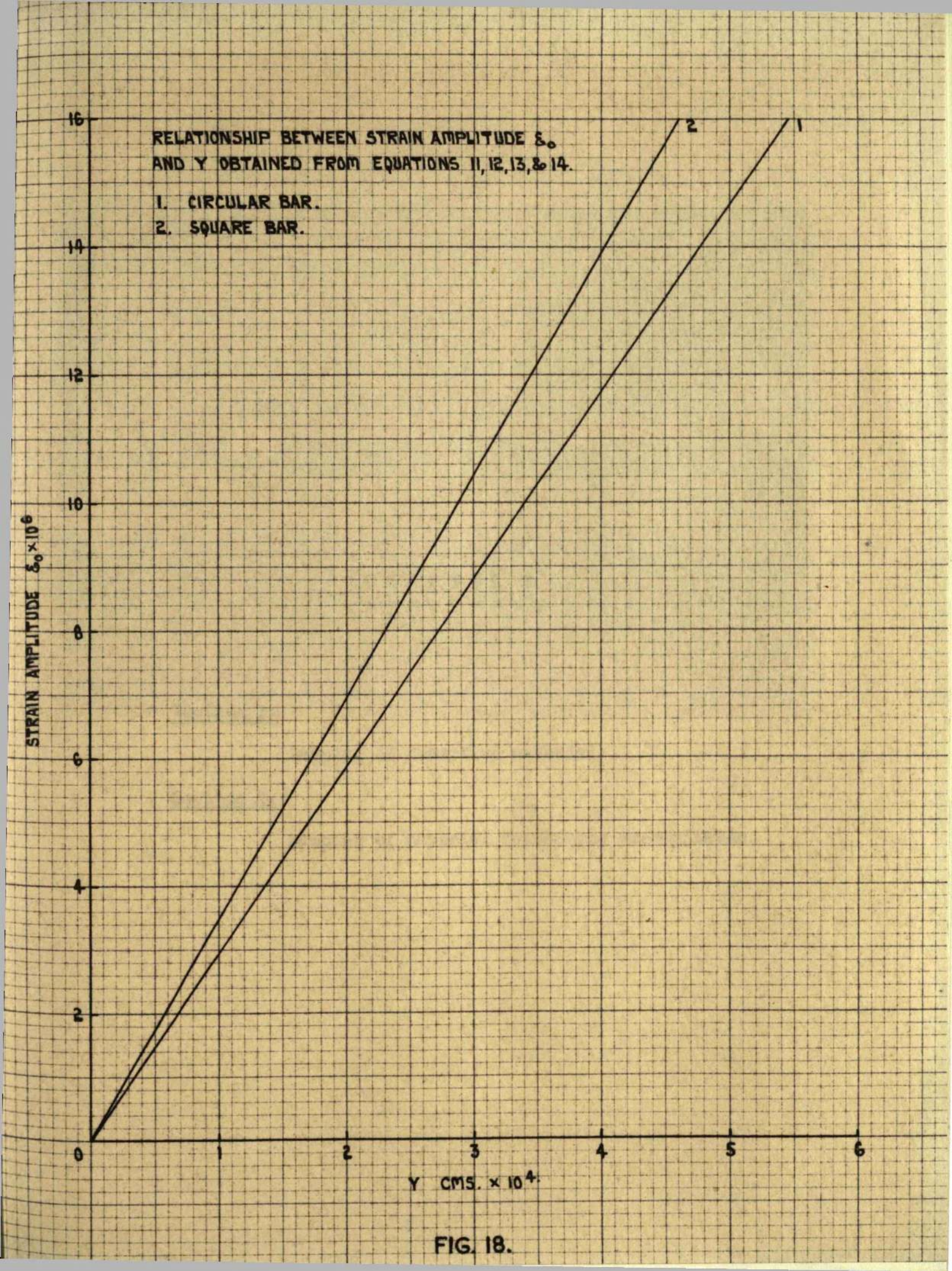
RELATIONSHIP BETWEEN STRAIN AMPLITUDE ε_o
AND Y OBTAINED FROM EQUATIONS 11, 12, 13, & 14.
1. CIRCULAR BAR.
2. SQUARE BAR.
1
2
STRAIN AMPLITUDE $\varepsilon_o \times 10^6$
16
14
12
10
8
6
4
2
0
1
2
3
4
5
6
Y CMS. $\times 10^4$

FIG. 18.

CHAPTER 3

Section 1.

Damping of defective material.

Section 2.

Damping of material containing precipitates.

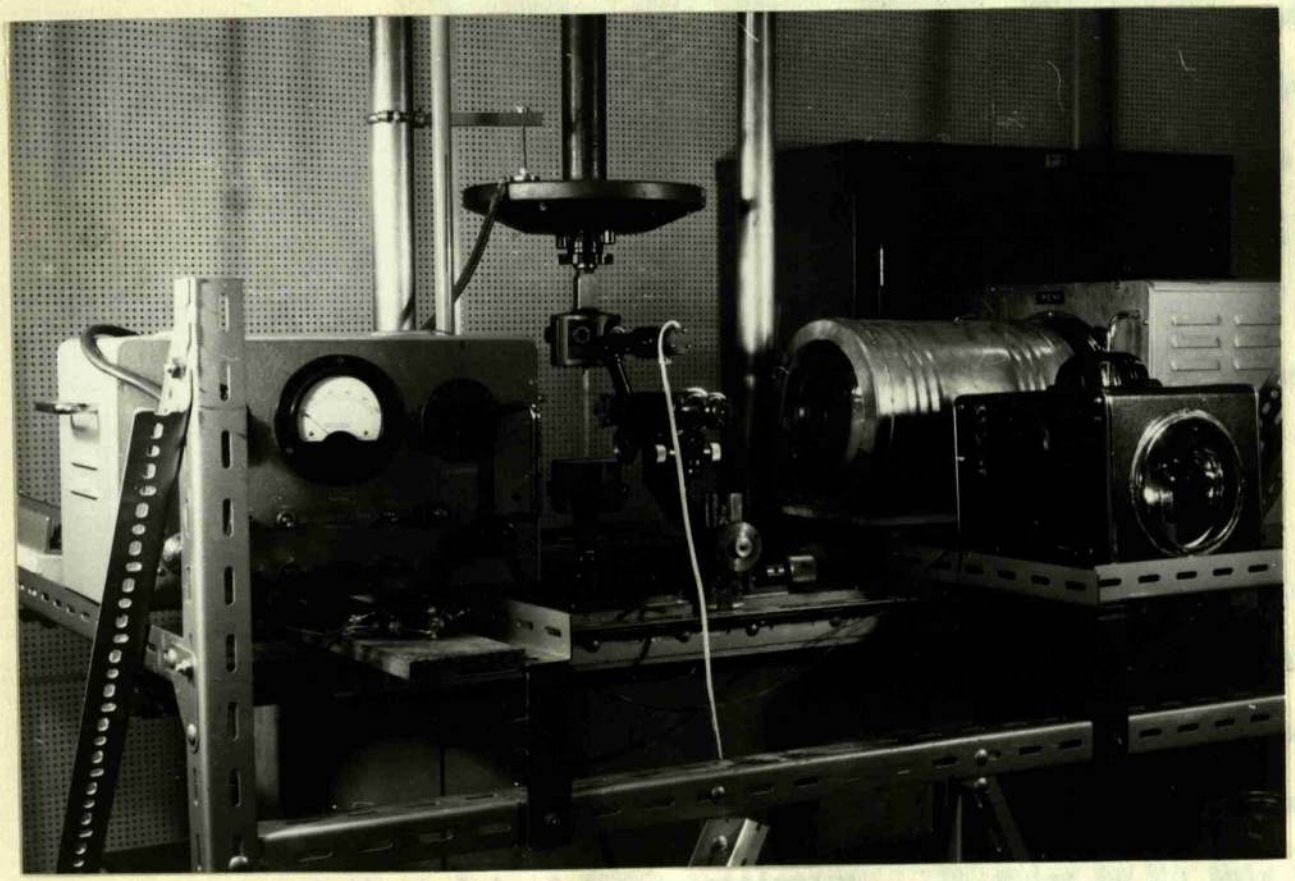

FIG. I

SECTION 1. DAMPING OF DEFECTIVE MATERIAL

Initial experiments were aimed at determining whether or not any large change occurs in the residual damping capacity of a metal which has been deformed by fatigue to the stage immediately prior to crack initiation as compared to metal with a crack initiated in it.

Experiments made to determine the effect of cavities and hot tears on damping capacity are also described.

Investigation of Fatigued Metal

The simplest method of investigating the first effect is to compare the damping capacity of metal which has been fatigued to the stage immediately prior to crack formation and compare its residual damping with specimens which have been fatigued just past the point of crack initiation. In order to do this some method must be used to localise the region in which the crack will start and also if possible by some means stop the test immediately a crack initiates. The former problem is surmounted by using specimens with a notch, which may be very small, and the latter by means of a special apparatus which will now be described and is shown opposite, Fig. 1.

Light from a stroboscope is collected by a converging lens and is then passed directly on to a reflecting glass slide in the microscope which deflects it on to the surface of the electrolytically

polished specimen being tested in a push-pull type fatigue machine. The reflected light is then viewed as in a normal metallurgical microscope. The stroboscope is fixed by a proximity meter which in turn uses the alternating capacity between a brass disc and the vibrating head of the testing machine. The stroboscope is thus synchronised with the fatigue machine and no manual adjustment is required. The vibrating specimen is then viewed as if stationary. The fatigue machine used throughout the present work is the 2-ton Amsler Vibrophore and is particularly suited for this type of work. Observations up to magnifications of 1500 are possible. During the fatigue test the surface of the metal in many cases becomes blackened by slip bands. This can make observations on crack formation difficult. This difficulty is overcome by using purely oblique illumination. To do this the light admitted to the glass slide is shut out and the stroboscopic beam which is almost parallel to the specimen surface is then reflected into the microscope by any irregularities on the specimen surface. The edges of a crack for example are readily defined by this type of illumination.

The specimens used were of 99·85% aluminium 3/16" square, and having a notch $\frac{1}{100}$" deep on two opposite faces. The specimens were annealed at 500°C. for 1.1/2 hours, after which they were electrolytically polished.+

+ The polishing procedure is described in Chapter 5.

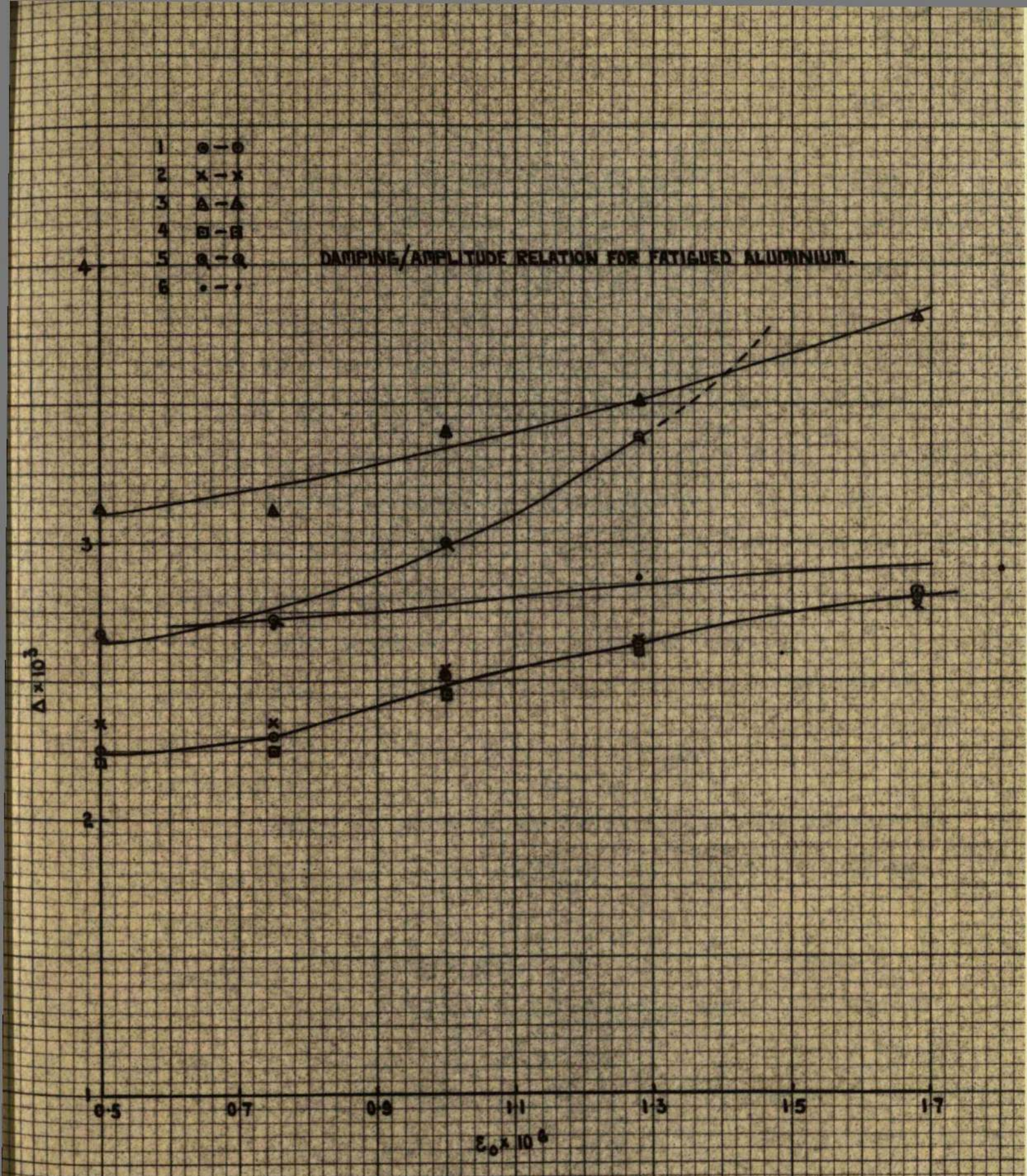
1 ●–●
2 ×–×
3 ▲–▲
4 ■–■
5 ◉–◉
6 •–•
DAMPING/AMPLITUDE RELATION FOR FATIGUED ALUMINIUM.
Δ×10³
4
3
2
1
0·5
0·7
0·9
1·1
1·3
1·5
1·7
ε₀×10⁴

FIG. 2.

It was thought that the effects of the fatigue machine clamps on the ends of the specimen would have little if any appreciable effect of the measured damping capacity since these end sections, 1·5 cms. long, both lie outside the nodes, and as was stated earlier, the ends of a transversely vibrating bar outside the nodes contribute very little to the actual damping capacity of the bar. Even so, the effect of the clamps was standardised by using a constant pressure obtained by means of a torque spanner. It was thus decided that the specimens could be fatigued and their recovered damping capacity measured without removing the ends.

After fatiguing at 5,000 cycles per minute for a specified duration the specimens were removed from the machine and left on cotton wool for four days. This ensured complete recovery of the metal.

The plots of damping against strain amplitude are shown in Figure 2 for the corresponding bars which received the following treatment.

Specimen No.	Treatment	Comments
1)	Fatigued 120,000 cycles at ± 2800 lbs/in^2	Not cracked
2)	Fatigued 140,000 cycles at ± "	Cracked at one notch
3)	Fatigued 160,000 cycles at ± "	Cracked at one notch
4)	Fatigued 231,000 cycles at ± "	Cracked at both notches
5)	Fatigued 147,000 cycles at ± "	Cracked at one notch
6)	Cold rolled and machined "	Not tested

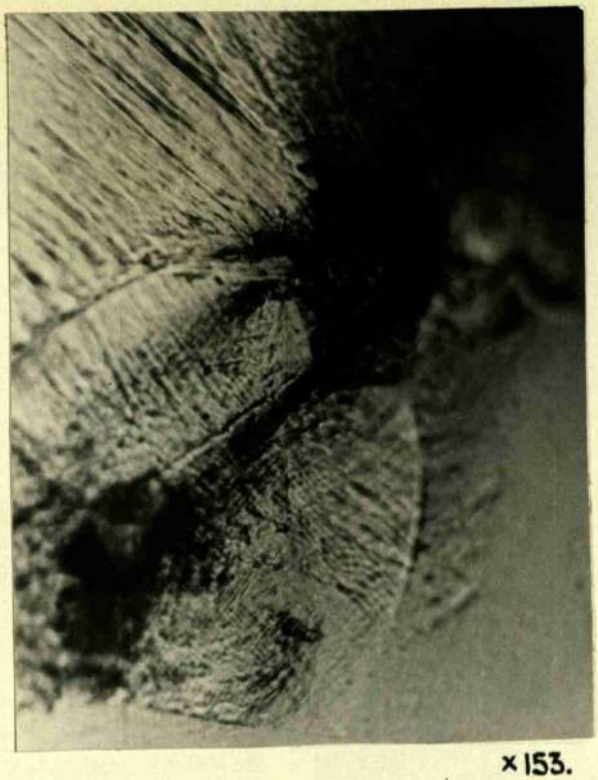

×153.

FIG. 3.

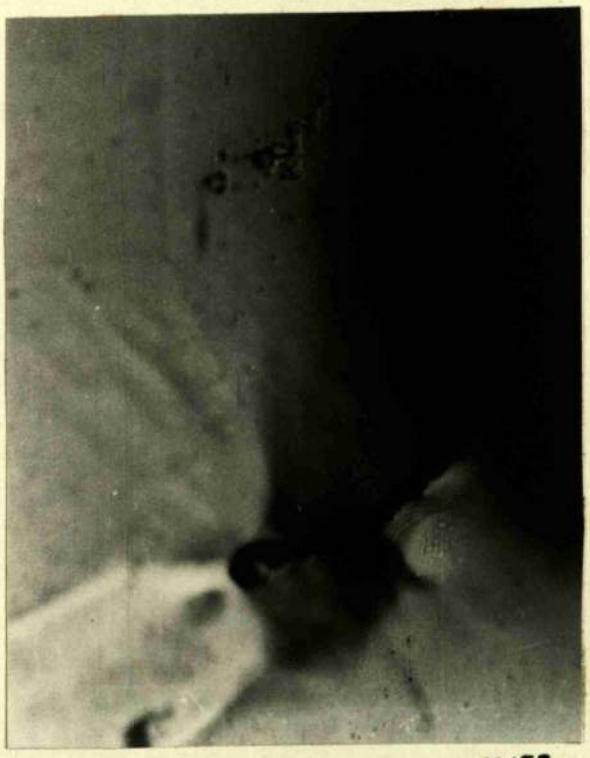

×153.

FIG. 4.

Discussion of Results

The most important feature of these results is their inconsistency. No distinction can be made between the uncracked bar fatigued for $1{\cdot}2 \times 10^5$ cycles, and for the two cracked bars fatigued at $1{\cdot}4 \times 10^5$ cycles and $2{\cdot}3 \times 10^5$ cycles. The latter bar was cracked at both notches. The results for these three bars are in fact similar to that for a hard worked machined specimen which has not been fatigued and has been included for comparison. To ensure that these specimens were in fact cracked they were given a subsequent electrolytic polish to remove slip traces and delineated grain boundaries. Photo-micrographs for specimens are shown before and after polishing in Figures 3 and 4. These show clearly the existence of a crack. The higher amplitude dependent damping of specimens 3 and 5 can not be accounted for by the existence of a crack since one of the cracks in specimen 4 possessed the longest surface trace of any bar investigated. The higher damping of these bars must result therefore from the residual dislocation damping. The residual damping due to dislocation motion for specimens subjected to fatigue has been shown by Valluri[99] to vary with the number of cycles which the material has been subjected to.

It can be concluded from the above results that the formation of a crack in fatigued metal is not accompanied by any large change in the residual amplitude dependent damping capacity of

the material. The results do indicate that the residual damping may vary with the number of cycles of stress which the specimen has been subjected to. Fromer and Murray[121] were unable to obtain any clear cut difference between a sound bar 80 inches long and a defective bar having a crack 8-10 inches in length in a transversely vibrating bar. They point out however that air damping with the large specimen size prevented the measurements from having any practical value. In a later paper Hanstock and Murray[25] show the damping of a specimen which has been cracked by fatigue to have a marked increase. The size of the crack however was much larger (approximately 3 cms long) than those investigated in the present work, and the rise in damping was most marked at strains ten times higher than the possible maximum obtainable with the present apparatus.

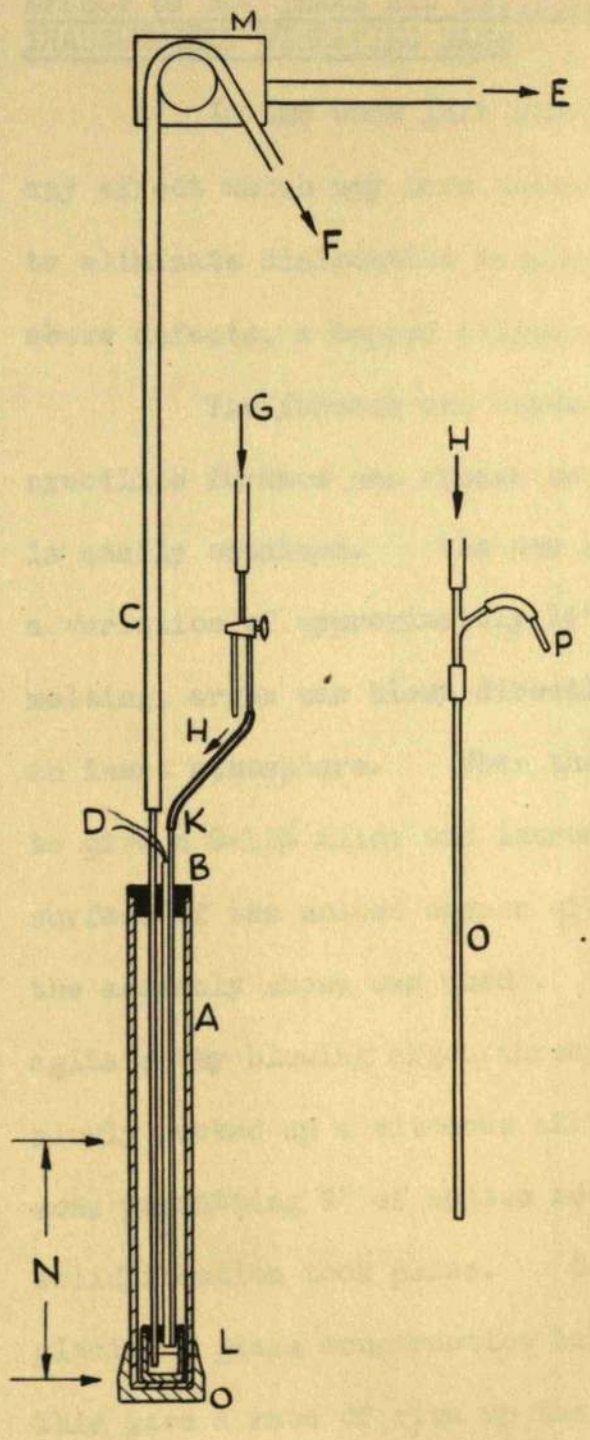

A - MULLITE TUBE
B - GRAPHITE TOP
C - RUBBER TUBE AND SAMPLING TUBE
D - THERMO COUPLE AND SHEATH
E - TO CLAMP
F - TO VACUUM PUMP
G - ARGON INLET
H - ARGON FOR BLOWING SILICON UNDER COPPER
K - ARGON FOR INERT ATMOSPHERE
L - MOLTEN COPPER
M - CLOCKWORK MOTOR
N - FURNACE HOT ZONE
O - TUBE FOR INTRODUCING SILICON
P - CONTAINER WITH SILICON

SCALE $\frac{1}{8}" = 1"$

FIG. 5.

EFFECT OF HOT TEARS AND CAVITIES ON THE DAMPING CAPACITY OF TRANSVERSELY VIBRATING BARS

In the work just discussed dislocation damping obscured any effect which may have occurred with crack initiation. In order to eliminate dislocation damping and also obtain specimens with the above defects, a copper silicon alloy was made up and cast.

The furnace and assembly used is shown in Fig. 5. A crucilite furnace was chosen because of the long hot zone which is easily obtained. The one shown gave a nine inch zone with a variation of approximately 14°C at 1100°C. During heating and melting, argon was blown directly into the crucible to give virtually an inert atmosphere. When the copper melted, sufficient silicon to give a 0·15% alloy was introduced by blowing it under the surface of the molten copper with the argon. For alloying purposes the assembly shown was used . The copper-silicon alloy was then agitated by blowing argon through the melt. The melt was then slowly sucked up a vitreous silica sampling tube, the long hot zone permitting 9" of molten metal to advance up the tube before solidification took place. Controlled suction was obtained by placing a glass construction between the pump and sampling rod. This gave a rate of rise up the tube of approximately 9.1/2" per minute. The procedure gave a good surface on the cast rods which were free from blow holes. For faster rates of suction, gas was entrapped in the rising liquid copper column making the rods useless.

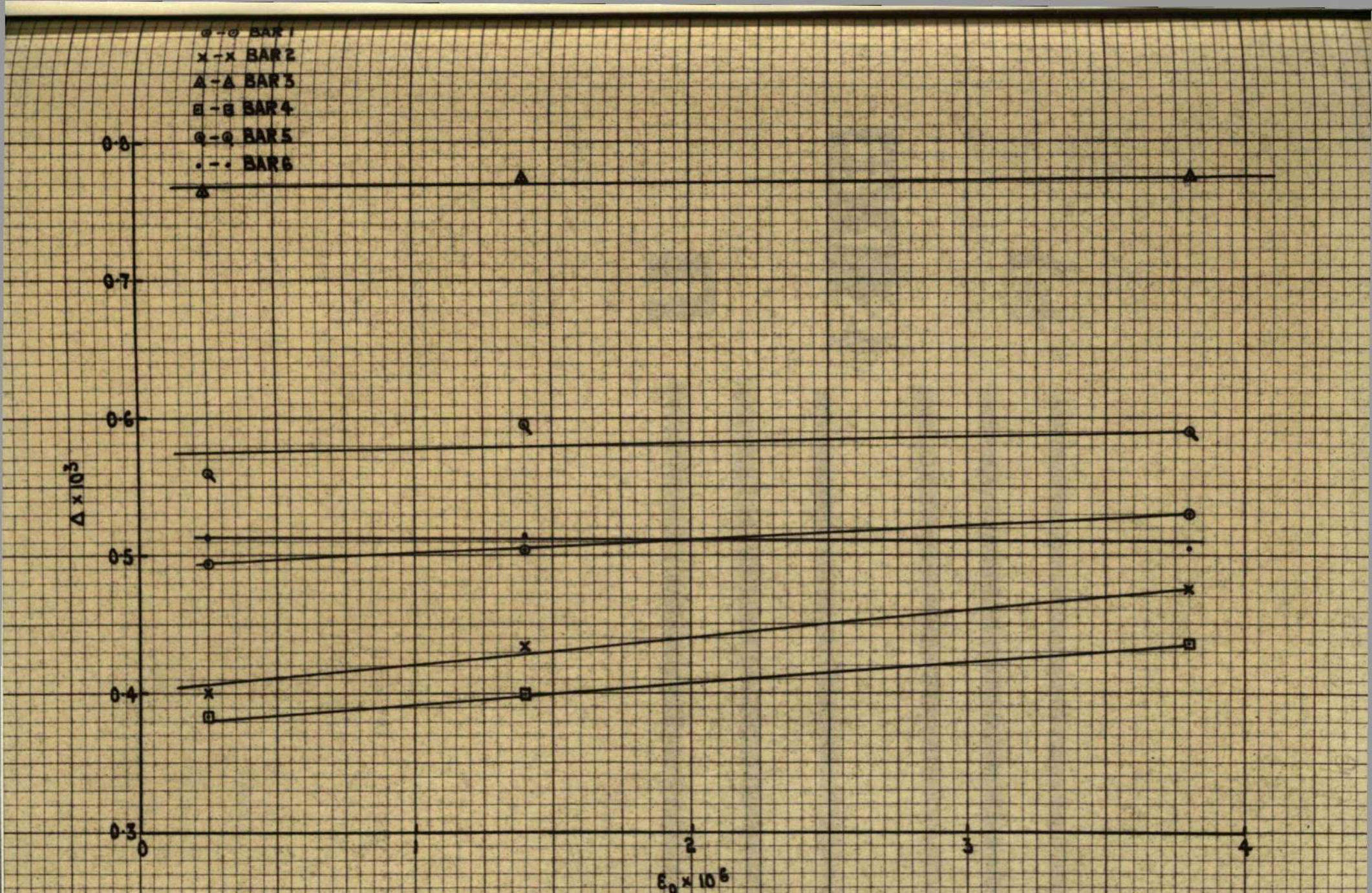
⊙-⊙ BAR 1
x-x BAR 2
Δ-Δ BAR 3
□-□ BAR 4
Q-Q BAR 5
•-• BAR 6
0·8
0·7
0·6
0·5
0·4
0·3
Δ x 10³
0
2
3
4
ε₀ x 10⁶

FIG. 6.

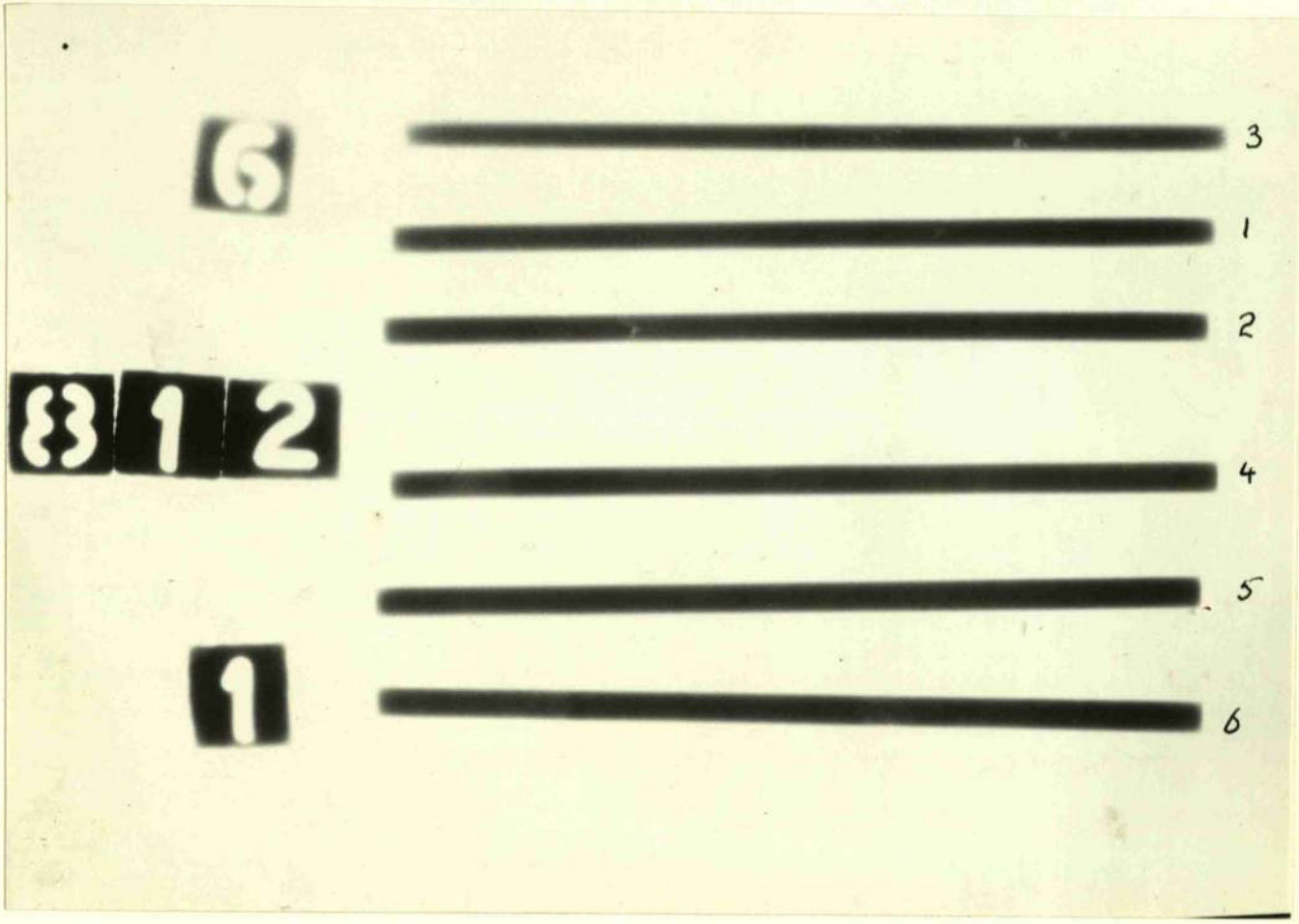

FIG. 7.

By simply lifting the sampling tube and copper column out of the furnace by hand, cooling was sufficiently rapid to give a copper rod with shrinkage cavities and hot tears. In order to cast sound rods use was made of a small clockwork motor as shown. This raised the evacuating tubing and in turn the sampking tube at 10 cms. per hour. This latter procedure gave sound copper bars which consisted of single crystals. On removal of the rods however and during subsequent machining the metal was so severely stressed that recrystallisation always took place. After solidification the rods were machined to 3/16" diameter by 10 cms. long. These bars were then annealed at 500°C for one hour to remove stresses caused by machining.

Results

The plots of damping capacity against strain amplitude are shown Fig. (6) for three sound rods and three defective rods. The bars were X-rayed, a print of which is shown in Fig. (7). As can be seen from this photograph, the three quickly cooled bars were all defective with specimen number (3) showing the greatest number of defects. This specimen also gave the highest damping results. Since any rise in internal friction in the case of defects is due to the rubbing of surfaces any damping due to this effect should be independent of amplitude. The relatively high amplitude dependent damping of specimen (3) agrees with this. It

is impossible to make any distinction between the other five specimens, and it must be concluded that either there were insufficient defects between the nodes of specimens (1) and (2) or that the effect of the support position obscured any small differences in their damping values.

Fromer and Murray[121] obtained excellent indication of the presence of porosity by damping measurements. However, their specimens were suspended at the nodes and a torsional mode of vibration was used. In this case relative motion between adjacent planes perpendicular to the ones of the specimen produces shear and thus good dissipative forces in cracks in that plane. With transverse vibrations however the paraxial filaments of the bar act independently and therefore affect the damping much less. It is of help to know that only in the case of extremely defective bars will the damping measurements be influenced to any extent, and since all the recovery work is made on extruded material, it is unlikely that any variation in future damping measurements will be due to internal defects.

SECTION 2. EFFECT OF PRECIPITATES ON INTERNAL FRICTION

At the start of this part of the work it was thought that a non-coherent precipitate might give rise to anomalous damping measurements other than those arising from dislocation motion. As will be shown, dislocation damping predominated over any other type. The results however in the light of dislocation theory proved most interesting. Use was made of the process of internal oxidation to obtain a non-coherent precipitate in a copper -0·2% silicon alloy.

Experimental Work

To determine the effect of the precipitate on the damping of copper, specimens of O.F.H.C. copper were also given an internal oxidation treatment. The result of this was simply to load the pure copper with oxygen without forming any scale or internal cuprous oxide.

To ensure a uniform grain size, all the specimens were vacuum annealed for 48 hours at 1040°C before internal oxidation.

All specimens were measured after vacuum annealing, then after internal oxidation.

Internal Oxidation Procedure

A low partial pressure of oxygen was obtained by containing the specimens in a copper cylinder 1.3/4" diameter by 1? cms. long, half filled with a mixture of equal amounts of cuprous oxide and

copper powders. This mixture gave a pressure of oxygen just below that required to form a layer of cuprous oxide in copper. One end of the tube was sealed by a close fitting copper disc brazed with a high melting α brass. The other end was sealed by thin copper foil, carefully shaped to fit tightly over the end of the tube. This in turn was tightly secured by copper wire. The copper powder used was 50 mesh and the cuprous oxide 200 mesh.

Because welding occurs between the copper and the copper powder during treatment the specimens had to be rested on a very thin porous refractory platform which, in turn rested on the oxidising mixture. The specimens were prevented from rolling together by small alundum shapes.

A temperature controlled platinum wound furnace was used for the internal oxidation experiments. The furnace had a 12.1/2 cms. long hot zone with a mean temperature deviation of $\pm$16°C. Two treatments were used for the Cu-0·2% Si material, These were:- 72 hours at 900°C for the partially oxidised specimens and 100 hours at 950°C for the fully oxidised specimens. These times and temperatures were decided upon by using equation (1) Chapter 1, Section 2. The depth of penetration of the oxidised region was measured on the microsections of several partially oxidised specimens and was found on the average to be 0·13 cms.

The pure copper specimens were given one treatment only

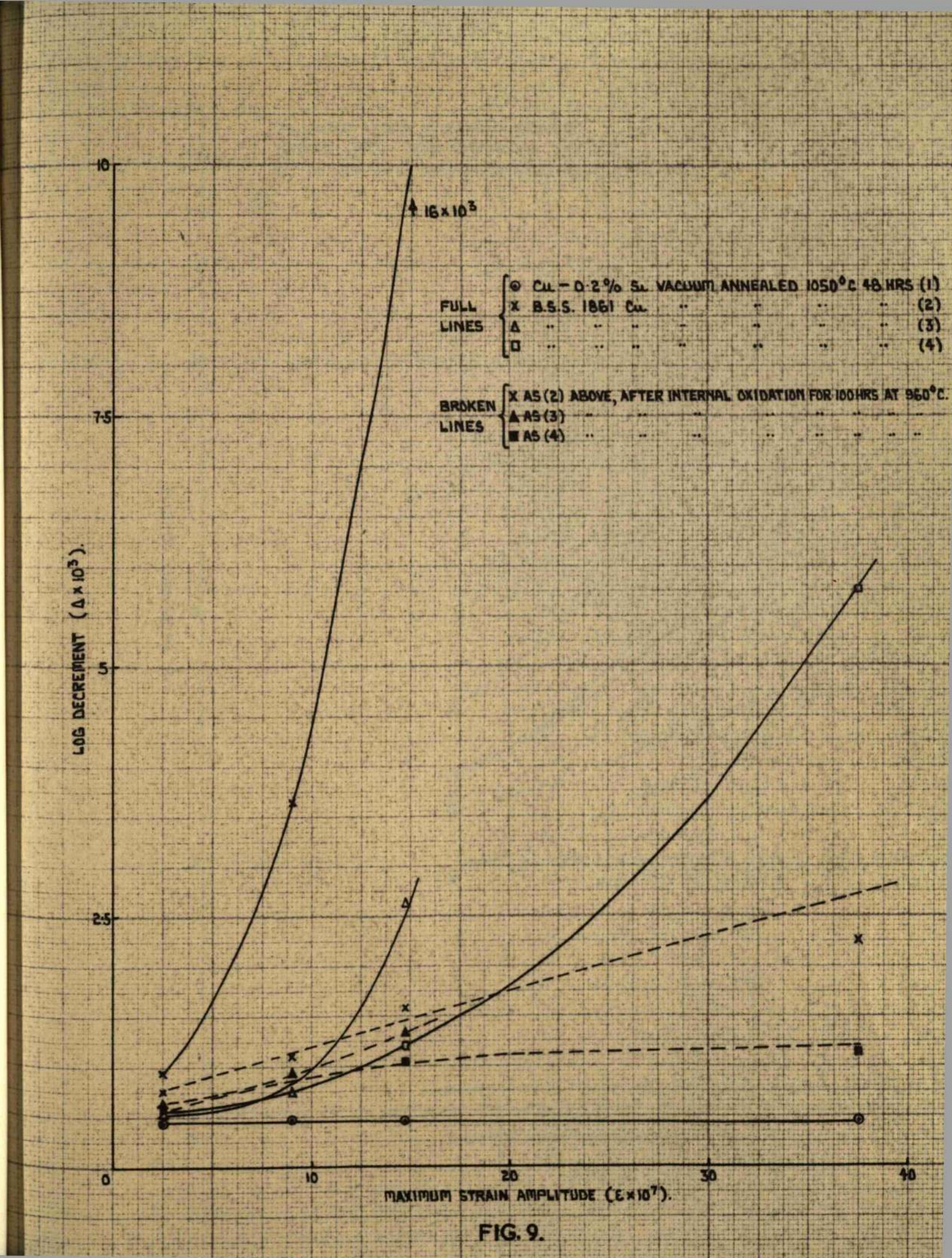
10
7·5
5
2·5
0
10
20
30
40
16 × 10³
LOG DECREMENT (Δ × 10³).
MAXIMUM STRAIN AMPLITUDE (ε × 10⁷).
FULL LINES
⊙ Cu – 0·2% Si. VACUUM ANNEALED 1050°C 48 HRS (1)
× B.S.S. 1861 Cu. .. .. (2)
Δ .. .. (3)
□ .. .. (4)
BROKEN LINES
× AS (2) ABOVE, AFTER INTERNAL OXIDATION FOR 100 HRS AT 960°C.
▲ AS (3) .. ..
■ AS (4) .. ..

FIG. 9.

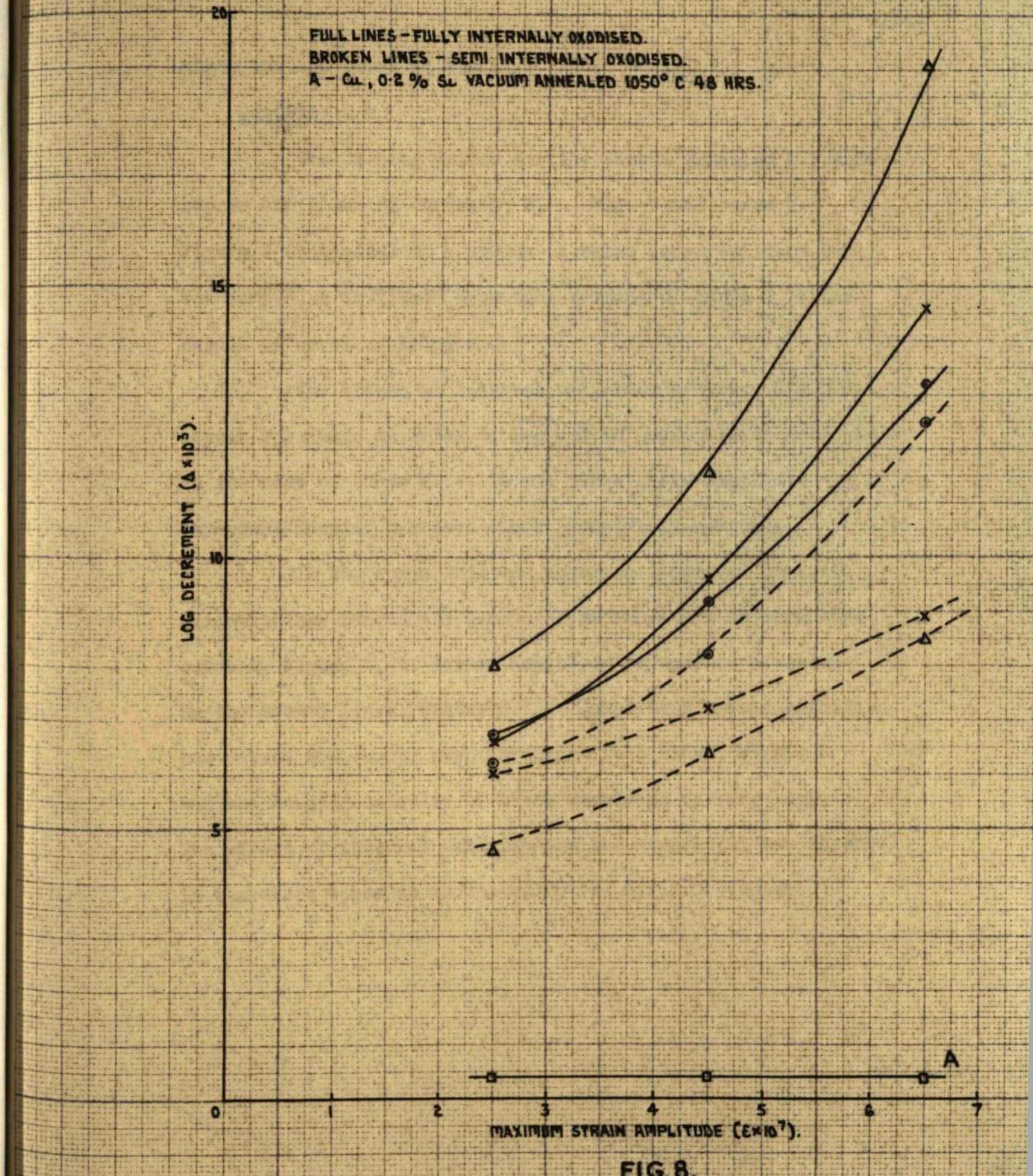
FULL LINES – FULLY INTERNALLY OXODISED.
BROKEN LINES – SEMI INTERNALLY OXODISED.
A – Cu., 0·2 % Si. VACUUM ANNEALED 1050° C 48 HRS.
LOG DECREMENT (Δ×10³).
20
15
10
5
0
1
2
3
4
5
6
7
A
MAXIMUM STRAIN AMPLITUDE (ε×10⁷).

FIG. 8.

which was 100 hours at 950°C.

Results

The damping values for the vacuum annealed O.F.H.C. copper are given by curves 2, 3, 4, Fig. 9 and curve 1. Figure 8 is typical of a vacuum annealed copper-silicon bar. The very high amplitude dependent damping of curve 2 is the result of careless handling.

The effect of internal oxidation of these O.F.H.C. copper specimens is quite marked and is particularly noticeable in the case of curve 2. In the three cases amplitude dependent damping has been almost completely removed.

In the copper-silicon specimens, partial internal oxidation has raised the damping from amplitude independence, curve A, Figure 8, to marked amplitude dependence as shown by the broken lines, Figure 8. Complete internal oxidation has raised the curves even further - full lines, Figure 8 - and the damping capacity of these specimens is very high. The effect of internal oxidation on the copper-silicon material is therefore opposite to the effect on O.F.H.C. copper.

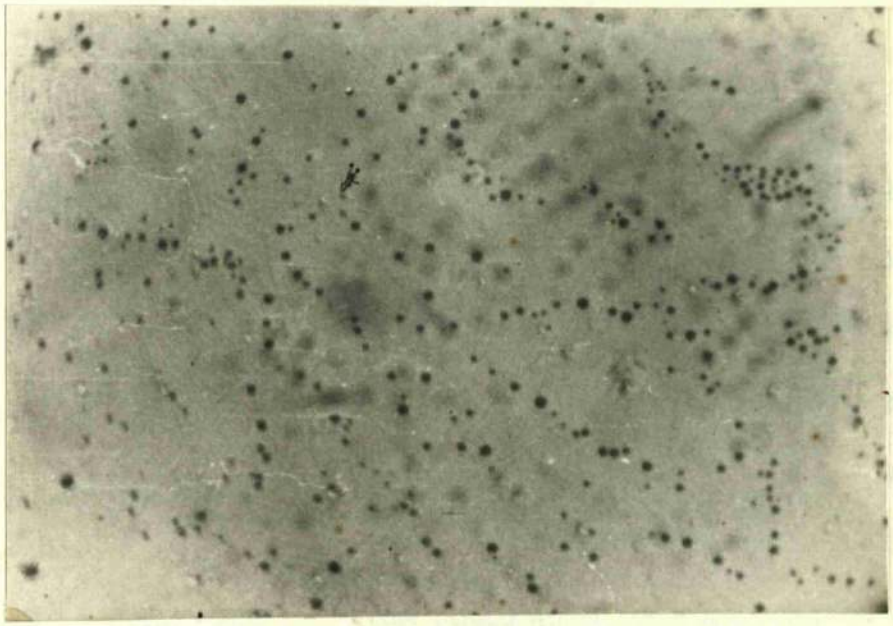

INTERNAL OXIDATION PRECIPITATE IN AN
·2% Si ALLOY TREATED AT 950°C FOR 100 HRS
X 500 (x3)

DISCUSSION

Perhaps the most significant difference between the fully internally oxidised copper-silicon specimens and the fully internally oxidised O.F.H.C. copper is the presence of silica particles in the former, since no oxide particles were found within the O.F.H.C. copper. The amount of oxygen present in the O.F.H.C. copper specimens, after internal oxidation, will probably be greater than in the internally oxidised copper-silicon alloy since in the latter case the oxidation front advances slowly while precipitation is taking place. It will be observed, however, that the damping values obtained for the internally oxidised copper-silicon alloy are higher than those for the vacuum annealed O.F.H.C. copper. Thus, the different amounts of oxygen present in the two sets of specimens cannot account for the high damping values of Fig. 8. The high amplitude dependent damping of the copper-silicon specimens must be a direct result of the presence of silica particles. The decrease in damping capacity, on internal oxidation of annealed O.F.H.C. copper is just as expected due to the pinning effect of oxygen on the dislocation lines.

The amplitude dependent results shown in Fig. 8 are characteristic of dislocation damping. It appears, therefore, that in some way, the silica particles are assisting in the formation of many loosely pinned dislocations. Shear stresses can develop round

a growing particle in a solid and also during cooling when different rates of contraction between the particle and matrix exist. These stresses can in turn create dislocations.

Parasnis and Mitchell[129] have observed this effect in crystals of silver chloride. In this case, large particles of what is assumed to be silver are surrounded by systems of decorated prismatic dislocation loops, figures of eight and concentric helical dislocations. It is demonstrated that the space required for the separation of further silver atoms upon silver particles inside the crystal is made available by the formation of the above types of dislocations and their subsequent glide. During cooling of silver chloride containing glass spheres, Jones and Mitchell[130] have noted that systems of prismatic dislocations can be created round the glass spheres. In metal, by direct observation of etch pits, Holden[123] has shown that large numbers of dislocations are generated round precipitates formed in an iron-carbon-silicon alloy; these are believed to arise from the shear stresses developed round the particles during cooling of the alloy. Huggins[122] has shown mathematically that large shear stresses can be caused by the anisotropic expansion or contraction of a precipitate in an isotropic matrix.

In the present work the shear stresses arising during growth of the silica particles and also during cooling may well create new dislocations round the particles and also free

lengths of dislocations which were already in the lattice simply by tearing them away from impurity pinning points. Such a sequence of events would partly explain the high amplitude dependent damping results shown in Figure 8.

The explanation given by Granato and Lucke[51] to account for the increase in damping after precipitation or internal oxidation is therefore oversimplified. The increased damping caused by precipitation will probably be due to a combination of three mechanisms, namely, a decrease in dissolved impurity or alloying element, the creation of dislocations round precipitates and the freeing of pinned dislocations by shear stresses in the vicinity of the precipitates.

C H A P T E R 4

Damping recovery after fatigue.

Experience gained while carrying out the work of Chapter 3 showed that experiments aimed at determining the mechanism of damping recovery after fatigue might be the most profitable method of investigating fatigue failure by internal friction, since it is possible that the process occurring during recovery would also be occurring during fatigue itself. The following experiments were aimed at determining the nature of this recovery process.

Experimental Procedure

The following work was carried out on O.F.H.C. copper vacuum annealed at 900°C for $1\frac{1}{2}$ hours, hard worked copper, and on 99·8% pure aluminium vacuum annealed at 500°C for $1\frac{1}{2}$ hours.

Copper The specimens were cut to 15 cm. lengths of 3/16" diameter rod and then annealed. After clamping in the fatigue machine a final alternating stress $\pm$ 10,680 lbs/in^2 was allowed to build up about a mean static stress of -480 lbs/in^2. The building up period of the stress was $0{\cdot}5 \times 10^5$ cycles after which fatigue was allowed to continue for a further 10^5 cycles. The stress mentioned is not exact since a slight belling of the specimen occurred; this was detected with the arrangement shown in Fig. 1 chapter 3. This slight belling was present in all the annealed specimens and was due to their dimensions and softness. The life of these specimens was approximately $2{\cdot}2 \times 10^6$ cycles and the given treatment therefore

LOW TEMPERATURE MEASUREMENT BOX

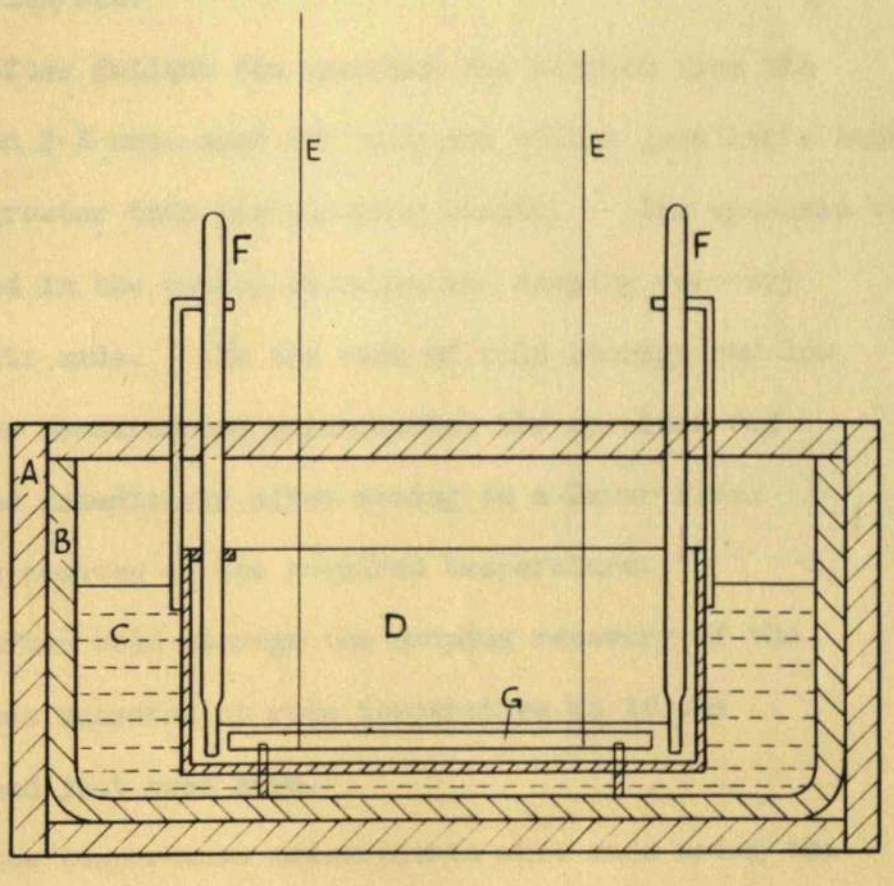

SCALE : 1" = 2"

A – FELT
B – GLASS TANK
C – ACETONE
D – COPPER JACKET
E – COTTON THREADS TO CRYSTALS
F – THERMOMETERS
G – SPECIMEN

FIG. 1.

amounted to just less than 5% of the fatigue life. The use of larger stresses gave rise to excessive belling of these specimens. The speed used for the tests on copper was 90 cycles/sec.

After fatigue the specimen was removed from the machine and 2·5 cms. sawn off each end with a jeweller's hacksaw. This was greater than the clamping length. The specimen was then placed in the cotton stirrups and damping recovery measurements made. In the case of cold storage and low temperature measurements experiments, the specimen was transferred immediately after sawing to a Dewar flask containing acetone at the required temperature.

After cold storage the damping recovery of the material was measured at room temperature as if the specimen had just been sawn.

Low temperature measurements were made using the low temperature box shown in Fig. 1. The thermometers gave the same temperature inside the copper jacket as in the acetone reservoir outside. These thermometers read just over 1°C high as they were not totally immersed. Transfer of the specimen from the Dewar flask into the copper jacket took approximately 30 seconds. The rise in temperature of the bar during this period is now known; however, initial measurements were not made for a further five minutes to give the temperature of the bar time to stabilise.

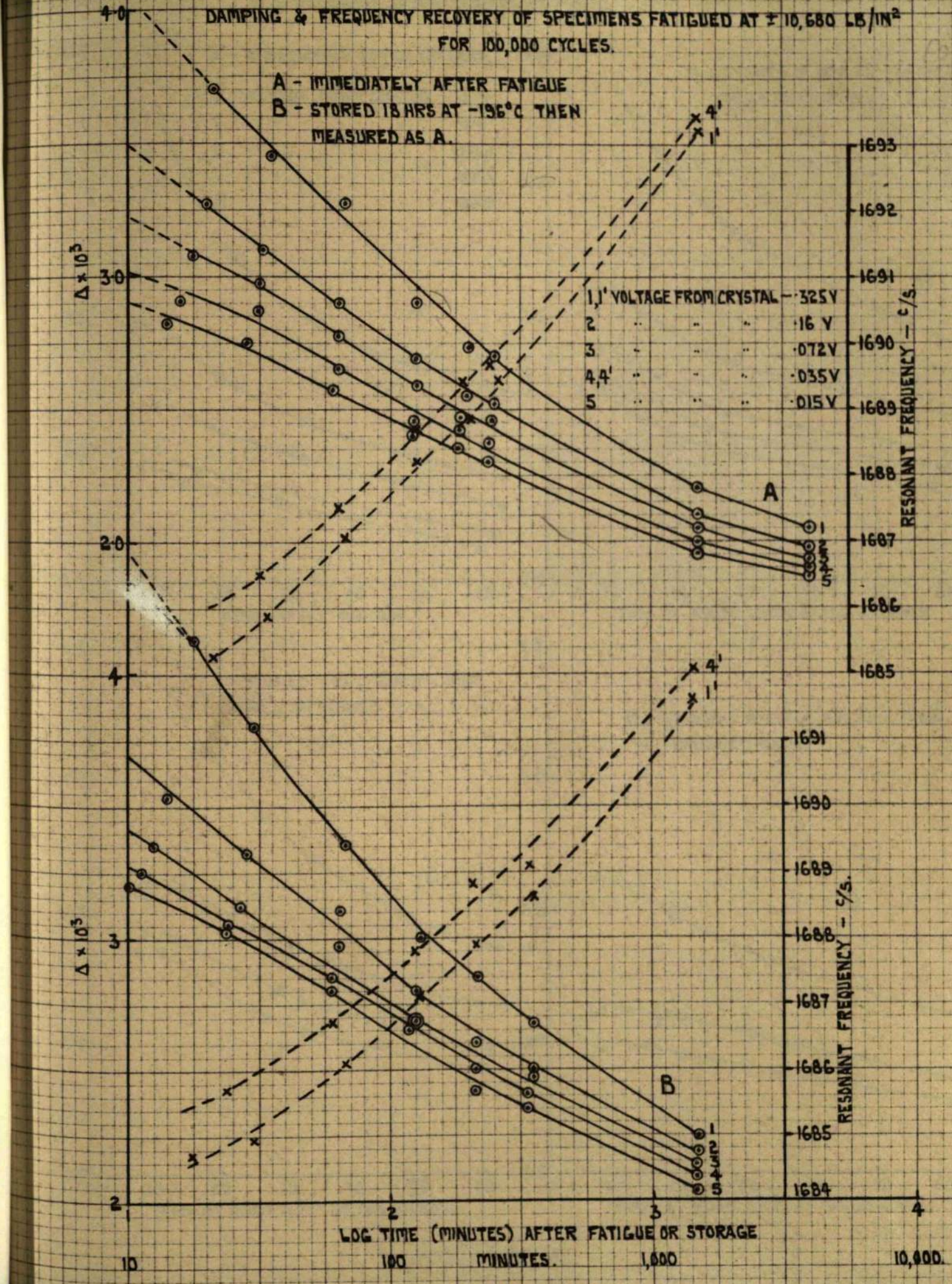
DAMPING & FREQUENCY RECOVERY OF SPECIMENS FATIGUED AT ± 10,680 LB/IN² FOR 100,000 CYCLES.
A - IMMEDIATELY AFTER FATIGUE
B - STORED 18 HRS AT -196°C THEN MEASURED AS A.
1,1' VOLTAGE FROM CRYSTAL - ·325V
2 " " " ·16 V
3 " " " ·072V
4,4' " " " ·035V
5 " " " ·015V
Δ x 10³
RESONANT FREQUENCY — c/s.
A
B
LOG TIME (MINUTES) AFTER FATIGUE OR STORAGE
10
100
MINUTES.
1,000
10,000.

FIG. 2

Δ - RECOVERY AFTER STORAGE AT −196°C, −40°C, −2°C.

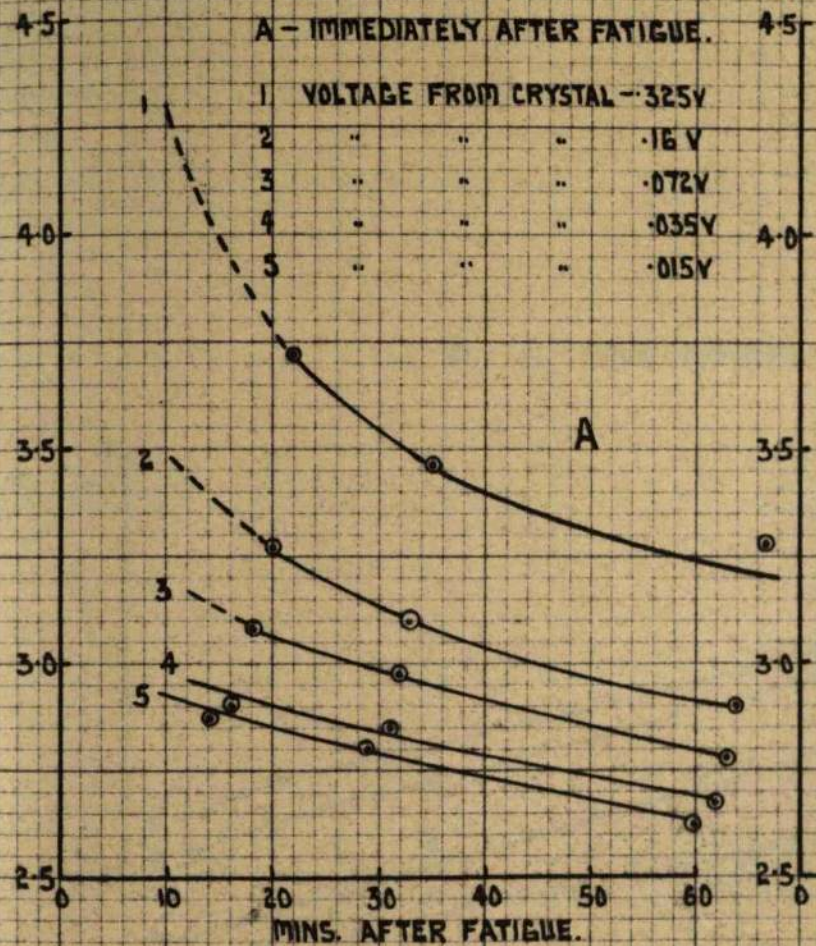

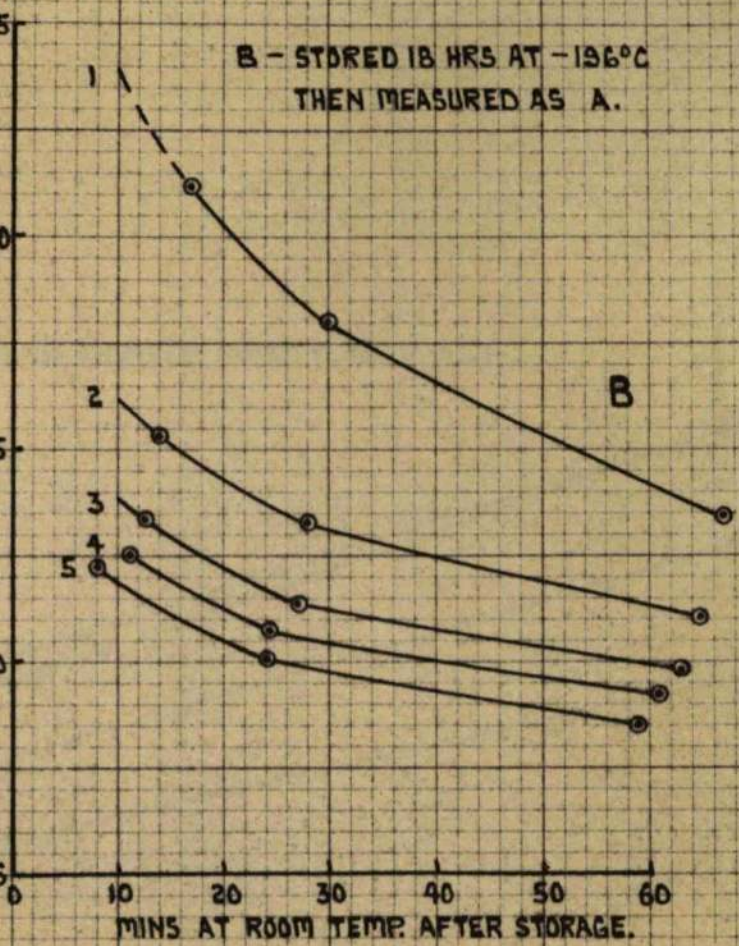

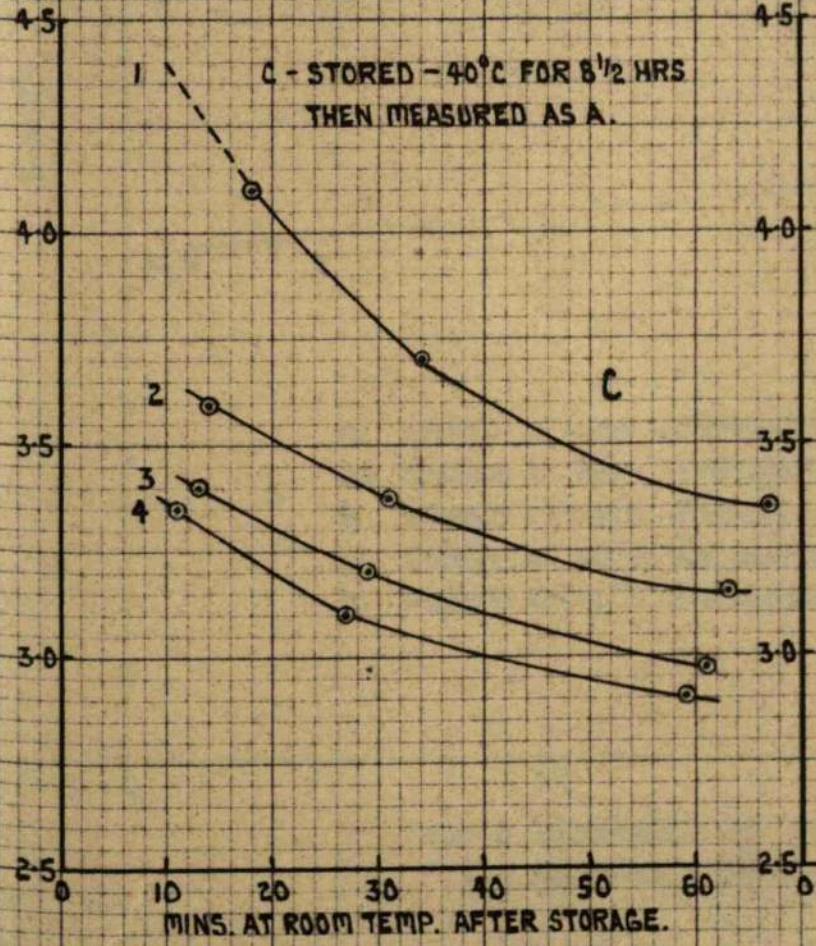

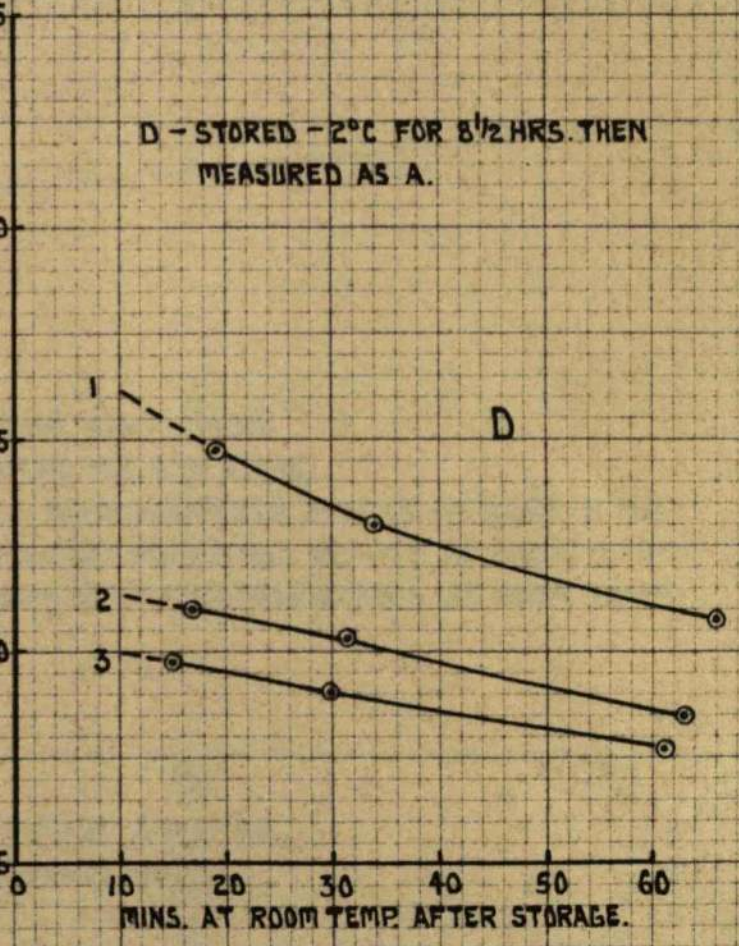

FIG. 3ABCD.

$\Delta - \varepsilon_0$ RELATIONSHIPS AS DERIVED FROM FIGS A,B,C,D.

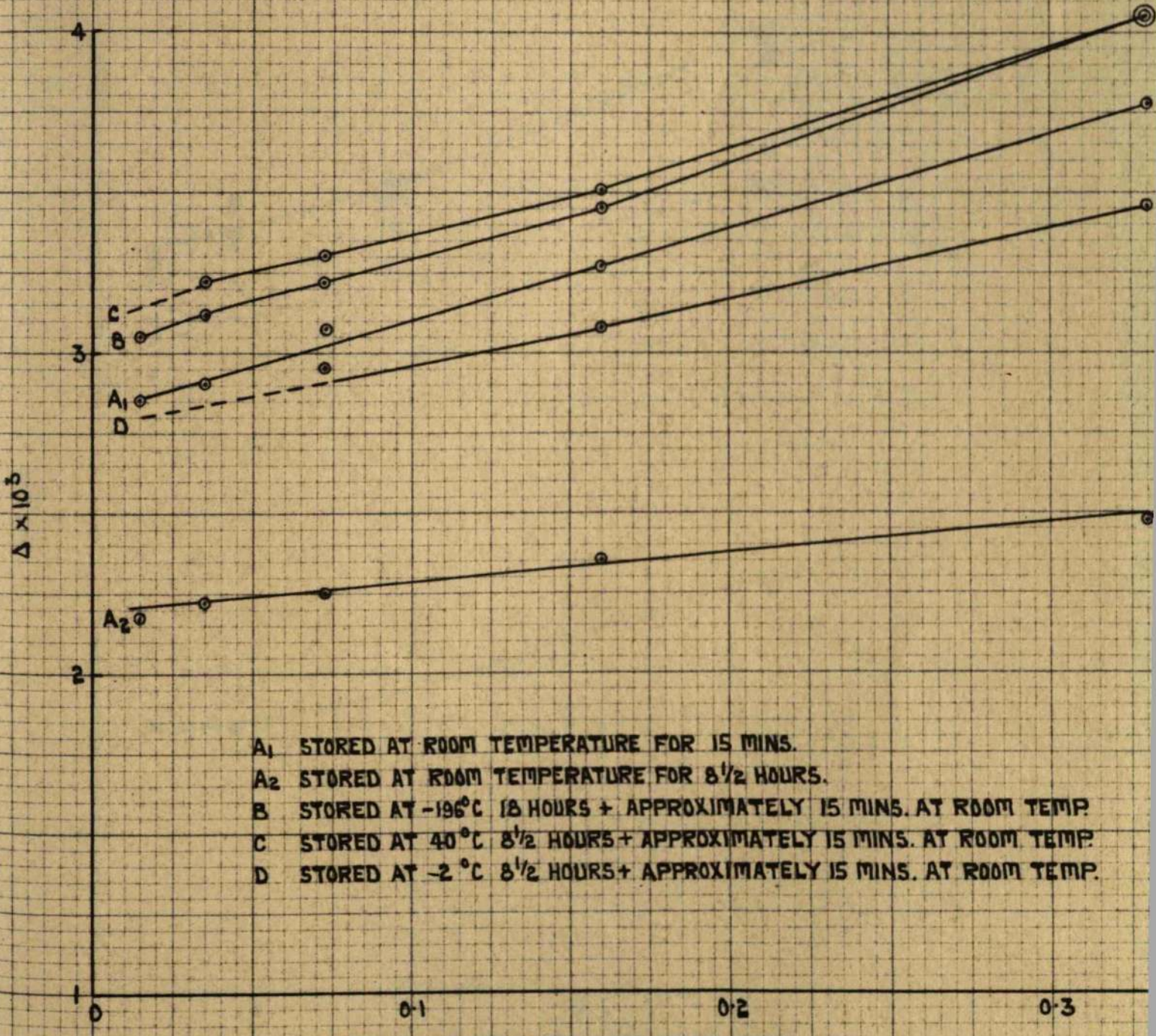

A_1 STORED AT ROOM TEMPERATURE FOR 15 MINS.
A_2 STORED AT ROOM TEMPERATURE FOR 8½ HOURS.
B STORED AT -196°C 18 HOURS + APPROXIMATELY 15 MINS. AT ROOM TEMP.
C STORED AT 40°C 8½ HOURS + APPROXIMATELY 15 MINS. AT ROOM TEMP.
D STORED AT -2°C 8½ HOURS + APPROXIMATELY 15 MINS. AT ROOM TEMP.

VOLTS GENERATED BY OUTPUT CRYSTAL.
[OR RELATIVE STRAIN AMPLITUDE].

FIG. 4.

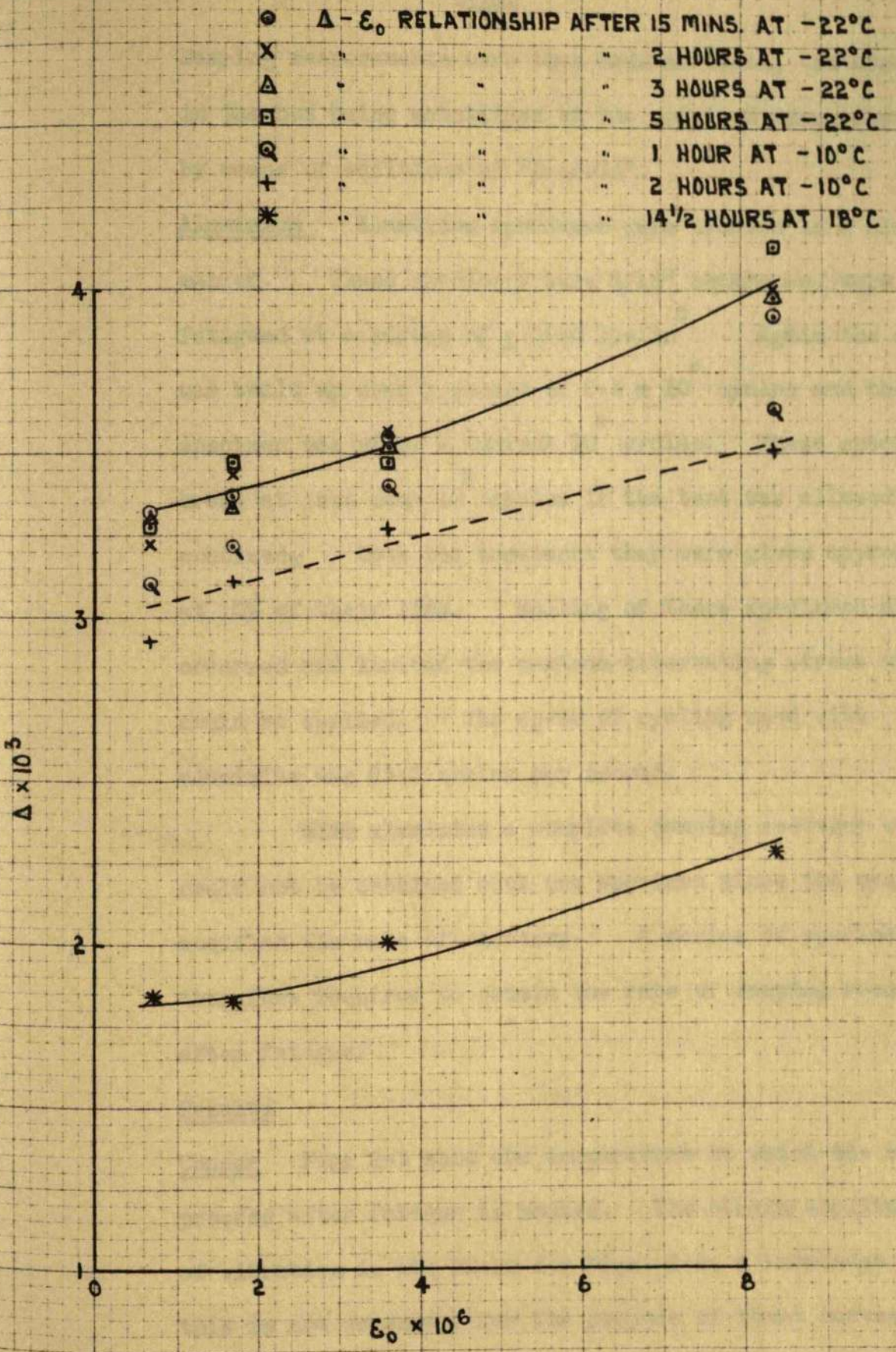
⊙ Δ - ε₀ RELATIONSHIP AFTER 15 MINS. AT -22°C
X " " " 2 HOURS AT -22°C
△ " " " 3 HOURS AT -22°C
⊡ " " " 5 HOURS AT -22°C
Q " " " 1 HOUR AT -10°C
+ " " " 2 HOURS AT -10°C
✱ " " " 14½ HOURS AT 18°C
Δ x 10³
4
3
2
1
0
2
4
6
8
ε₀ x 10⁶

FIG. 5.

Damping measurements were then made as usual, the acetone in the box being maintained at the required temperature $\pm \frac{1}{2}$°C by means of additions of "Dricold".

Aluminium Aluminium specimens were treated in a similar manner. These specimens were 3/16" square and were fatigued at a stress of $\pm$ 2250 lbs/in^2. Again the stress was built up over a period of $0{\cdot}5 \times 10^5$ cycles and the specimen was given a further 10^5 cycles. These specimens broke at just over 10^6 cycles if the test was allowed to continue; thus the treatment they were given approximated at 10% of their life. Belling of these specimens also occurred and limited the maximum alternating stress which could be applied. The speed of cycling used with aluminium was 83·5 cycles per second.

With aluminium a complete damping recovery curve could not be obtained with one specimen since the measurements modified the rate of recovery. A series of specimens was therefore required to obtain the rate of damping recovery after fatigue.

Results

Copper Figs. 2-5 show the temperature at which the recovery process after fatigue is halted. The strain amplitude of vibration is not known for Figs. 2-4; a knowledge of this is not necessary for the purpose of these curves.

Fig. 2A gives typical damping recovery measurements

made over a range of strain amplitudes for a fatigued bar. Similar results are shown in Fig. 2B for a bar which has been stored for 18 hours in liquid nitrogen between the end of fatigue, and recovery measurements. A notable feature of these curves is the higher rate of decrease of Δ for higher amplitudes of measurement. A corresponding increase in Young's Modulus as shown by the frequency measurements (for relationship between E and f see equation 3, chapter 2) accompanies the recovery of damping. Again the largest frequency recovery is associated with the higher amplitude of measurement. Figs. 3A,B,C and D show that recovery appears to be halted completely at temperatures of -196°C and -40°C, whilst some recovery has taken place during storage at -2°C. These curves have been replotted in Figure 4 and this shows rather more clearly that recovery starts to operate at some temperature between -40°C and -2°C.

Fig. 5 is the damping-strain amplitude relationship obtained from one bar which was held at -22°C in the low temperature measuring box. Over a period of 5 hours no recovery is observable. When the temperature was raised to -10°C the $\Delta - \varepsilon_a$ curve showed that measureable recovery had taken place in the first hour at this temperature. The range in which the mechanism causing recovery starts to operate is therefore between -22°C and -10°C.

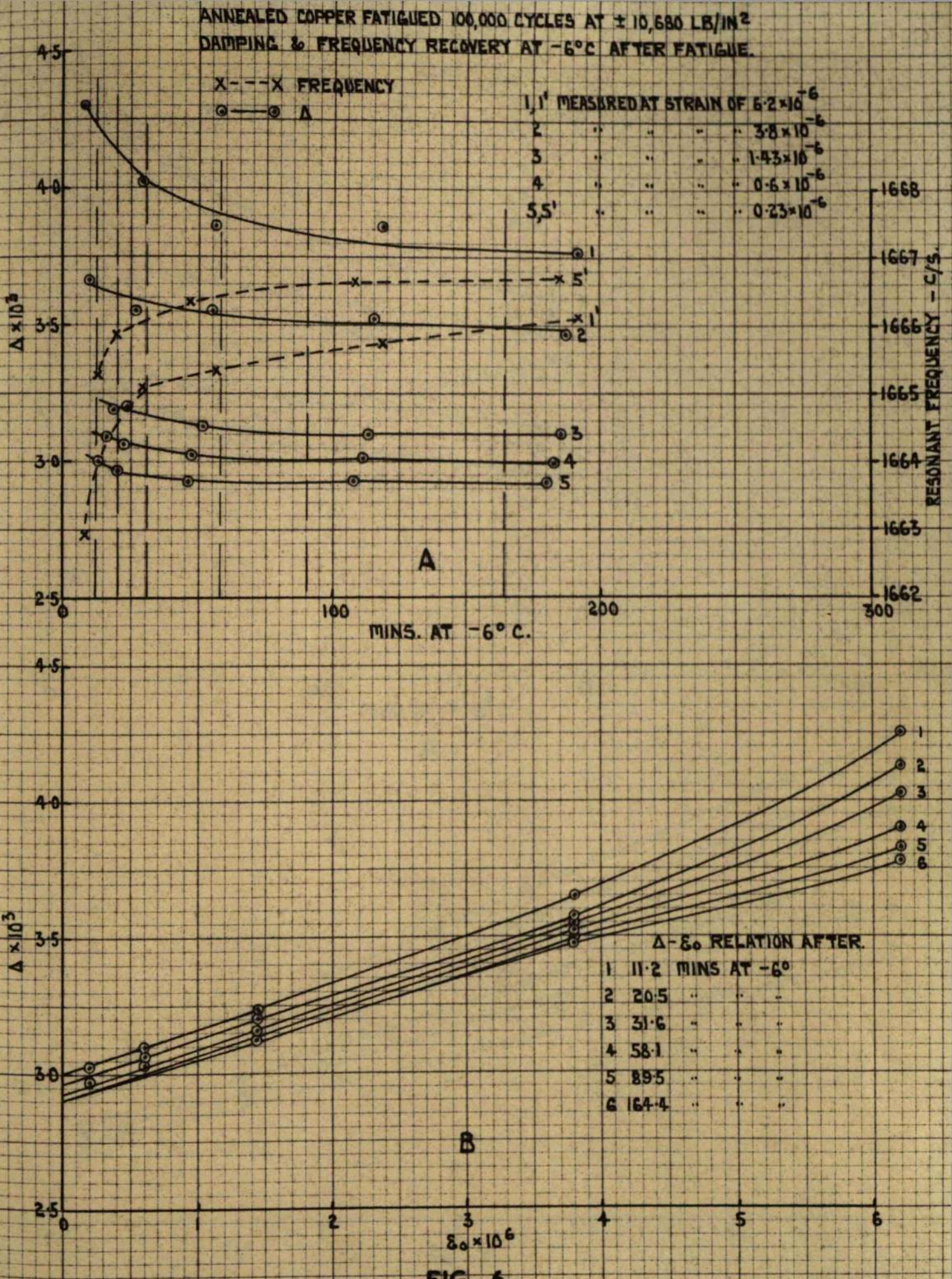
ANNEALED COPPER FATIGUED 100,000 CYCLES AT ± 10,680 LB/IN²
DAMPING & FREQUENCY RECOVERY AT −6°C AFTER FATIGUE.
X---X FREQUENCY
⊙——⊙ Δ
1,1' MEASURED AT STRAIN OF 5·2×10⁻⁶
2 " " " " 3·8×10⁻⁶
3 " " " " 1·43×10⁻⁶
4 " " " " 0·6×10⁻⁶
5,5' " " " " 0·23×10⁻⁶
Δ×10³
RESONANT FREQUENCY − C/S.
MINS. AT −6° C.
A
Δ−ε₀ RELATION AFTER.
1 11·2 MINS AT −6°
2 20·5 " " "
3 31·6 " " "
4 58·1 " " "
5 89·5 " " "
6 164·4 " " "
B
ε₀×10⁶

FIG. 6.

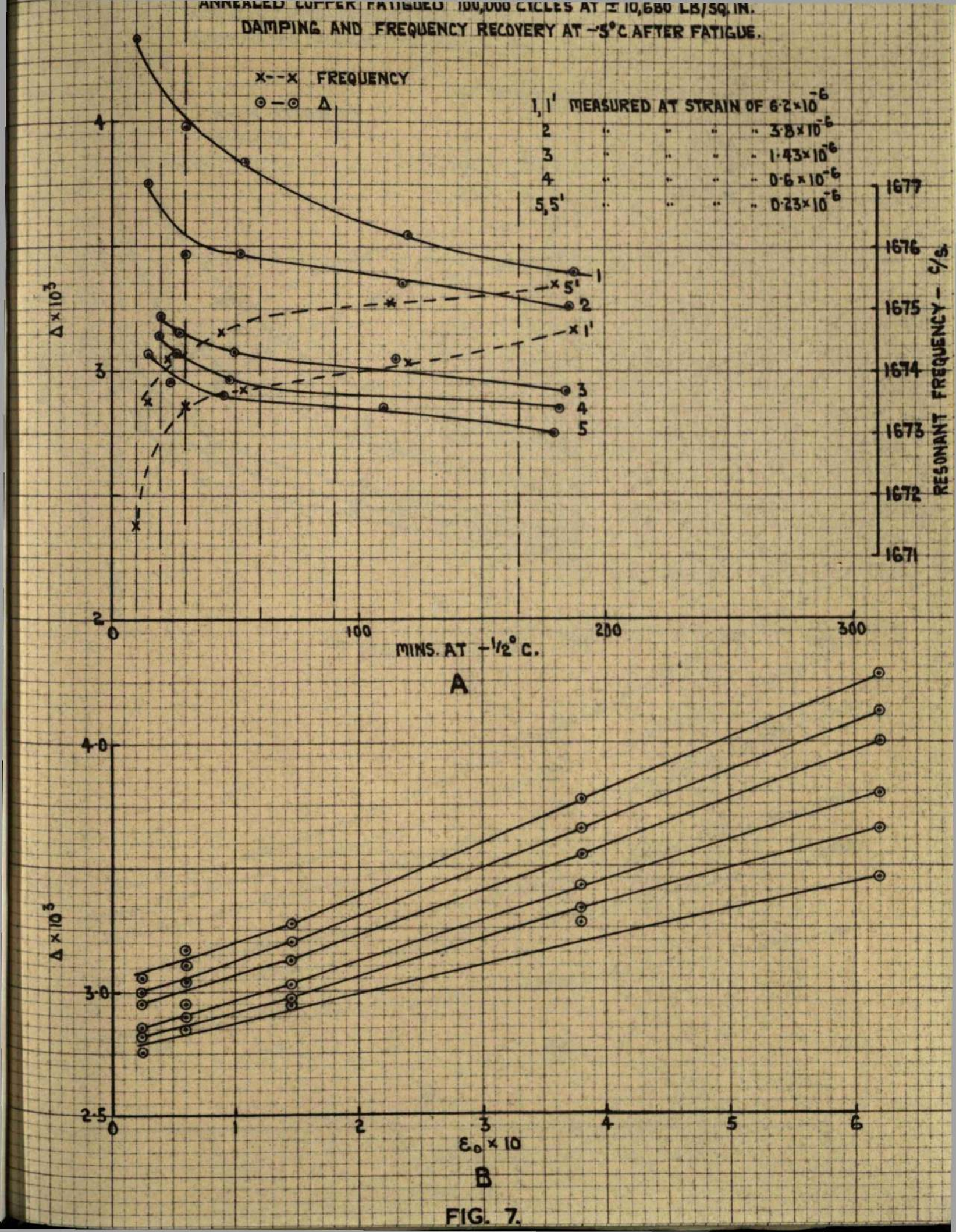
ANNEALED COPPER FATIGUED 100,000 CYCLES AT ± 10,680 LB/SQ. IN.
DAMPING AND FREQUENCY RECOVERY AT −5° C AFTER FATIGUE.
x--x FREQUENCY
⊙—⊙ Δ
1, 1' MEASURED AT STRAIN OF 6·2×10⁻⁶
2 " " " " 3·8×10⁻⁶
3 " " " " 1·43×10⁻⁶
4 " " " " 0·6×10⁻⁶
5, 5' " " " " 0·23×10⁻⁶
Δ×10³
RESONANT FREQUENCY — C/S
1677
1676
1675
1674
1673
1672
1671
4
3
2
0
100
200
300
MINS. AT −½° C.
A
4·0
3·0
2·5
Δ×10³
0
1
2
3
4
5
6
ε₀×10
B

FIG. 7.

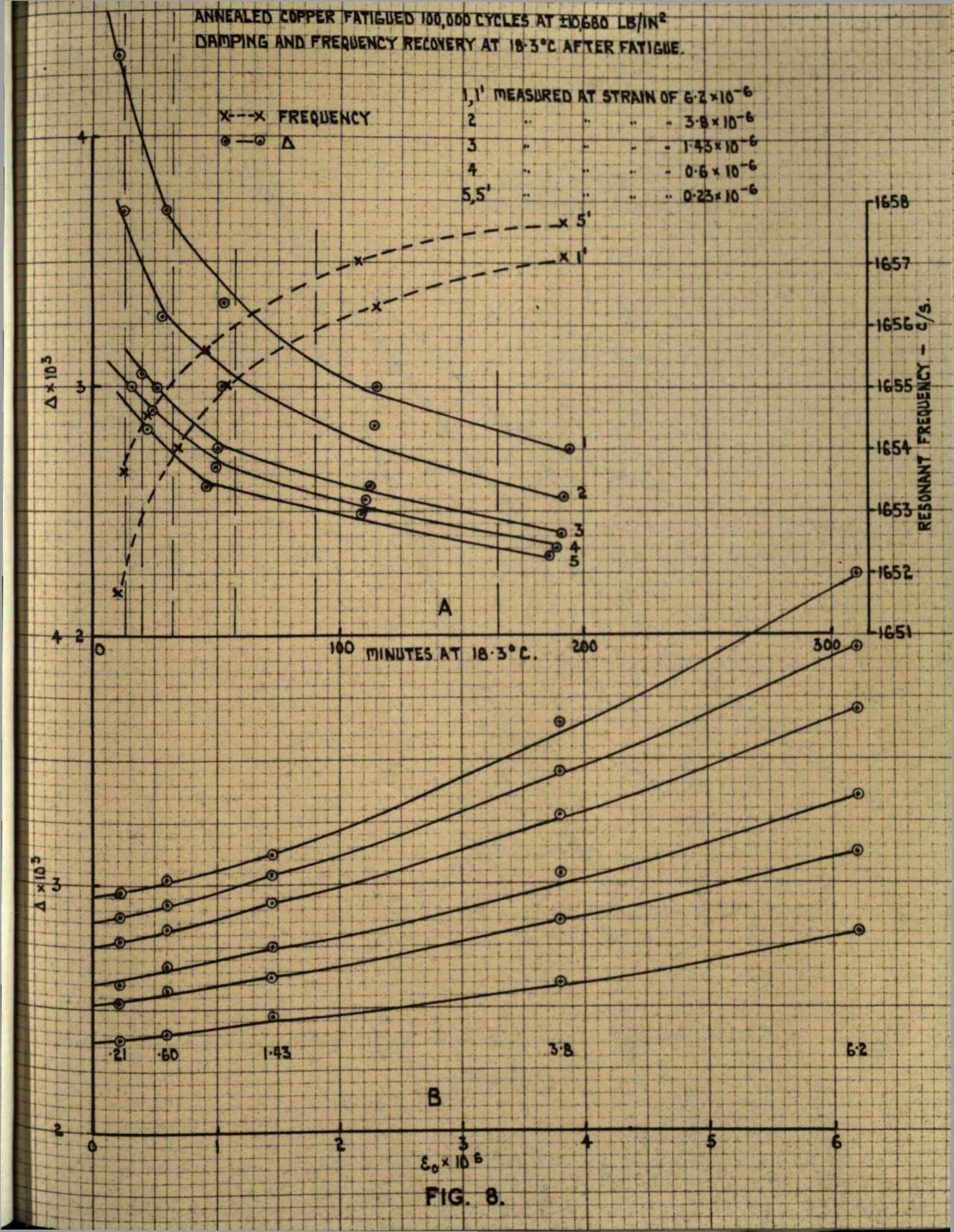
ANNEALED COPPER FATIGUED 100,000 CYCLES AT ±10,680 LB/IN²
DAMPING AND FREQUENCY RECOVERY AT 18·3°C AFTER FATIGUE.
1,1' MEASURED AT STRAIN OF 6·2×10⁻⁶
2 " " " " 3·8×10⁻⁶
3 " " " " 1·43×10⁻⁶
4 " " " " 0·6×10⁻⁶
5,5' " " " " 0·23×10⁻⁶
x---x FREQUENCY
⊙—⊙ Δ
Δ×10³
RESONANT FREQUENCY - c/s.
MINUTES AT 18·3°C.
A
B
ε₀×10⁶
·21
·60
1·43
3·8
6·2

FIG. 8.

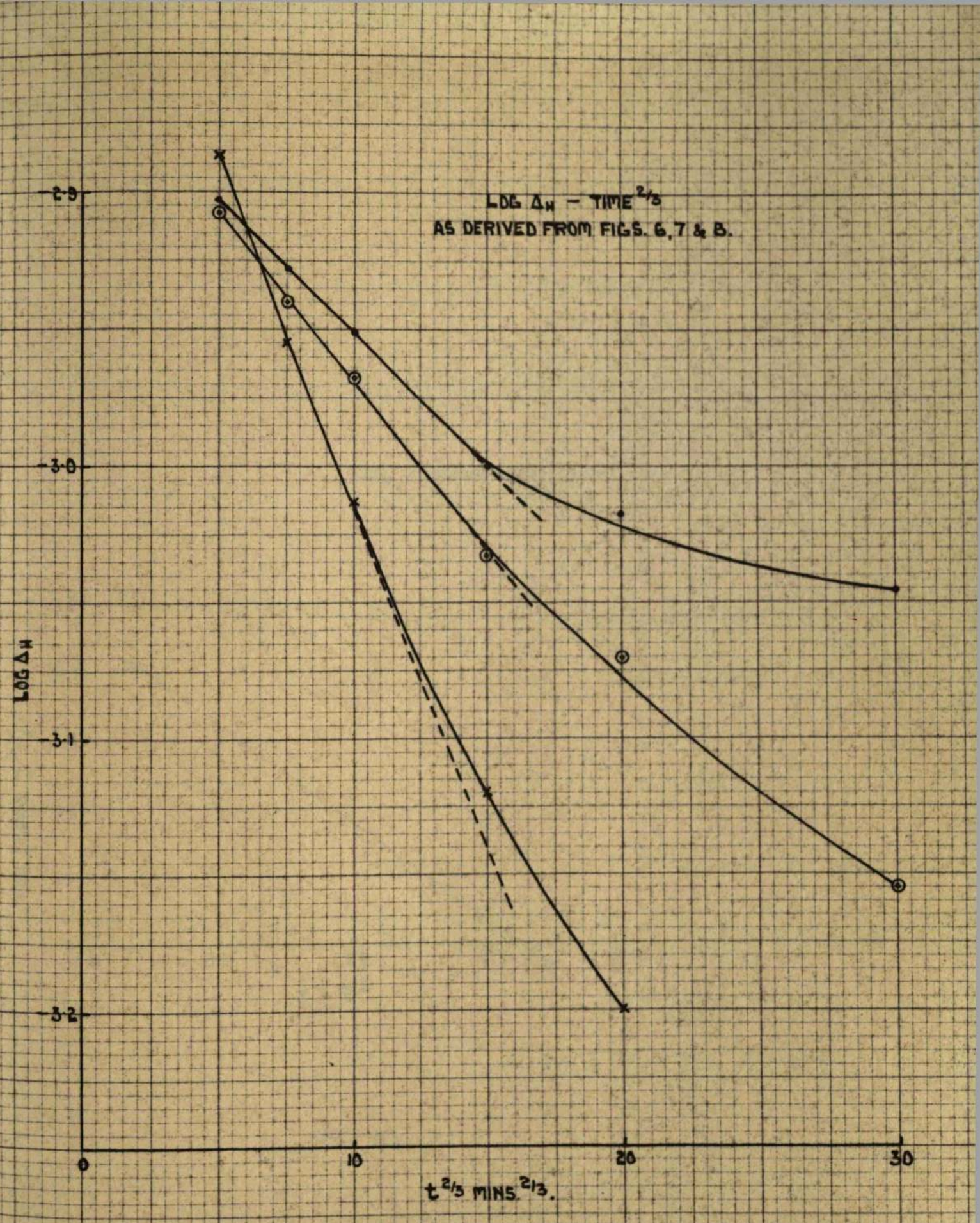
LOG Δ_H – TIME $^{2/3}$
AS DERIVED FROM FIGS. 6, 7 & 8.
-2·9
-3·0
-3·1
-3·2
LOG Δ_H
0
10
20
30
$t^{2/3}$ MINS. $^{2/3}$.

FIG. 9.

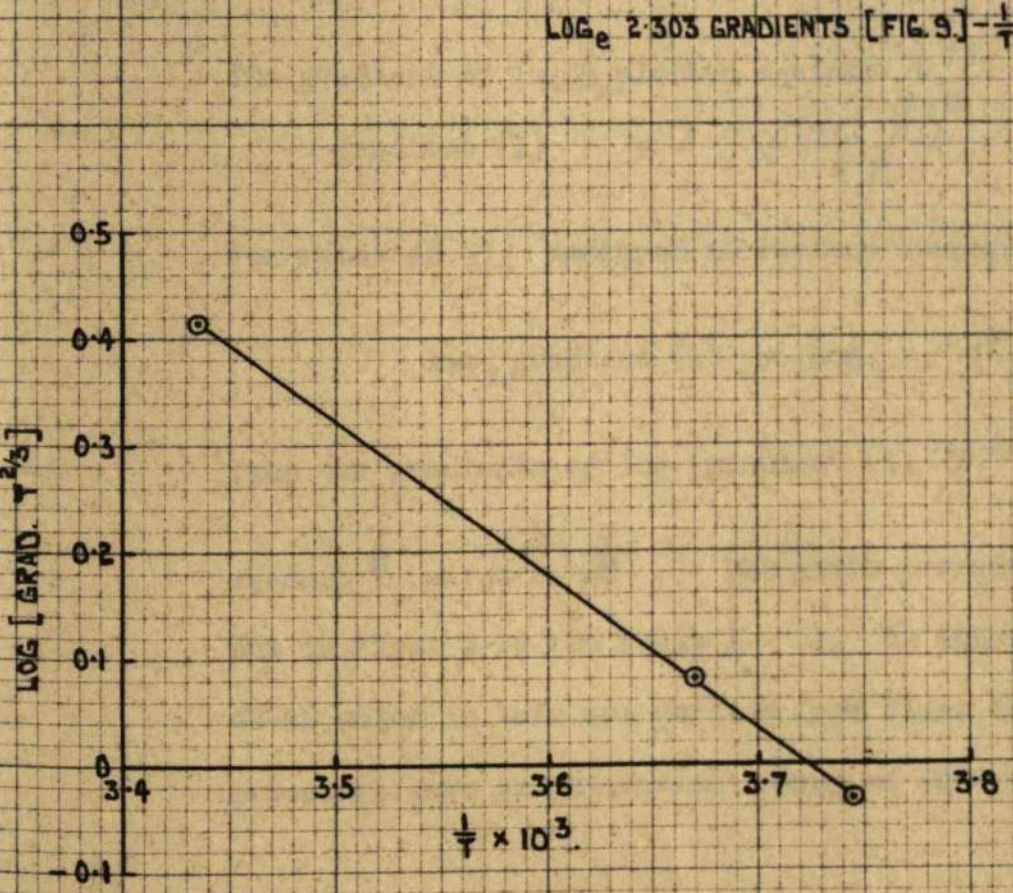
LOG$_e$ 2·303 GRADIENTS [FIG. 9] $-\frac{1}{T}$
0·5
0·4
0·3
0·2
0·1
0
−0·1
LOG [GRAD. $T^{2/3}$]
3·4
3·5
3·6
3·7
3·8
$\frac{1}{T} \times 10^3$.

FIG. 10.

The purpose of results plotted in Fig. 6-10 is to determine the activation energy of the recovery process which may be derived as follows.

Using Beshers equation - equation (21) chapter 1 section 3

$$\text{Log}_e \Delta_H = \text{Log}_e \Delta_3 - \beta' t^{2/3}$$

$$= \text{Log}_e \Delta_3 - \gamma\rho \left(\frac{AD_0 e^{\frac{Q}{KT}}}{KT} t\right)^{2/3}$$

The gradient of $\log \Delta_H$ plotted against $t^{2/3}$ gives

$$\text{gradient (1)} = \gamma\rho \left(\frac{AD_0 e^{-\frac{Q}{KT}}}{KT}\right)^{2/3}$$

For rates of Δ_H measured at various temperatures then

$$\log_e \text{gradient (1)} = \text{Log}_e \gamma\rho \left(\frac{AD_0}{K}\right)^{5/3} - \frac{2}{3}\text{Log}_e T - \frac{2}{3}\cdot\frac{Q}{KT}$$

Thus the gradients of log (gradient (1) $T^{2/3}$) plotted against $\frac{1}{T}$ gives $\frac{2}{3}\cdot\frac{Q}{K}$. The above procedure is followed out in Figs. 6-10 and Table 1. Δ_H is obtained from Figures 6B-8B which in turn are derived from Figs. 6A-8A. This procedure gave an activation energy of 9870 cals/mole.

$\Delta - \varepsilon_0$ RELATIONSHIPS DURING RECOVERY AFTER:-
1 - CLAMPING ONLY. 2 - PULLED IN TENSION. 3 - FATIGUE.

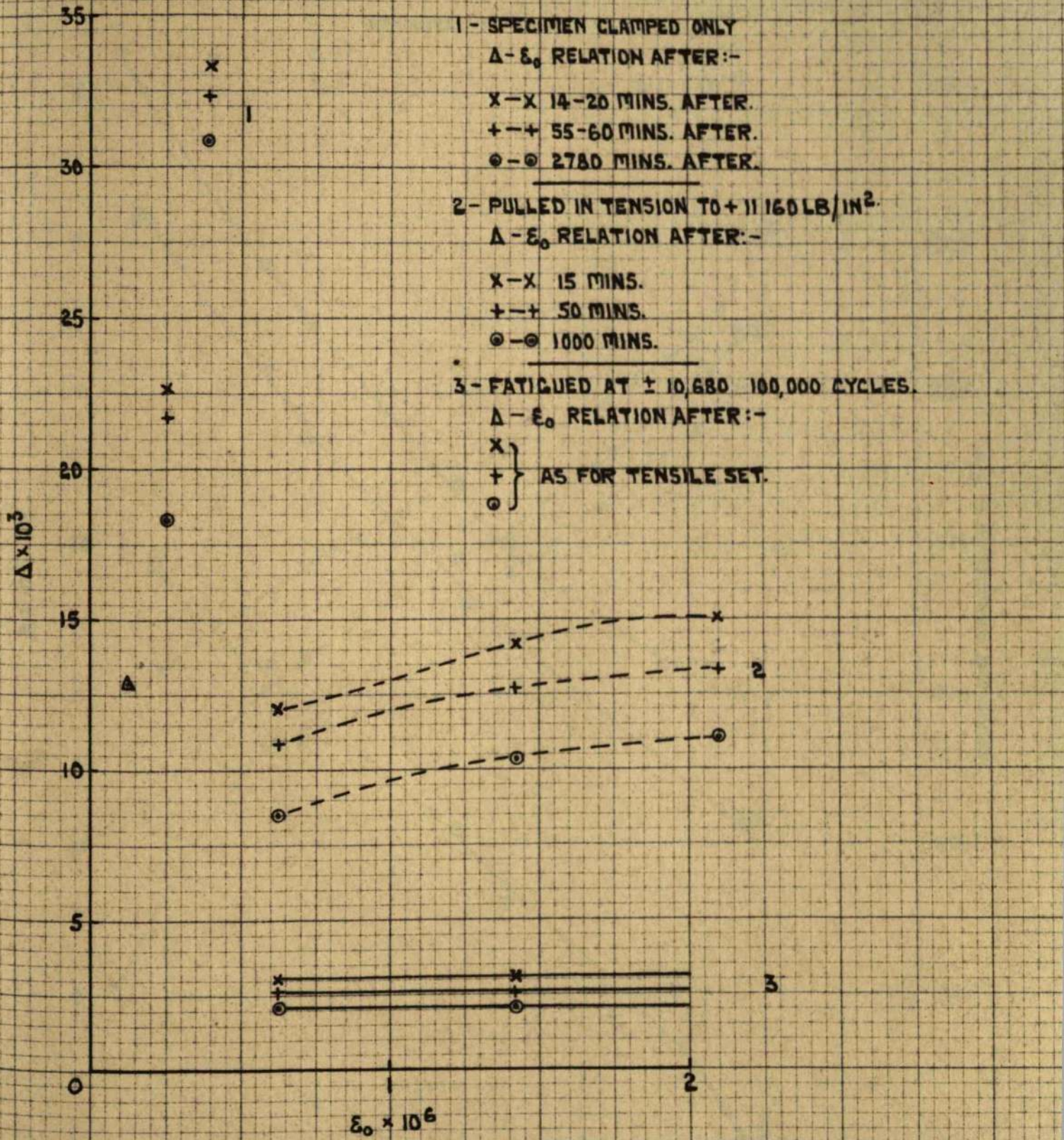

1 - SPECIMEN CLAMPED ONLY
$\Delta - \varepsilon_0$ RELATION AFTER:-

X - X 14-20 MINS. AFTER.
+ - + 55-60 MINS. AFTER.
⊙ - ⊙ 2780 MINS. AFTER.

2 - PULLED IN TENSION TO + 11 160 LB/IN^2.
$\Delta - \varepsilon_0$ RELATION AFTER:-

X - X 15 MINS.
+ - + 50 MINS.
⊙ - ⊙ 1000 MINS.

3 - FATIGUED AT ± 10,680 100,000 CYCLES.
$\Delta - \varepsilon_0$ RELATION AFTER:-
X, +, ⊙ } AS FOR TENSILE SET.

FIG. 11.

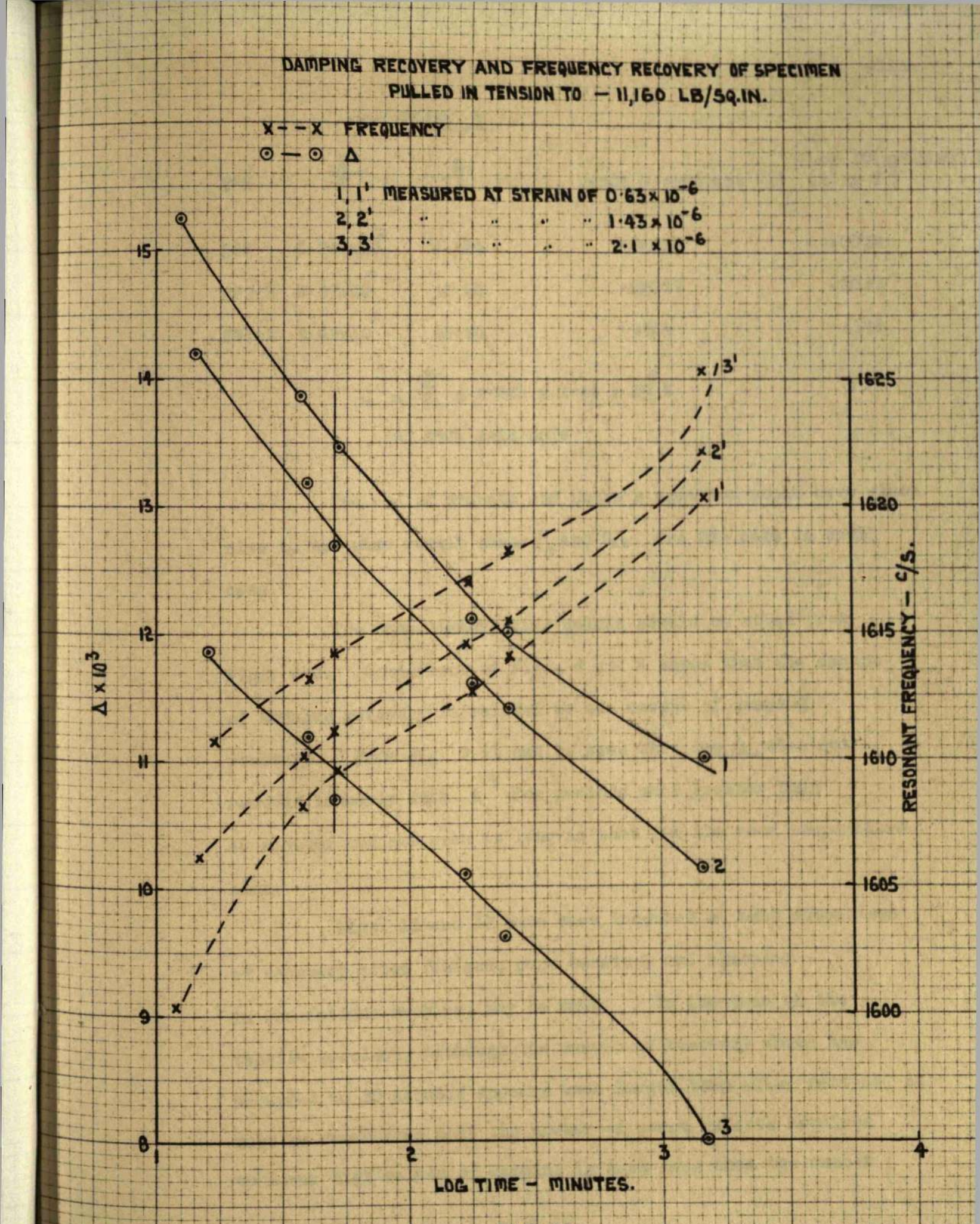
DAMPING RECOVERY AND FREQUENCY RECOVERY OF SPECIMEN PULLED IN TENSION TO — 11,160 LB/SQ.IN.
X — X FREQUENCY
⊙ — ⊙ Δ
1, 1' MEASURED AT STRAIN OF 0·63 × 10⁻⁶
2, 2' " " " " 1·43 × 10⁻⁶
3, 3' " " " " 2·1 × 10⁻⁶
Δ × 10³
RESONANT FREQUENCY — C/S.
LOG TIME — MINUTES.
15
14
13
12
11
10
9
8
1
2
3
4
1625
1620
1615
1610
1605
1600
x 3'
x 2'
x 1'

FIG. 12.

TABLE 1

T°K	$\frac{1}{T}$	$T^{\frac{2}{3}}$	2·303 x gradient (1)	Log 10(gradient x (1) x $T^{\frac{1}{3}}$
267	$3 \cdot 745 \times 10^{-3}$	41·45	·02237	-·0334
272·5	$3 \cdot 67 \times 10^{-3}$	42·04	·02829	·0795
291·3	$3 \cdot 43 \times 10^{-3}$	43·94	·5909	·4143

$$Q = \frac{3}{2} \times 2 \cdot 303 \times 1 \cdot 44 \times 10^{-3} K$$

$$= 9878 \text{ cals/mole}$$

The use of Granato and Lucke's equation would have given rise to the same result since ε_0 and C_{10} are the same in each case.

Two other interesting points should be noted from Figs. 6-9. Comparison of Figs. 6 and 8 shows that the amount of modulus recovery is related to the amount of damping recovery. From Fig. 9 it can be seen that log Δ_H does not recover linearly with $t^{2/3}$ for periods much greater than 40 minutes and not even as long as that for the room temperature case.

Figs. 11 and 12 have been inserted so that comparison of recovery after fatigue, pure tension, and clamping in the fatigue machine, may be made. In the case of the tensile specimen, although the amount of recovery which has occurred in 50 minutes appears much larger than after fatigue, it must be remembered that the number of point defects required to lower high values of damping is much less than the number

$\Delta - \varepsilon_0$ RELATIONSHIP FOR FATIGUED ALUMINIUM AFTER STORAGE AT 18° C FOR VARIOUS TIMES.

1 ⊙—⊙ 8-16 MINS. AFTER FATIGUE.
2 ×—× 20-28 MINS. " "
6 Δ—Δ 7 HOURS " "
4 •—• 1¾ HOURS " "
5 +—+ 3 HOURS " "
3 ⊙ ⊙ 45-53 MINS. " "

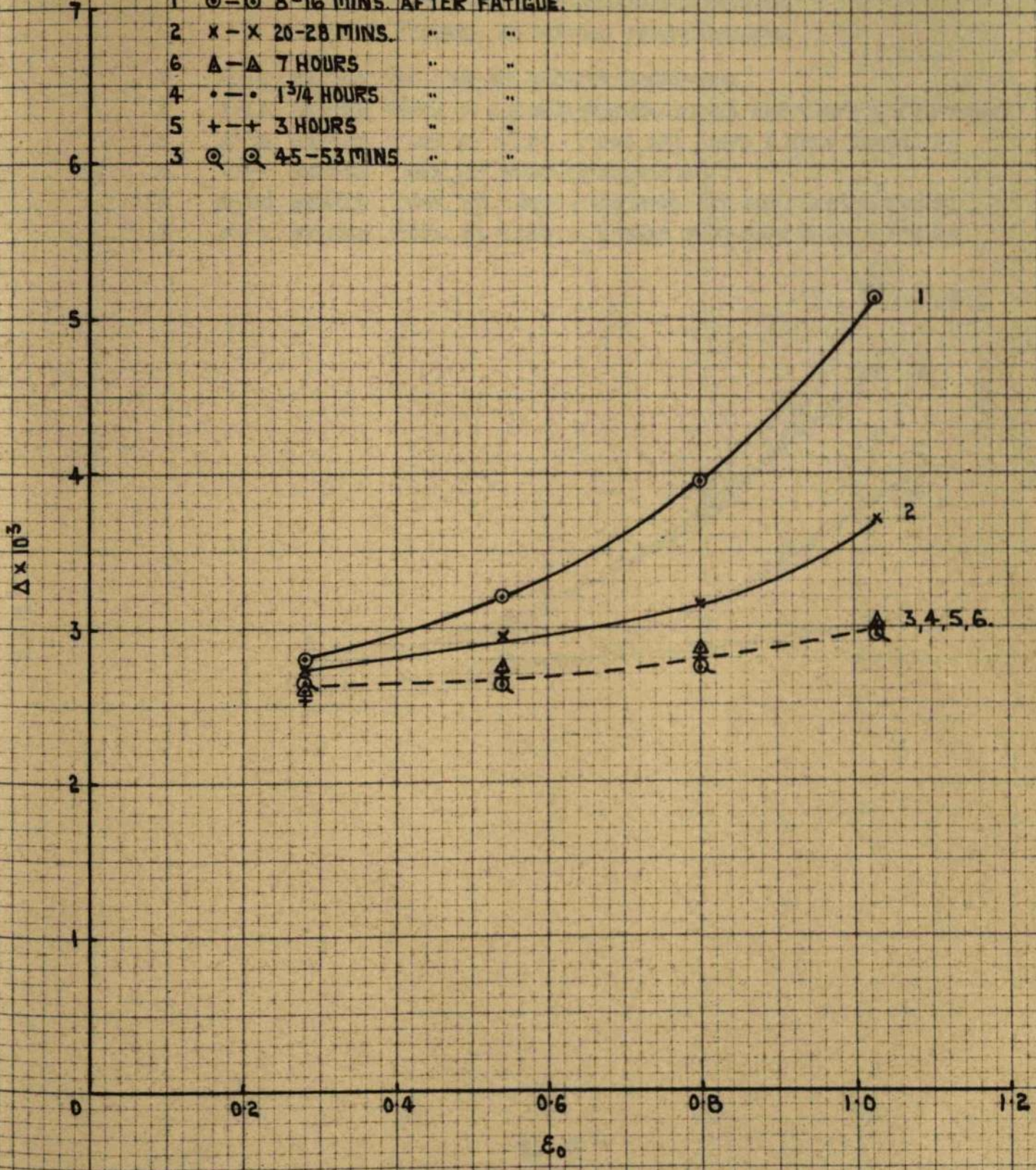

FIG. 13.

$\Delta - \varepsilon_0$ RELATIONSHIP FOR FATIGUED ALUMINIUM
AFTER STORAGE AT VARIOUS TEMPERATURES.

1 ⊙–⊙ RESTED 7½ MINS. AT ROOM TEMPERATURE.
2 x–x RESTED 7 HRS. IN LIQUID NITROGEN + 4 MINS. BET. −196°C & 0°C + 7 MINS.
5 Δ–Δ RESTED 7 HRS. AT −20°C + 1 MIN. BET. −20°C & 0°C + 7 MINS.
6 •–• RESTED 7 HRS. AT ROOM TEMPERATURE.
4 ⊙–⊙ RESTED 7 HRS. AT −40°C + 1½ MINS. BET. −40°C & 0°C + 7 MINS.
3 +–+ RESTED 7 HRS. AT −60°C + 2 MINS BET. −60°C & 0°C + 7 MINS.

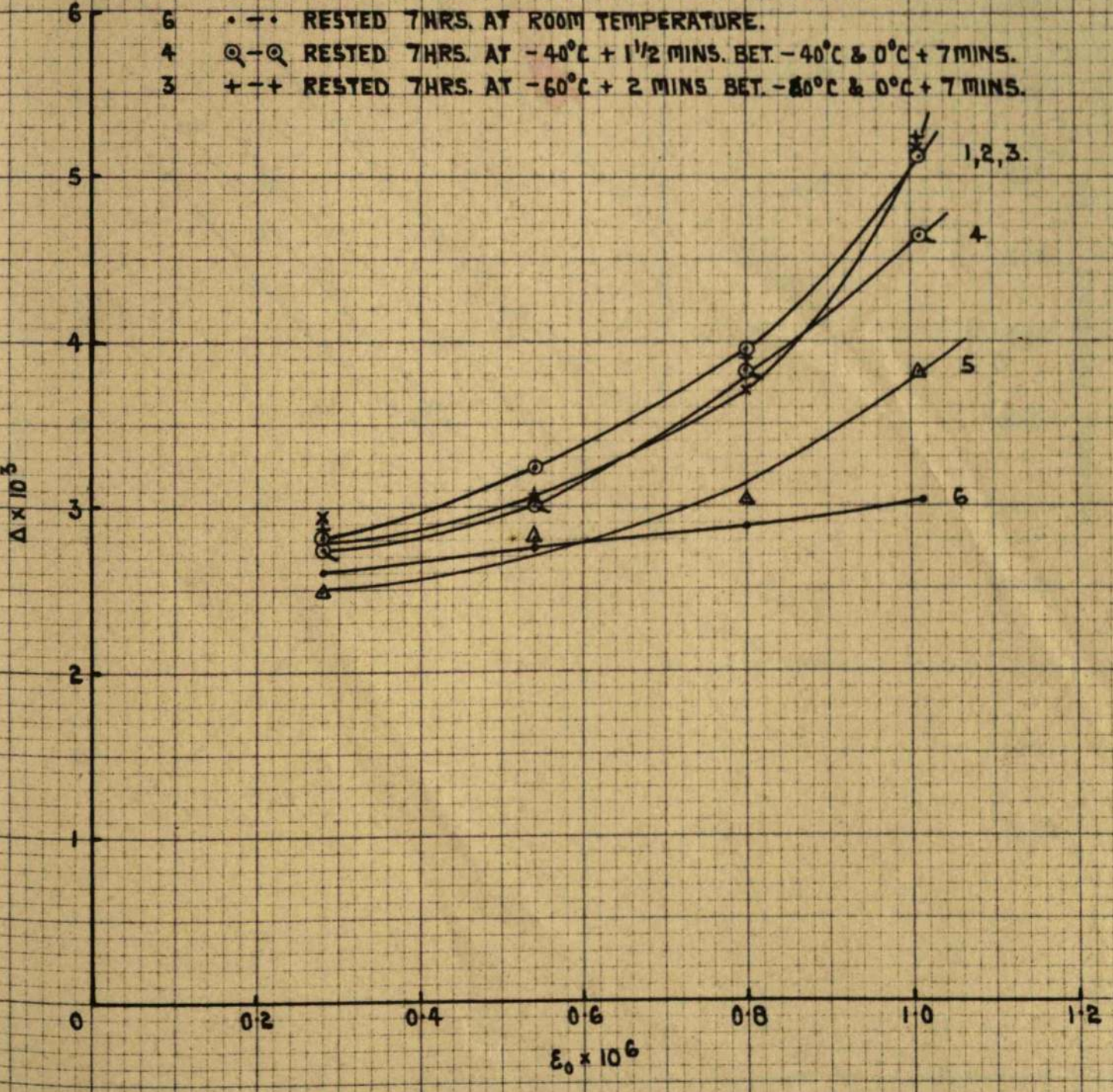

FIG. 14.

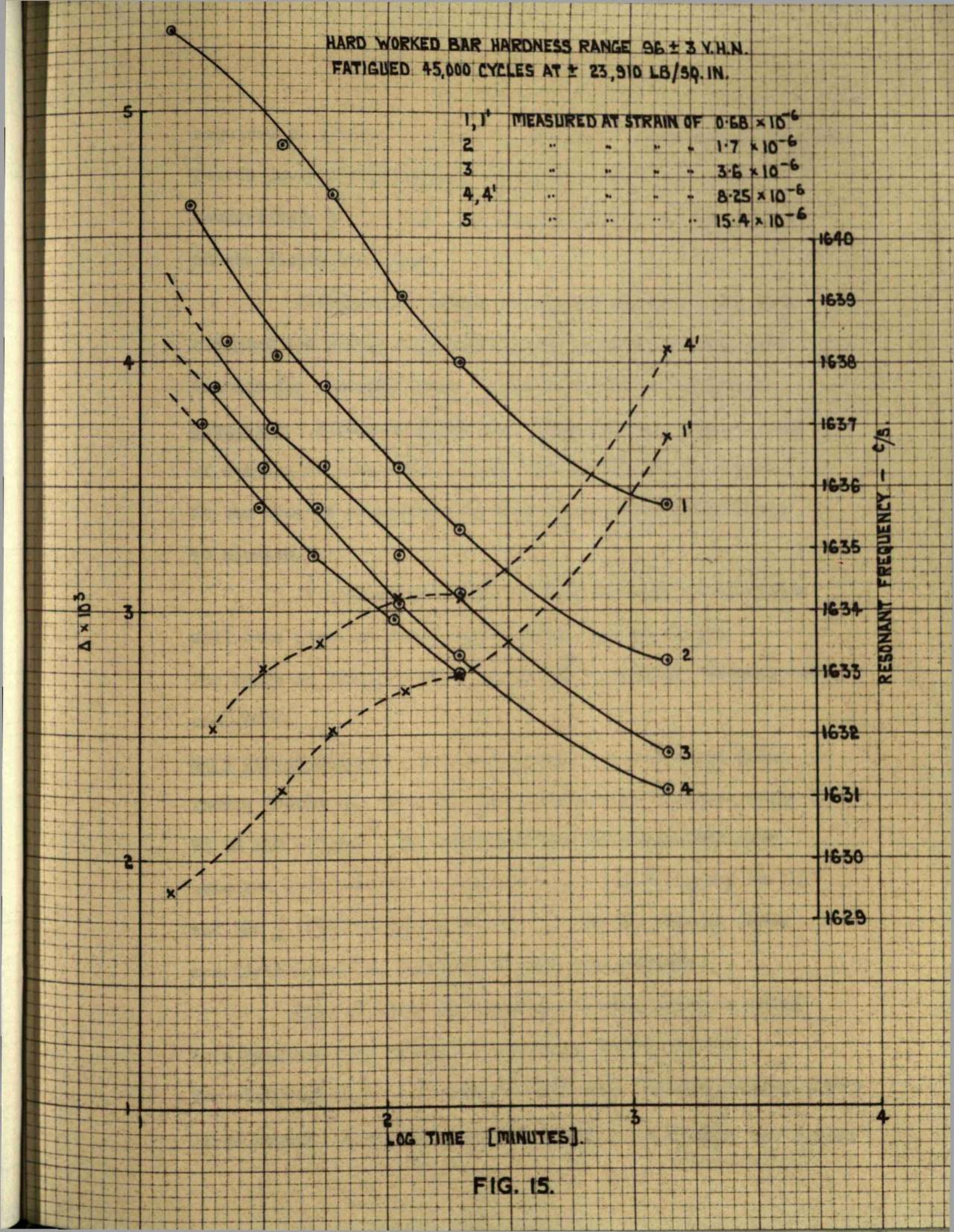
HARD WORKED BAR HARDNESS RANGE 96 ± 3 V.H.N.
FATIGUED 45,000 CYCLES AT ± 23,910 LB/SQ. IN.
1, 1' MEASURED AT STRAIN OF 0·68 × 10⁻⁶
2 " " " " 1·7 × 10⁻⁶
3 " " " " 3·6 × 10⁻⁶
4, 4' " " " " 8·25 × 10⁻⁶
5 " " " " 15·4 × 10⁻⁶
Δ × 10³
RESONANT FREQUENCY − C/S.
LOG TIME [MINUTES].
1
2
3
4
5
1640
1639
1638
1637
1636
1635
1634
1633
1632
1631
1630
1629

FIG. 15.

required to lower low values of damping. This arises from the fourth power and exponential dependence of Δ_I and Δ_H respectively on L_c i.e. the concentration of point defects on the dislocation line.

Fatigue has lowered the high damping arising from clamping and sawing to a much greater extent than has pure tension for the same load. This in itself is important.

Aluminium Figure 13 shows that after fatigue, the recovery of damping in aluminium is much more rapid than in copper. In the case of aluminium, recovery is complete after about 40 minutes.

It appears from Fig. 14 that recovery in aluminium will take place at lower temperatures than in copper. The range in which recovery is halted is probably between -40°C and -60°C.

Hard Worked Copper The hard worked copper received from Thomas Bolton and Sons Ltd. had a continuous hardness range from 90 to 110 V.H.N. Specimens for the following work were selected with hardness ranges of 96 $\pm$ 3 V.H.N. (group No. 1) and 106 $\pm$ 3 V.H.N. (group No. 2). During fatigue these specimens showed no tendency to bell transversely.

Fig. 15 shows the damping recovery which occurred in a specimen from group 1 fatigued at 23,910 lbs/in^2. for 45,000 cycles. A comparatively high initial damping with a large amount of recovery is noteworthy. A similar bar pulled

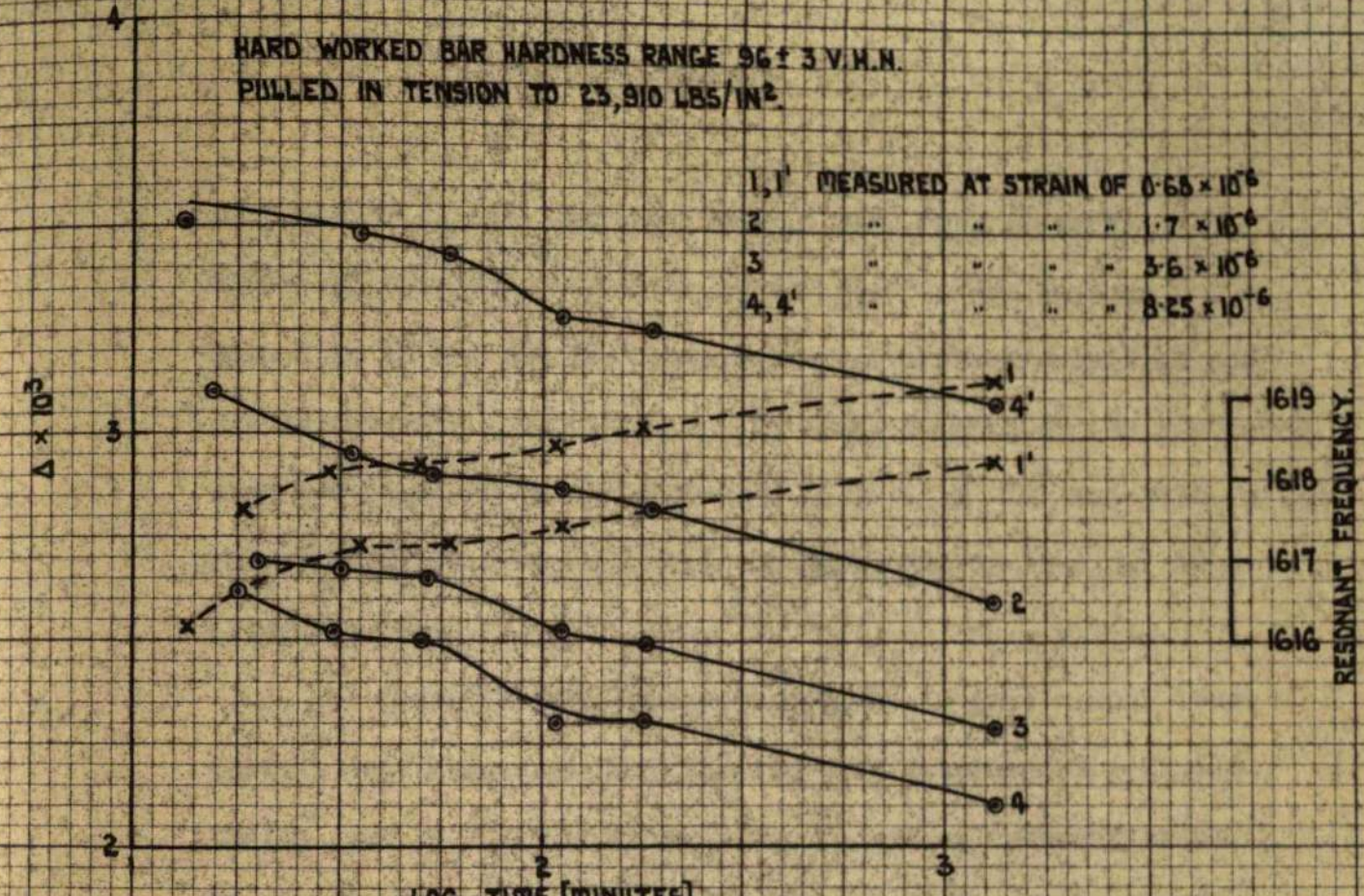
HARD WORKED BAR HARDNESS RANGE 96 ± 3 V.H.N.
PULLED IN TENSION TO 23,910 LBS/IN².
1,1' MEASURED AT STRAIN OF 0·68 × 10⁻⁶
2 " " " " 1·7 × 10⁻⁶
3 " " " " 3·6 × 10⁻⁶
4,4' " " " " 8·25 × 10⁻⁶
Δ × 10³
4
3
2
1
2
3
LOG TIME [MINUTES].
1619
1618
1617
1616
RESONANT FREQUENCY.

FIG. 16.

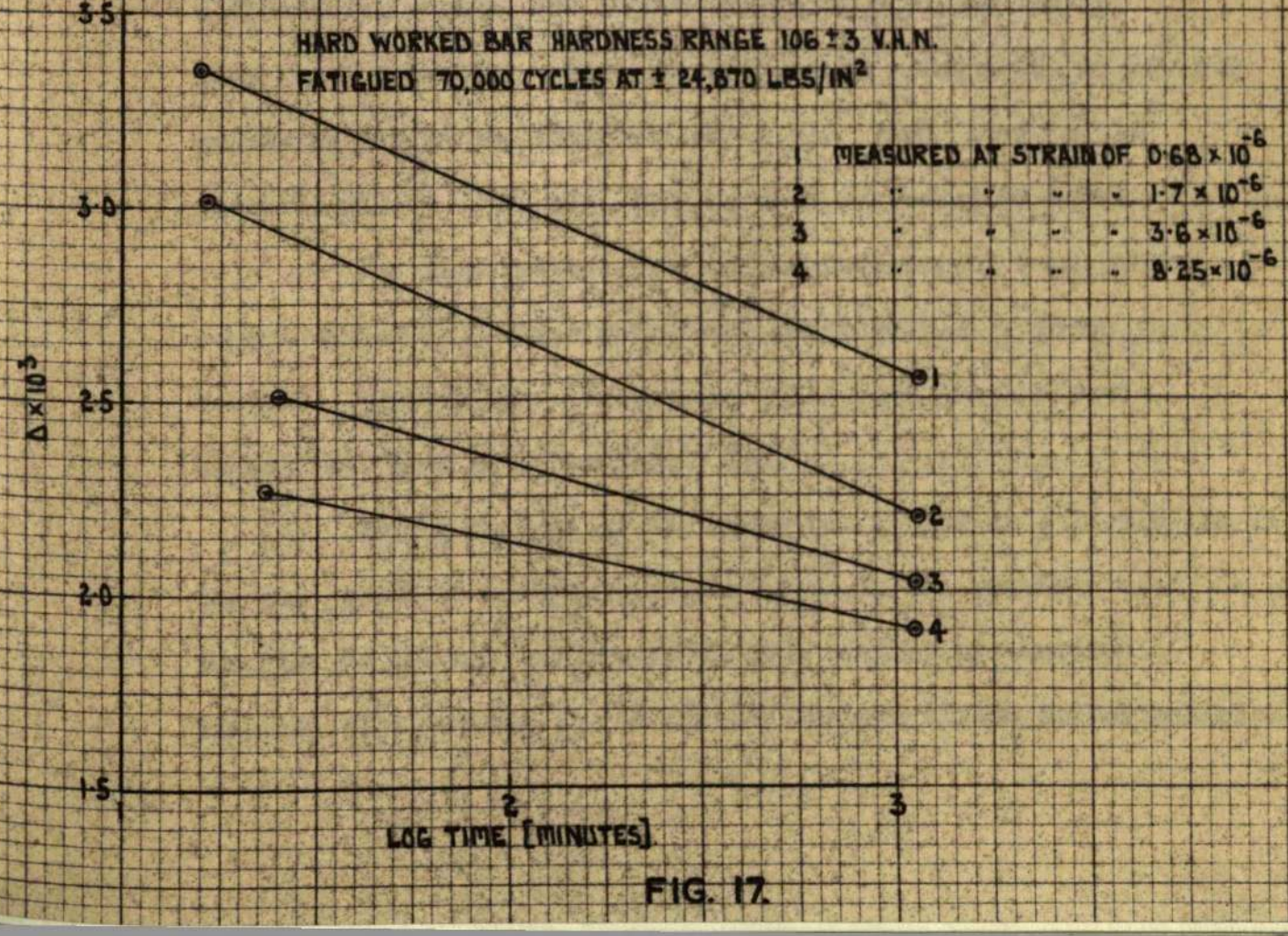
HARD WORKED BAR HARDNESS RANGE 106 ± 3 V.H.N.
FATIGUED 70,000 CYCLES AT ± 24,870 LBS/IN²
1 MEASURED AT STRAIN OF 0·68 × 10⁻⁶
2 " " " " 1·7 × 10⁻⁶
3 " " " " 3·6 × 10⁻⁶
4 " " " " 8·25 × 10⁻⁶
Δ × 10³
3·5
3·0
2·5
2·0
1·5
2
3
LOG TIME [MINUTES].

FIG. 17.

to + 23,910 lbs/in^2 in pure tension gave rise to very different results. In this latter case as can be seen From Fig. 16 the initial damping was not particularly high and little recovery took place. The final damping of the specimens used for Figs. 15 and 16 decreased to $2{\cdot}74 \times 10^3$ and $2{\cdot}56 \times 10^3$ respectively at a measuring strain amplitude of $15{\cdot}4 \times 10^6$, after one week.

Material from hardness group No. 2 gave a much lower initial amplitude dependent damping when fatigued at $\pm$ 23,910 lbs/in^2 and Fig. 17 shows the lower amount of recovery which also took place. This initial damping of the higher hardness material could be raised however, by fatiguing at a higher alternating stress, and 40,000 cycles at $\pm$ 28,700 lbs/in^2 gave initial damping values of $2{\cdot}99 \times 10^3$ and $4{\cdot}03 \times 10^3$ for measuring strain amplitudes of 68×10^6 and $15{\cdot}4 \times 10^6$ respectively. This high damping then recovered as usual.

The high initial damping and recovery of hard worked copper caused by fatigue was always reproducible. On no occasion, however, was the damping after pure tension ever higher than that shown in Figure 16.

During fatigue of the group No. 1 bars at $\pm$ 23,910 lbs/in^2 the bar tended to heat up considerably; in the specimen used for Fig. 15 the bar was prevented from heating by continual swabbing with acetone. A further feature of the softer material

was that the input power to the fatigue machine had to be increased continuously during the test. This indicates an increase in damping of the material associated with softening. No warming of the harder material occurred during fatiue at 24,870 lbs/in^2 (Fig. 17) and the power required remained constant; the tendency of the specimen to heat up and the necessity for increased input power was present, however, when the hard material was fatigued at 28,700 lbs./in^2.

Recovery of the hard worked material after fatigue appeared to be halted at just below room temperature i.e. between 5°C and 15°C. Insufficient results however were obtained for this temperature range to be known definitely.

Discussion of Results.

The higher the rate of recovery of both damping and Young's Modulus which occur with higher measuring strain amplitudes is in accordance with the Granato and Lucke equation (18) chapter 1 section 3. The amplitude dependence of both E and Δ verify that the damping arose from dislocation motion.

Figs. 2-6 all lead to the conclusion that the damping and modulus recovery of the annealed and fatigued copper is stopped when the specimen is cooled to some temperature between -10°C and -20°C. The similarity between the present results and those obtained by Barnes, Hancock and Silk[64] on quenched and irradiated copper is very marked. In the latter case recovery must

be due to vacancy dislocation interaction since neither quenching nor irradiation will modify the dislocation density to any great extent.

In aluminium the greater speed of room temperature recovery and the lower temperature at which it will proceed both indicate a lower activation energy for the recovery mechanism. The results on aluminium are similar to those obtained by Valluri[99] who measured Δ_I recovery after fatigue. In the latter case recovery was complete after approximately 30 minutes.

Both the present results and those obtained by Valluri in turn are very similar to those obtained by Levy and Metzger[59] after quenching aluminium.

The similarity between recovery after fatigue as compared with recovery after quenching or irradiation is strong evidence that the recovery arises from migration of vacancies to dislocations.

The activation energy as derived from Figs. 6-10 is much lower than the accepted value for vacancy migration in copper, i.e. about 16,000 calories/mole[18,19]. Great weight cannot be placed on the value derived from the present work since the curves of Figs. 6B, 7B and 8B do not obey an exponential law in the first place. The recovery is also complicated by the fact that the material used is polycrystalline and as will be shown in chapter 5 the fatigue structure developed in

the present tests was exceedingly non-homogeneous, many grains did not show any fatigue structure at all. The concentration of vacancies would, therefore, vary greatly from grain to grain. It is also probable that dislocation interaction modified the recovery process, particularly in heavily deformed grains. The activation energy obtained is certainly much too low to arise from diffusion of impurities to the dislocation.

The divergency of the log $\Delta_H/t^{2/3}$ plot in Fig. 9 is to be expected when using the recovery theory of either Beshers or Granato and Lucke. This arises because both these theories are based on the Cottrell-Beilby equation 16 chapter 1 section 3, which assumes that the overall concentration of mobile point defects C_{10} remains constant. This is not true during recovery since C_{10} is being reduced by vacancies which have migrated to dislocations and also by vacancies forming clusters which can then collapse to give dislocation loops. This would give rise to the deviation shown in Fig. 9.

Quenching and irradiation experiments have shown that vacancies, by migrating to the dislocations and interacting with them, can give rise to a decrease in damping with time after either of these treatments. It has been shown in other published work discussed in chapter 1 section 1 that vacancies are created abundantly during fatigue. It seems reasonable to assume therefore, that the decrease in damping which occurs during

annealing at room temperature after fatigue is likewise caused by the gradual migration of vacancies to dislocations and subsequent interaction with them. The temperatures below which the recovery is halted in copper and aluminium in the present work is further evidence that the effect arises from vacancy migration.

The results shown in Figure 11 are important. They show that cyclic stressing has reduced the initial damping measurements much more than a similar stress applied in pure tension. This means that a cyclic stress can reduce the mobility of dislocations much more than a similar tensile stress. It is not possible to say from the present results whether or not this reduction is due to point defects or dislocation interaction arising during fatigue. The results however are in agreement with those obtained by Broom and Ham[30] who, by means of tensile stress-strain curves, have shown that this hardening is a pronounced feature of annealed material subjected to fatigue. They have also shown that this hardening can most satisfactorily be explained by point defect hardening.

Recently[127] these workers have fatigued copper single crystals at 78°K and determined the effect of annealing at various temperatures on the tensile strength. They stated that a maximum hardness was obtained after 30 minutes at 210°K and no further hardening was observed even after 2500 minutes at 293°K. The hardening at 210°K was attributed to

divacancies migrating to the dislocations. Damping capacity are measurements, however, much more sensitive to dislocation motion than are stress-strain curves, and the present damping measurements show that recovery can continue for periods of several days at room temperature. It is probable therefore, that hardening continued on the experiments of Broom and Ham for longer periods than was realised, the stress-strain curves not being sensitive enough to show this.

The high damping caused by fatigue of hard worked copper is further proof, supplementing that already discussed in chapter 1, section 1 that softening can occur during fatigue. It is not possible to compare directly the results obtained on hard worked copper with those obtained from annealed copper since the initial structures and the fatigue stresses used in each case were vastly different. However, it appears that the recovery process in the hard worked material after fatigue also arises from a dislocation-vacancy interaction mechanism.

The hardening of annealed metal and the softening of work hardened metal by the same mechanism, i.e. fatigue, is not incompatible and one basic mechanism based on point defects is put forward to account for both these phenomena. This mechanism is described in chapter 5.

Conclusions

It has been established with fair certainty that

vacancies are created during fatigue, and that their mobility can cause hardening of the structure by pinning of dislocations during annealing at room temperature. It has also been shown by damping capacity measurements that fatigue at room temperature can restrict subsequent dislocation motion to a much greater extent than the same stress applied in pure tension. The high damping capacity which can result in work hardened metal after it has been subjected to a sufficiently high alternating stress is further evidence that softening of work hardened metal can occur during fatigue.

CHAPTER 5

Optical and Electron Microscope Studies of Fatigued Surfaces.

OPTICAL AND ELECTRON MICROSCOPE STUDIES OF FATIGUED METALS

In the review of the theories dealing with the causes of fatigue failure, mention was made of the probability of cracks forming due to the notch effect of slip bands or grain boundaries. During the fatigue of the specimens of aluminium used in Chapter 3, observations were made of the development of slip bands and crack initiation using the technique described in that chapter. These observations were supplemented by ordinary optical and electron microscope studies of the surfaces resulting from deformation by fatigue. Similar studies were also made on copper.

Before reliable observations on deformed metals can be made with the electron microscope it is necessary for the specimen to have a good surface before the start of deformation. In the present case this was done by the following procedure. Both aluminium and copper specimens were emeried through the usual stages down to 000 paper. They were then annealed and the required surface was subsequently obtained by electrolytic polishing. A potentiometric type circuit was constructed which suited both metals. The solution used for aluminium consisted of 200 ml perchloric acid in 1000 ml ethyl alcohol. The cathode consisted of a cylindrical aluminium sheet. The specimen was rotated vertically in the solution which was heated up to some temperature between 75-80°C. This solution temperature was found to be critical and when polishing was carried out at lower temperatures pitting was severe. The optimum voltage was found to be 24 volts

for a duration of two to five minutes.

The copper was polished in a solution of 700 ml orthophosphoric acid and 350 ml distilled water. In this case the specimen was rotated underneath the copper cathode and made an angle of 45° with the horizontal. Vertical polishing gave severe pitting. The specimens were polished for 7-10 minutes at 1·3v. Temperature was not found to be critical.

Using the above methods an excellent surface finish was obtained on both copper and aluminium. Optical observations were made using the Vickers projection microscope, and all electron microscope studies were made with the Metro.-Vickers E.M.3.

Replicas for electron microscope examination were made by the following technique specially developed for this present work.

Perspex (1/2" x 1/2" x 1/16") previously washed in warm soapy water followed by distilled water was clamped on to the surface to be examined with a pressure of a few lbs/in^2 and the assembly was heated for one hour at 120°C. The perspex impression was then removed from the specimen and carbon evaporated on to it under high vacuum. To protect this carbon film a layer of nitrocellulose was deposited on to the surface from a 2% solution in amyl acetate. Thus treated the replica was examined under the light microscope and a grid placed on the area of interest. A small disc of paper was placed on the grid of slightly smaller diameter than the grid, so that the rim of the grid was just visible. Gummed paper was then

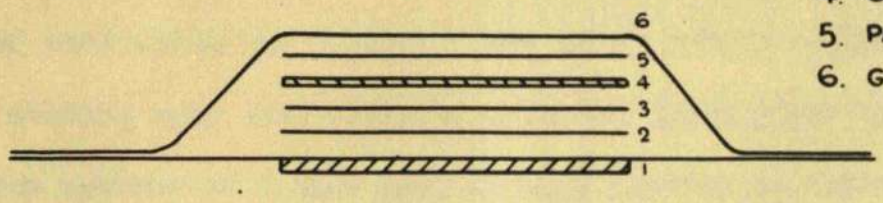

1. AREA TO BE EXAMINED
2. CARBON FILM
3. NITRO CELLULOSE
4. GRID
5. PAPER
6. GUMMED PAPER

FIG. 1.

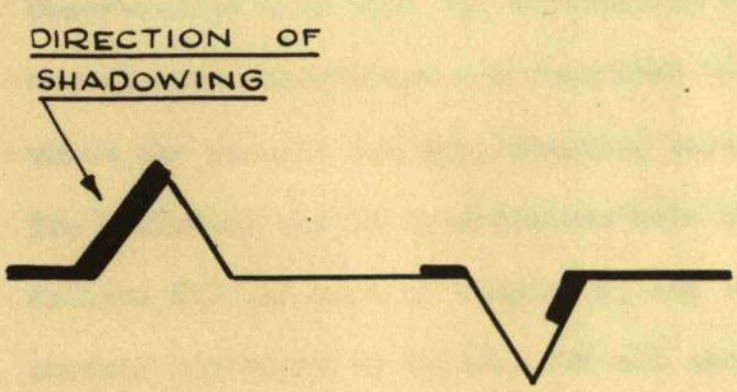

POSITIVE SHADOWED CARBON REPLICA.

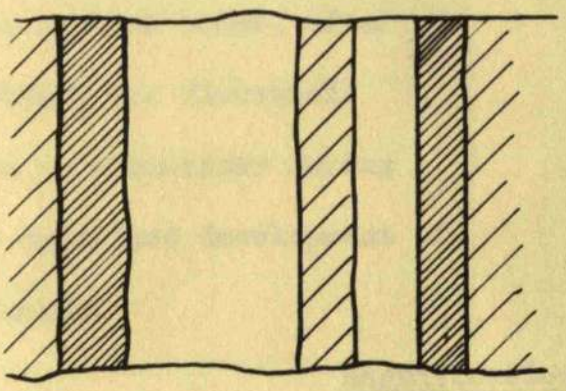

RESULTING PRINT FROM ELECTRON MICROSCOPE PHOTOGRAPH

FIG. 2.

stuck on the whole of the replica, covering the paper and grid and holding it in place. This complete assembly is shown in Fig. 1. Soaking overnight in chloroform removed the perspex, the gum of the paper used being insoluble. The grid, carbon replica and nitro cellulose coating were then released from the brown paper and placed with carbon upwards on a wire mesh in amyl acetate to remove the nitrocellulose and thus leave the positive carbon replica seated on the grid. The replica was then given a final wash in distilled amyl acetate, after which it was shadow cast with gold-palladium at an angle of 18°.

The resulting prints made from the photographs taken in the electron microscope may be interpreted with the aid of Fig. 2. Observations made with the stroboscope technique, optical microscope, and electron microscope are described below in that order, after which the results all supplementing each other, are discussed. The following direct observations were made on a specimen during fatigue for the work of Chapter 3, and the described development of surface structure is typical for all speciments.

Fatigued up to	Comments	Magnification Used
0-2000 cycles	Stress building up to ± 2250 lbs/in^2 slip bands appearing at notch; these bands are fine, straight and evenly spaced	x100
3,000 to 5,000 cycles	Slip bands at both notches becoming darker	x100
6,000 cycles	Waxy slip lines appearing; slip bands starting to develop away from notch	x100

7000 cycles	Slip bands forming in many grains at centre of specimen	x100
8000 to 15,000 cycles	Slip bands continuing to darken and broaden; some grains noted apparently quite free from slip	x100
25,000 cycles	Still no reflected oblique illumination observed	x500
35,000 cycles	Many bands appear to be continuous across grain boundaries	x100
38,000 cycles	Slip bands showing up under oblique illumination and forming what appears to be extruded material	x500
72,000 cycles	High extrusions observed throughout slip bands. These stand proud of the metal and it is possible to focus the microscope on top of them	x500

Throughout the observations it was noted that slip bands would often stop short of grain boundaries and then approach gradually. Grain boundaries stopped some slip bands for the duration of the test, other slip bands however were observed to continue over grain boundaries and develop in an adjacent grain; this process could occur over several grains.

Normally a crack formed in the specimen after $1{\cdot}4 \times 10^5$ cycles. It usually occurred at a notch and in a grain boundary which had become darkened at a very early stage of the fatigue test. These cracks propagated either in grain boundaries or through grains. It was noted that if the crack entered an actual grain, then the grain often darkened due to dense slipband formation. Even in these dark regions, however, it was still usually possible to observe

BRACKETED MAGNIFICATION IS THAT USED FOR REPRODUCTION

FIG 4 x 150 (x3)

FIG 6 x 150 (x3)

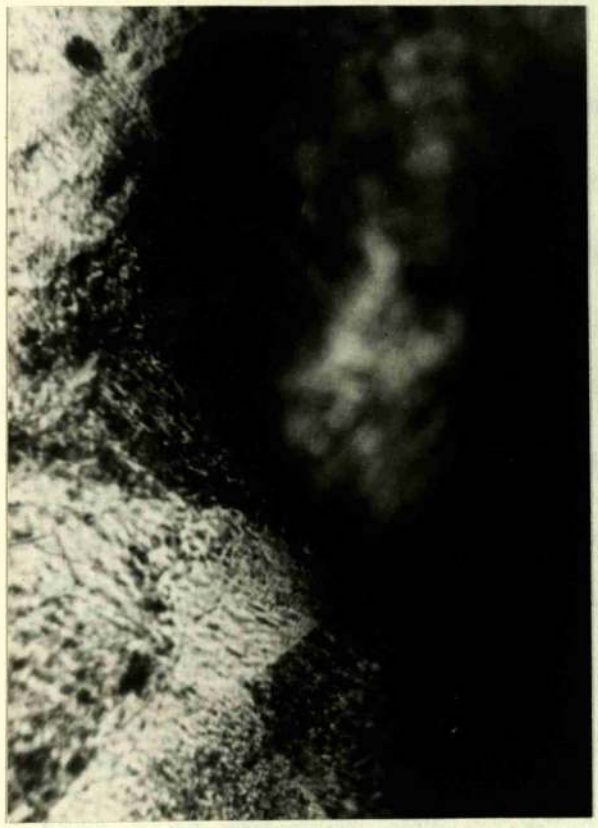

FIG 3 x 150 (x3)

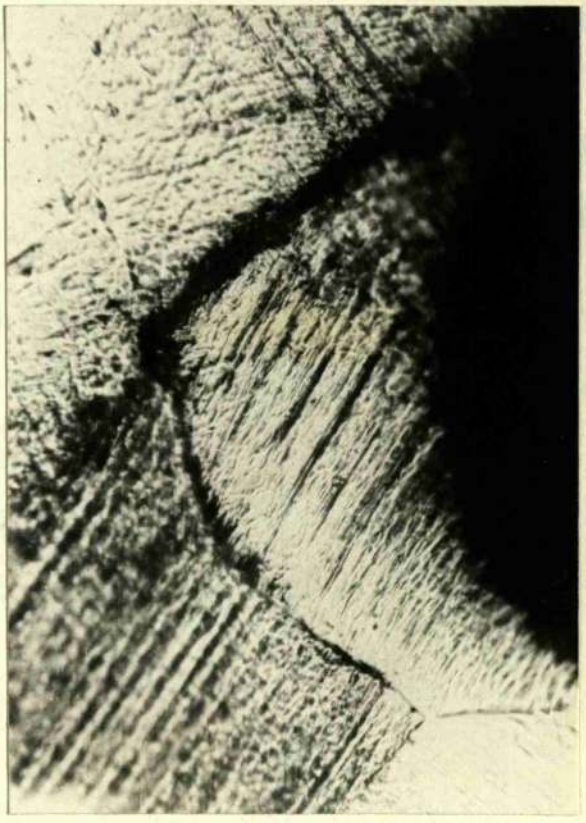

FIG 5 x 150 (x3)

the progress of a crack by means of oblique illumination. This observation is an indication of the high stresses which exist at the tip of a crack.

The above observations of slip bands continuing across grain boundaries are in agreement with the observations of Thomson[38] made on copper and also of Smith[39] on aluminium, and discussed in Chapter 1. There is no doubt that the observed cracks started at grain boundaries. Figs. (3) and (5) show what appears to be cracks starting at boundaries. By means of subsequent electrolytic polishing and removing all traces of slip bands, these regions were shown to be cracks, Figs. (4) and (6). Figs. 3 and 4 Chapter 3 show a further example of this. Recently Smith[39] has also observed cracks originating in grain boundaries in annealed aluminium at room temperature; this type of crack initiation was suppressed by fatiguing at -73°C. Smith suggested that the lower melting point of aluminium was the cause of grain boundary cracking. Kemsley[17] however has shown that intercrystalline fatigue cracks form in annealed copper when high stresses are used ($\pm$ 25,000 lbs/in^2) while crack initiation and propagation was either transcrystalline or along twin boundaries at low stresses. Kemsley has attributed intercrystalline failure to surface wrinkling and the formation of valleys at grain boundaries which in turn act as stress raisers.

It may be concluded from the observations made to date that high stresses tend to give intercrystalline fracture. The

total life of the specimens shown by Smith was 227,000 cycles, which indicates that a high stress was used.

In the present work the life of the specimens were approximately 140,000 cycles and it is expected that high stresses would be set up in the region of the notch. It is noteworthy that delineation of the same grain boundaries at the notch occurred very early in the test.

The bulk of microscope investigations of fatigued surfaces have been concentrated on slip band development and crack initiation in these regions. As a result of this the present theories of crack initiation have been developed to account for transcrystalline failure. As far as the writer knows, no exact model has been proposed which will account for intercrystalline failure.

The causes of intercrystalline failure proposed by Kemsley for annealed copper fatigued at high stresses cannot be applied directly to the present results obtained with aluminium since, as will be shown, extreme surface deformation also takes place inside the grains and this will probably give rise to stress concentrations at least comparable with the delineated grain boundaries. The lower melting point of aluminium may be of importance as suggested by Smith.

Attempts were made to take a cine film recording of the development of surface structure during fatigue. These were successful only at magnifications of x25. At higher magnifications it was necessary to use a Paillard Bolex Reflex camera for maintaining

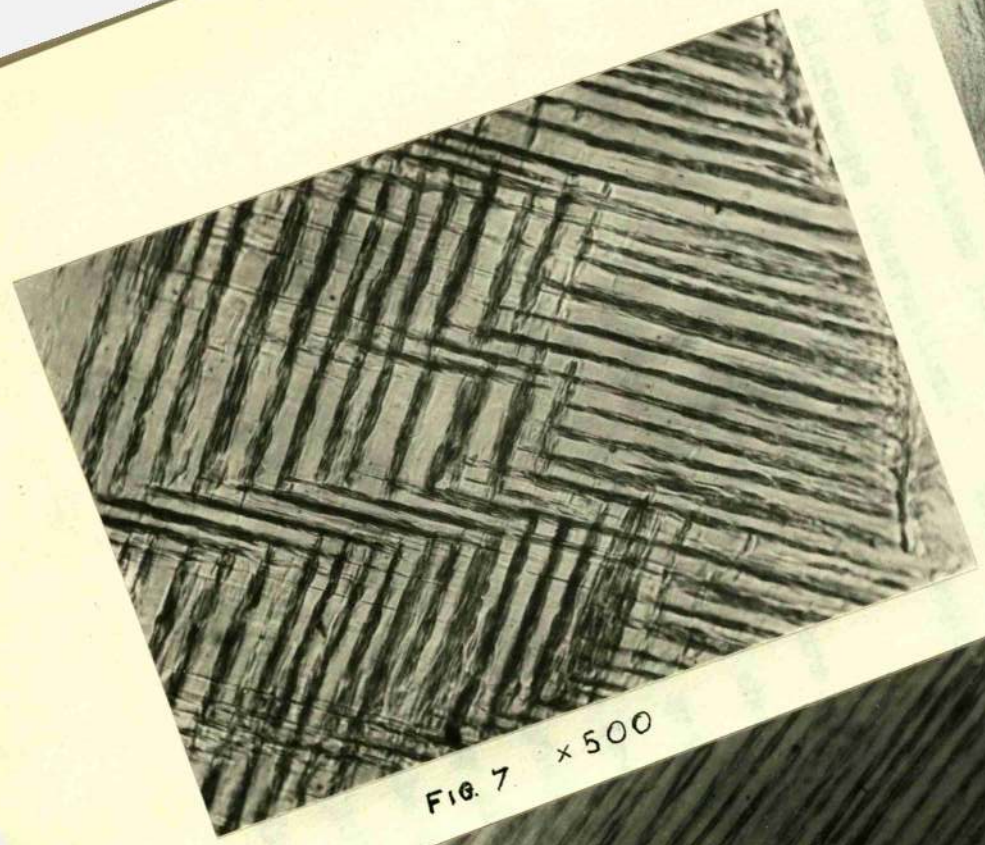

FIG. 7 ×500

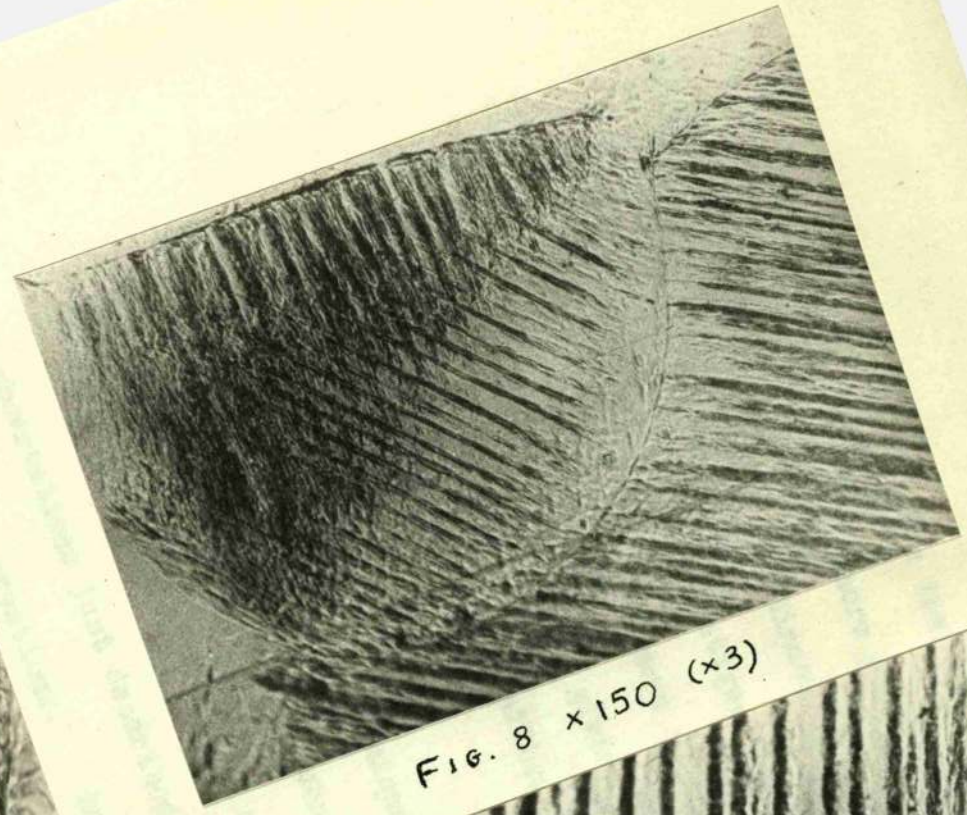

FIG. 8 ×150 (×3)

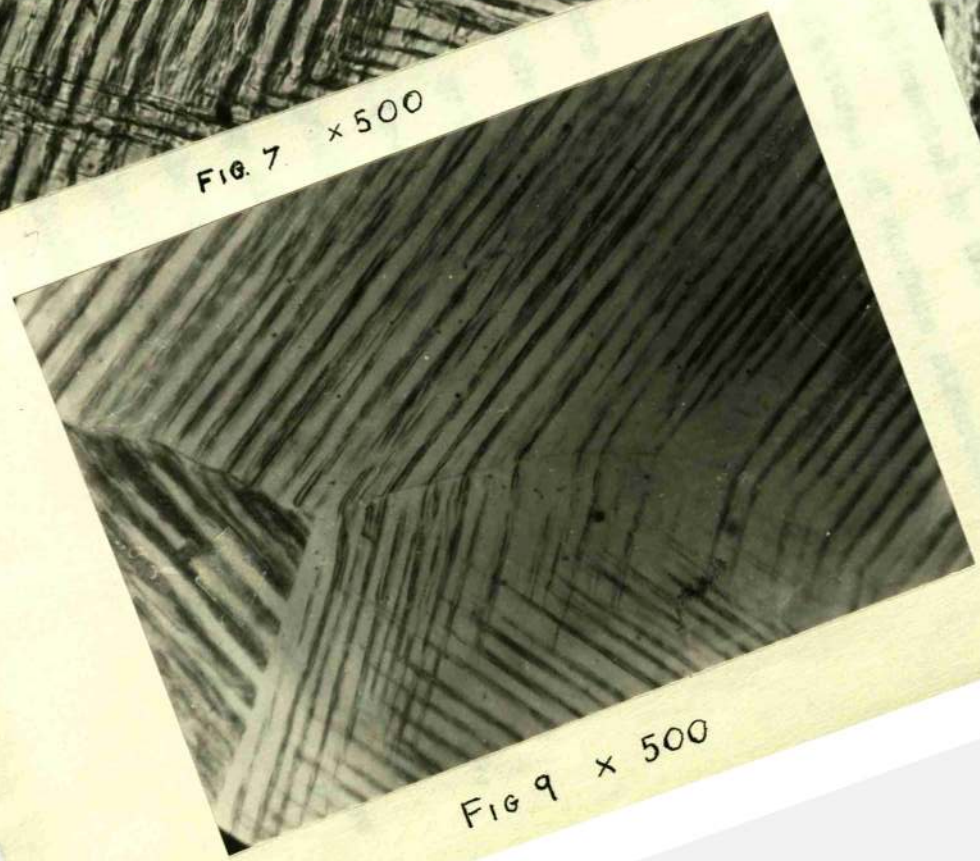

FIG 9 × 500

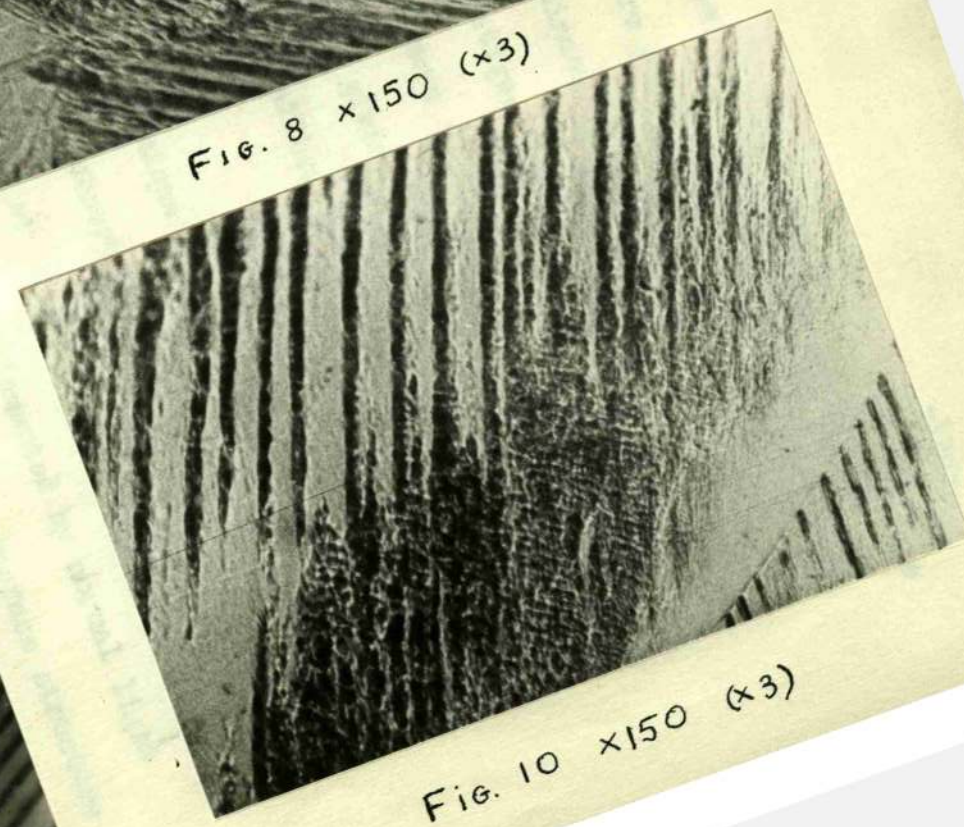

FIG. 10 ×150 (×3)

sharp focus, and for this camera insufficient lighting was obtainable from the stroboscope. With a more powerful light source however it would be possible to make a continuous photographic recording at magnifications up to x 500 of fatigue failure. Even at x 25 using a Bell and Howell cine camera it was necessary to use Ilford H.P.S. film developed in Ergol, giving a photographic speed of 1500 Weston. At these low magnifications little information could be obtained from the cine film.

The stroboscopic technique could have wide application in fatigue studies especially for observing rates of crack propagation and the effect of second phases or inclusions on these rates. The observations just described are supplemented by normal light microscope observations. Relevant features of surface structure due to fatigue were noted and photographed in the cases of aluminium and copper.

Typical fatigue structure as observed on the aluminium specimens used in Chapter (3) is shown in Figs. (7) and (8). Figure (9) shows slip bands crossing a grain boundary and developing in an adjacent grain. Even at these low magnifications, it is possible to note the complexity of the striations formed in fatigued aluminium. Figure (8) suggests that the waxy slip shown, and typical also of iron, depends on the direction which the operating slip plane is making with the applied stress; Fig (10) however shows that localised stress conditions in a grain are more likely to be responsible. Indeed, a

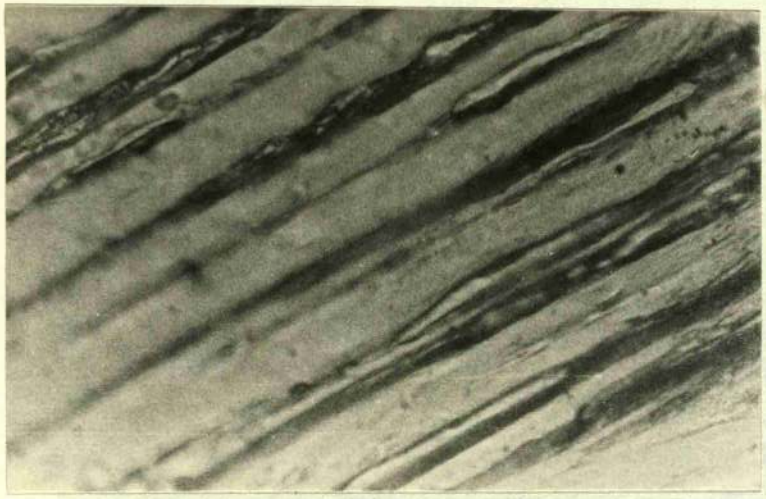

Fig. 11 x 720 (x 3)

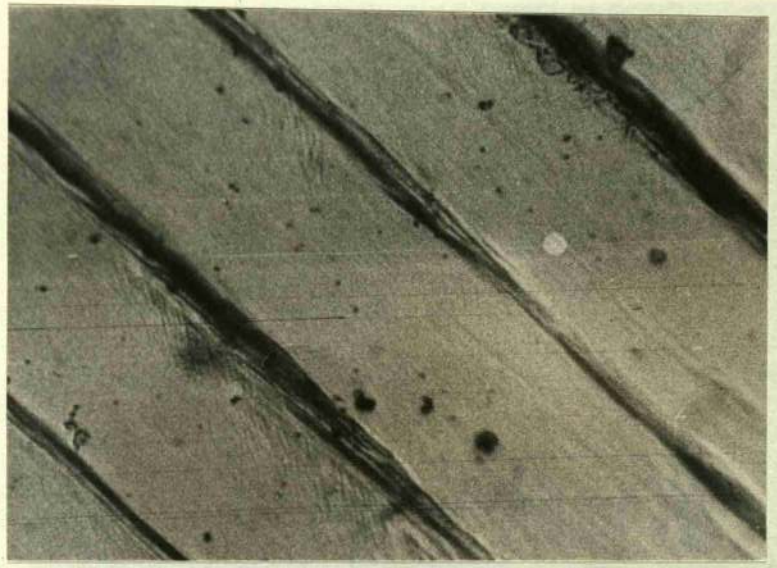

Fig. 12 x 720 (x 3)

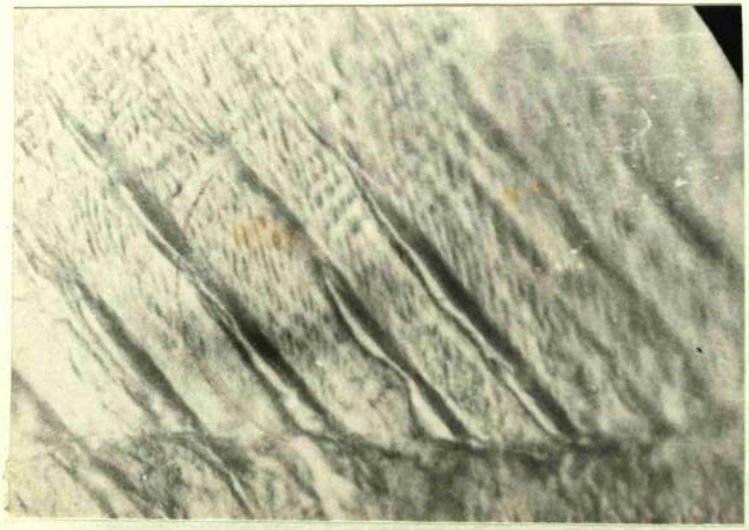

Fig 13 x 720 (x 3)

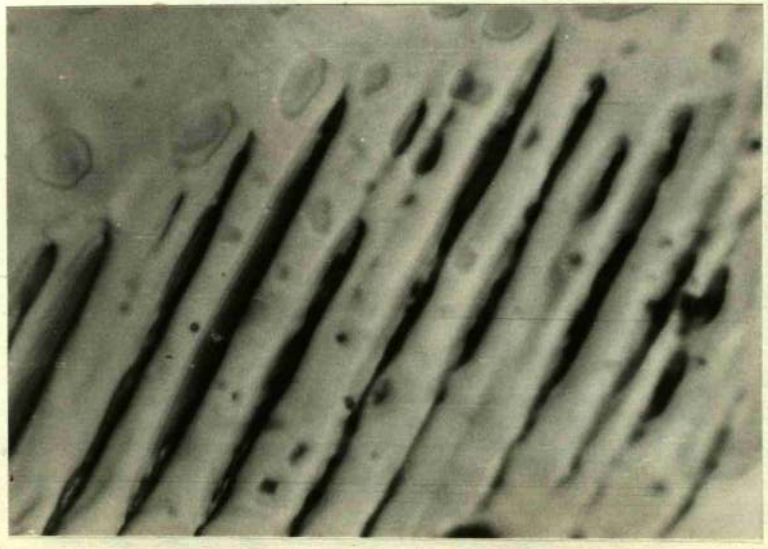

Fig. 14 x 720 (x 3)

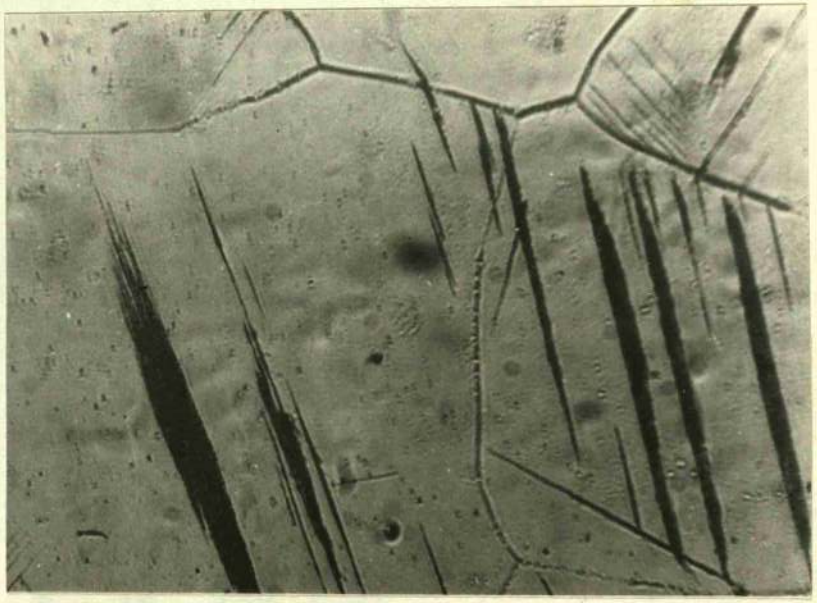

FIG. 15 × 25 (×3)

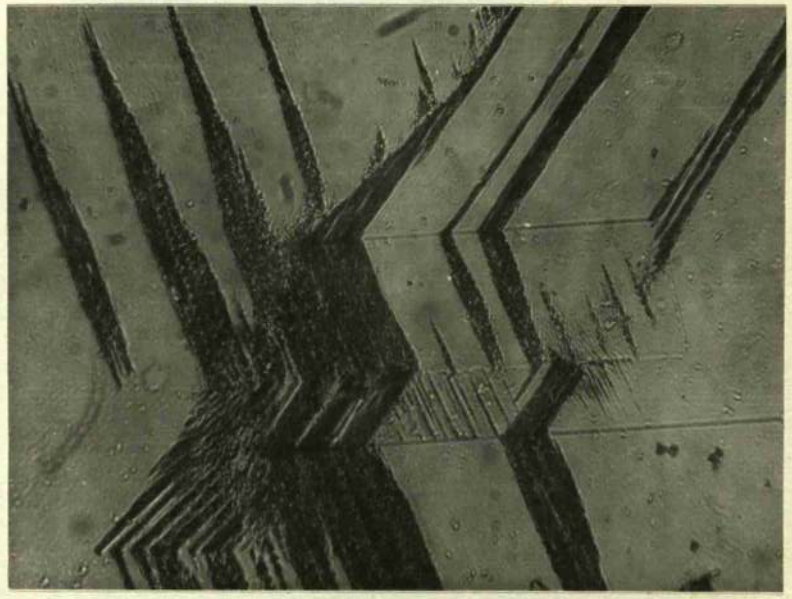

FIG. 16 × 250 (×3)

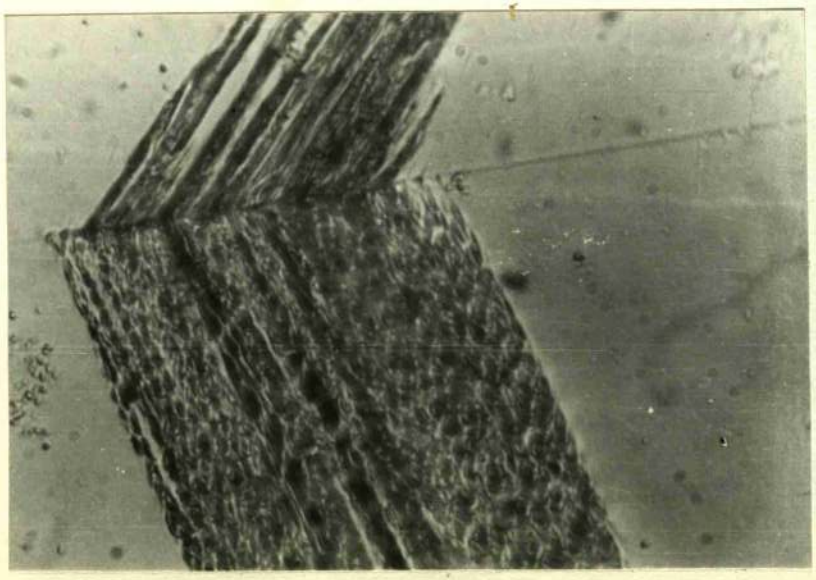

FIG. 17 × 830 (×3)

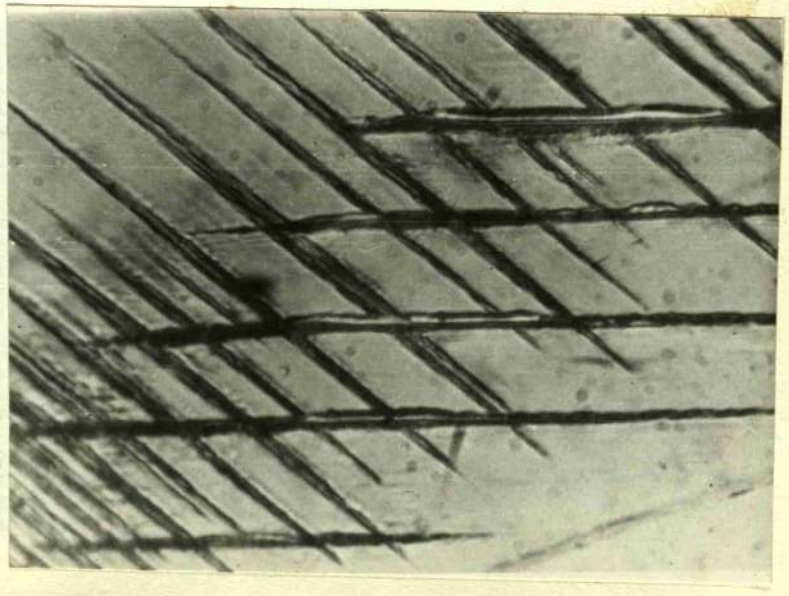

FIG. 18 × 830 (×3)

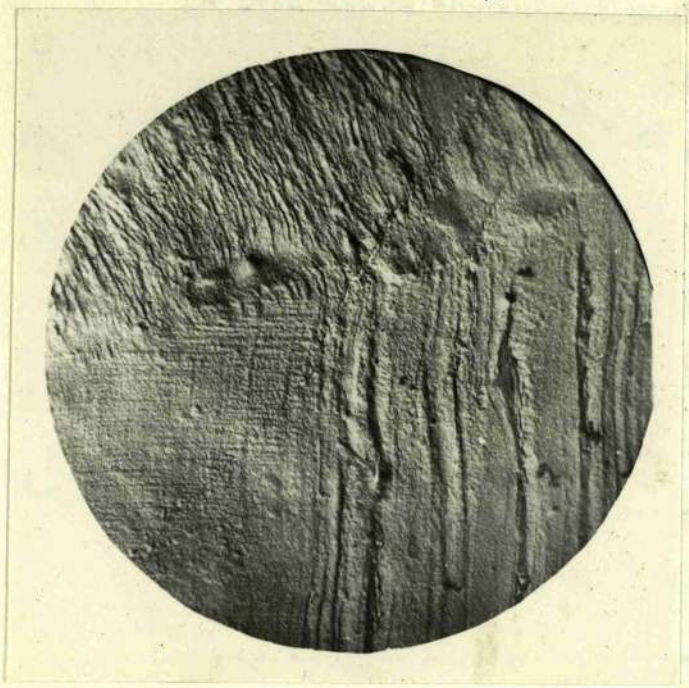

Fig. 20

All electron microscope photomicrographs taken at approximately x 8000.

Fig. 21.

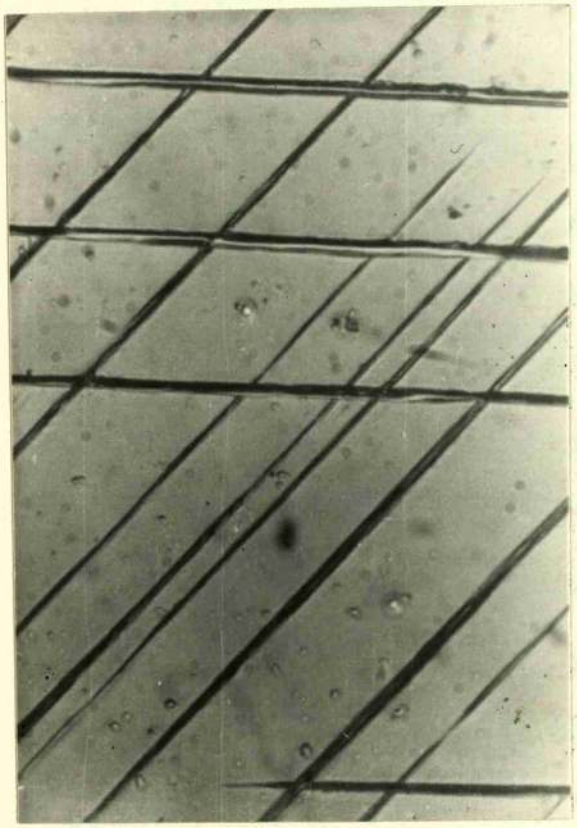

Fig. 19 x 830 (x3)

feature of fatigue deformation is the non-homogeneous distribution of slip bands throughout specimens as a whole and inside grains themselves. Figs. (11), (12) and (13) show the fatigue structure at higher magnifications. Fig. (11) shows what appears to be valleys in the case of some striations and erupted material in others. Fig. (12) shows other striations which demonstrate the grooving effect more clearly; and Fig. (13) shows clearly smooth films of material rising above the surface of the metal. Subsequent electrolytic polishing of these surfaces firstly removes most of the surface features; traces of the coarse structure featured in Figs. (12) and (13) however are left. The valleys appear more rounded while the films of material are removed or partly left depending on their initial size. Fig.(14) shows some of the larger films which remain after electrolytic polishing. No estimate was made of the depth of metal removed by polishing.

Fatigue Structure of Copper as Studied using the Light Microscope

It should be pointed out that in the specimens examined large regions were present on which no fatigue structure was apparent.

The specimens used for this work were annealed bars 3/16" square by 10 cms. long machined from rolled 3/16" B.S.S. 1861 sheet copper. The stress used was $\pm$ 10,680 lbs/in^2 about a mean of -480 lbs.

Figure (15) shows typical fatigue structure of copper. This demonstrates clearly the non-homogeneous distribution of slip bands. The majority of bands are stopped by grain boundaries; however, some propagate across them. Twin boundaries do not affect

the development of slip bands to the same extent as grain boundaries as can be seen from Figs.(16) and (17). Slip bands often stop long before reaching a grain boundary. Even at x 1300 the fine structure of these broad slip bands was not at all clear. The characteristics of fatigue bands in copper are quite different from those of aluminium, no waxy slip lines such as shown in Fig. (10) being observed in the former.

Fig. (18) shows valleys in some of the striations and also well developed films of material rising above the surface similar to those observed in aluminium. Fig. (19) shows that these films can extend unbroken for considerable distances along the length of a slip band.

Electron Microscope Studies of Fatigued Surfaces in Aluminium

The direction of shadowing is indicated by the arrow placed beside each photomicrograph.

Fig. (20) shows slip bands meeting at a grain boundary. The typical waxy structure of fine slip lines in aluminium can be seen clearly on the left hand side of the boundary. From this figure and the circled region in Fig. (23) an indication is obtained of the cause of the waxy appearance. It appears to be the result of very fine cross slip occurring frequently throughout the slip lines. In Fig.(21) slip lines can be seen stopping short of a grain boundary.

As was noted with the light microscope surface wrinkling inside the grains of aluminium was often very marked; this is demonstrated

FIG. 22

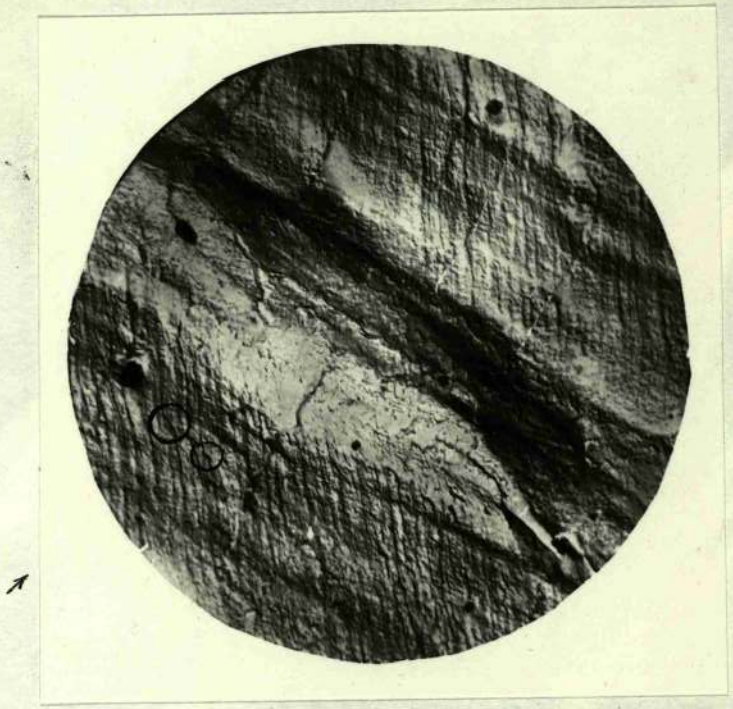

FIG. 23.

FIG. 24

FIG. 25

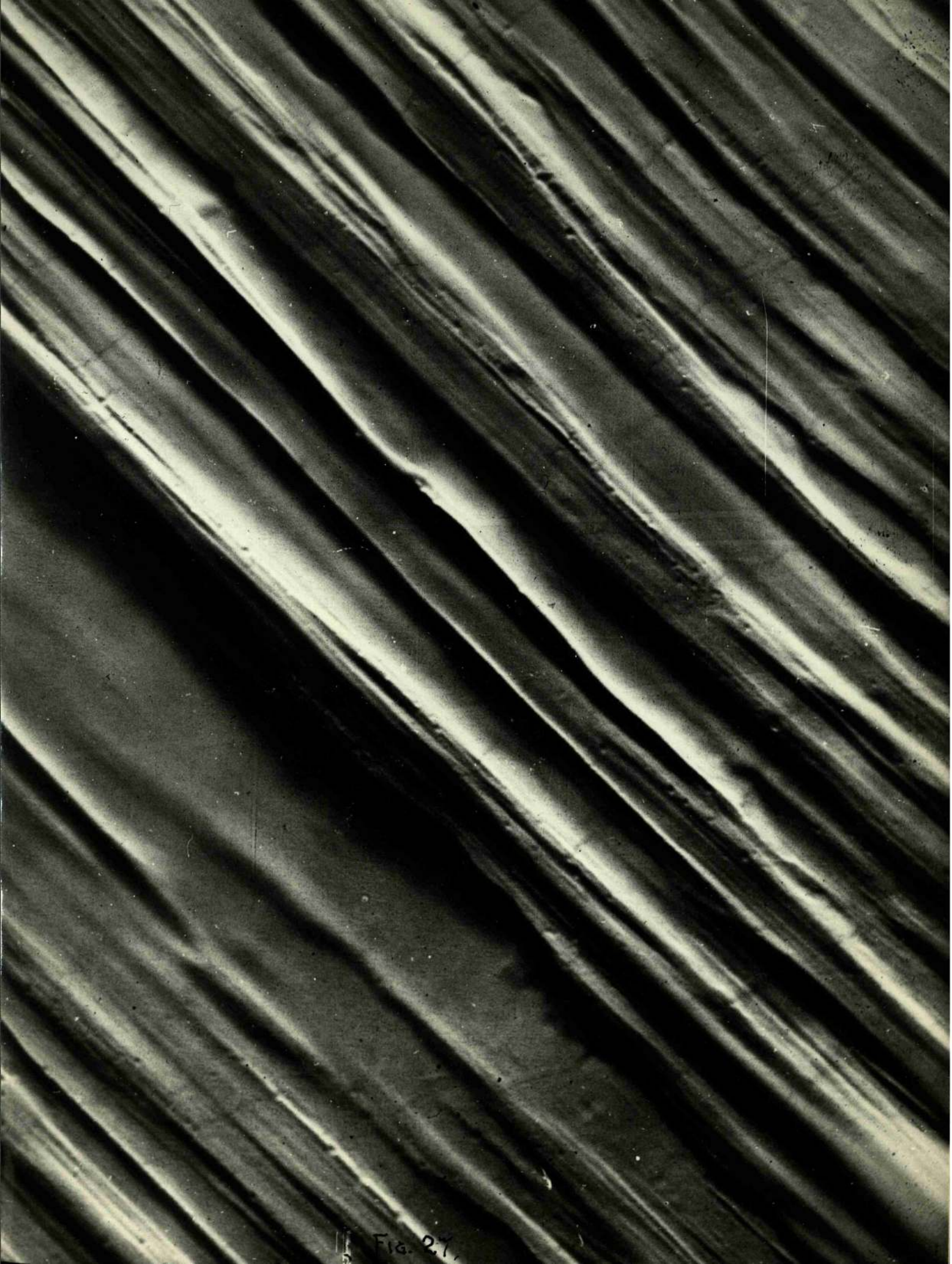

Fig. 27.

more clearly with the electron microscope.

Figs. (22) and (23) show narrow and very broad intrusions respectively, the intrustion of Fig.(23) being part of a broad band crossed by fine waxy slip. Figs.(24) and (25) show narrow and broad extrusions respectively. The torn extrusion in Fig.(24) in particular appears to be composed only of a thin film of material. In Fig.(26) the general surface distortion which can occur during the development of coarse slip striations can be seen.

Fig. (27)+ is a transmitted light photograph of one of the fatigued aluminium specimens. This was taken by means of a new replica technique developed for examining surfaces with the light microscope. A cellulose acetate replica is made of the surface to be examined. The replica is next heavily shadowed with chromium after which it is coated with formvar for protection. The total magnification of Fig. (27) is approximately x 9000 and the structure shown is comparable with that shown in the electron micrograph of Fig.(26); i.e. the severe surface wrinkling which can arise during fatigue is clearly demonstrated.

Electron Microscope Studies of Fatigued Copper

As with aluminium the structure of well developed slip bands was resolved to a much greater extent than was possible

---

+ The photomicrograph was kindly taken by D.H. Page of the British Paper and Board Industry Research Association.

FIG 26

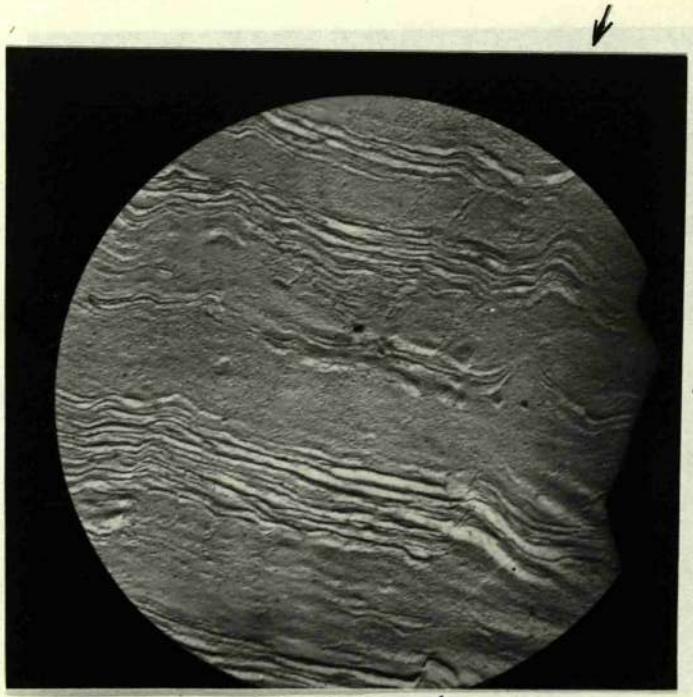

FIG 28

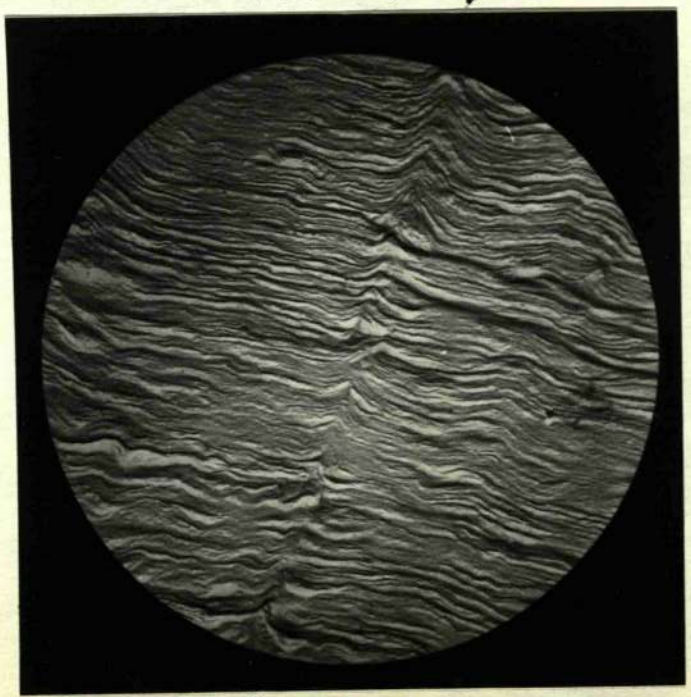

FIG 29

FIG 30

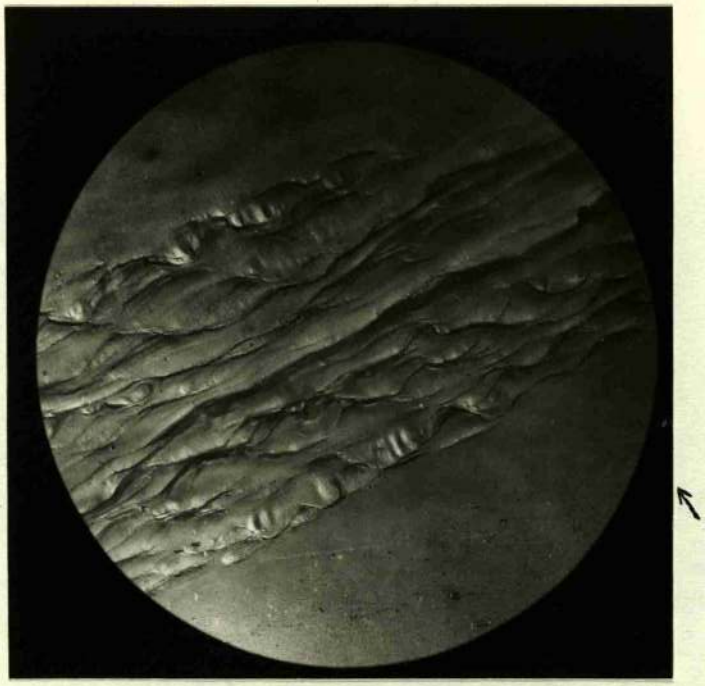

Fig 32.

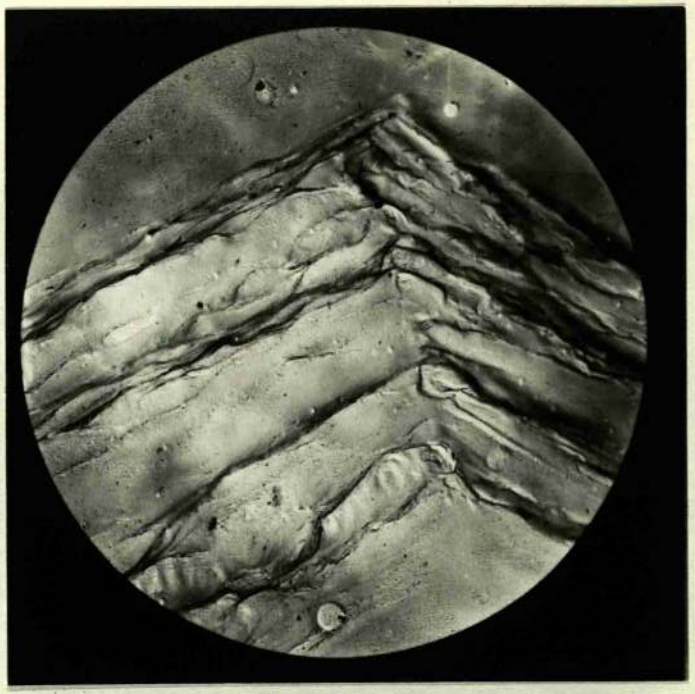

Fig. 31

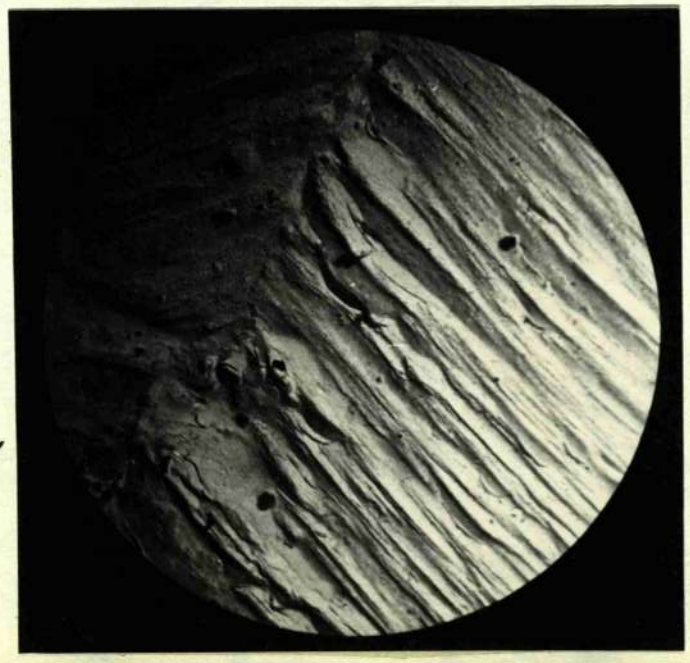

Fig. 33

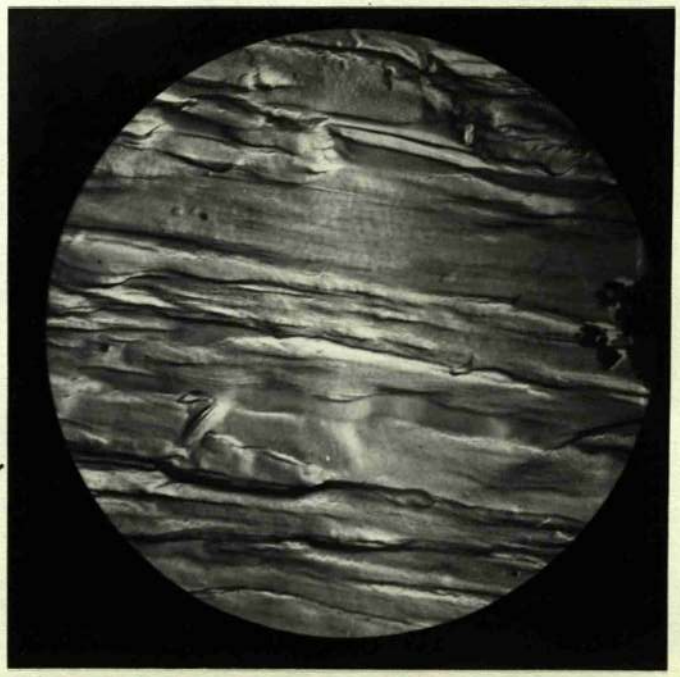

Fig. 34

using the light microscope.

Figs. (28), (29), (33) and (34) are taken from a specimen cycled to fracture by a stress of $\pm$ 10,680 lbs/in^2 about a mean of -480 lbs. Figs. (30), (31) and (32) are taken from a specimen cycled for 100,000 cycles, approximately 1/20th of its life at the same stress as above. The fine structure of fatigue slip bands in copper can be seen in Fig.(28) and Fig.(29). In both the above cases disturbance of the surface is small. The kinking of the slip bands in the region indicated by the arrows was observed frequently and at present no explanation can be found which might account for it. Figs. (30) and (31) both show slip bands crossing a twin boundary; Fig. (30) demonstrates well how a broad band can be composed of several small bands such as the one at the bottom of the picture. In both these figures extrusions and intrusions are apparent, surface wrinkling is quite severed in the case of Fig.(31). Figs. (32), (33) and (34) all show the composition of well developed slip bands. In all these figures extrusions and intrusions can be seen in various stages of development. It should be noted that the metal in Fig.(33) has been fatigued for approximately twenty times the number of cycles for that in Fig. (32). The areas in between slip bands in Figs.(28), (30), (31) and (32) all appear to be free from slip; this does not rule out the possibility that slip has occurred in these regions and is too fine to be resolved with the technique and electron microscope used, or that it has left no surface markings.

Discussion of Observations

The optical and electron microscope studies just described give rise to many questions which must be answered before the problem of fatigue is understood.

The delineation of grain boundaries and the initial initiation of cracks in grain boundaries at high stress has already been discussed. It should be noted however that these high stresses were localised to the region of the notches in the specimens described. The bulk of the material was subjected to alternating stresses which were low enough to give typical fatigue structure. This is demonstrated by Fig.(8) which shows fatigue structure stopping well inside a grain. To verify this both the aluminium and copper were tested for asterism. The specimens so tested were those which had received the highest stresses applied to annealed materials in this work. Figure 35 shows a back reflection X-ray diffraction photograph taken from a region between the notches of specimen (5) Chapter 3 where apart from the actual vicinity of the notch, the stress will be at its highest; three other such photographs were taken of fatigued aluminium used in the present work and all gave sharp spots typical of Figure 35. Figure 36 is a typical result obtained from a copper specimen. For the sake of comparison an annealed specimen which had been stressed by 8% in tension was examined and the severe arcing of the spots is shown in Fig.37. Fatigue of hard worked material and fatigue of annealed metal cycled at low stresses always gives rise to

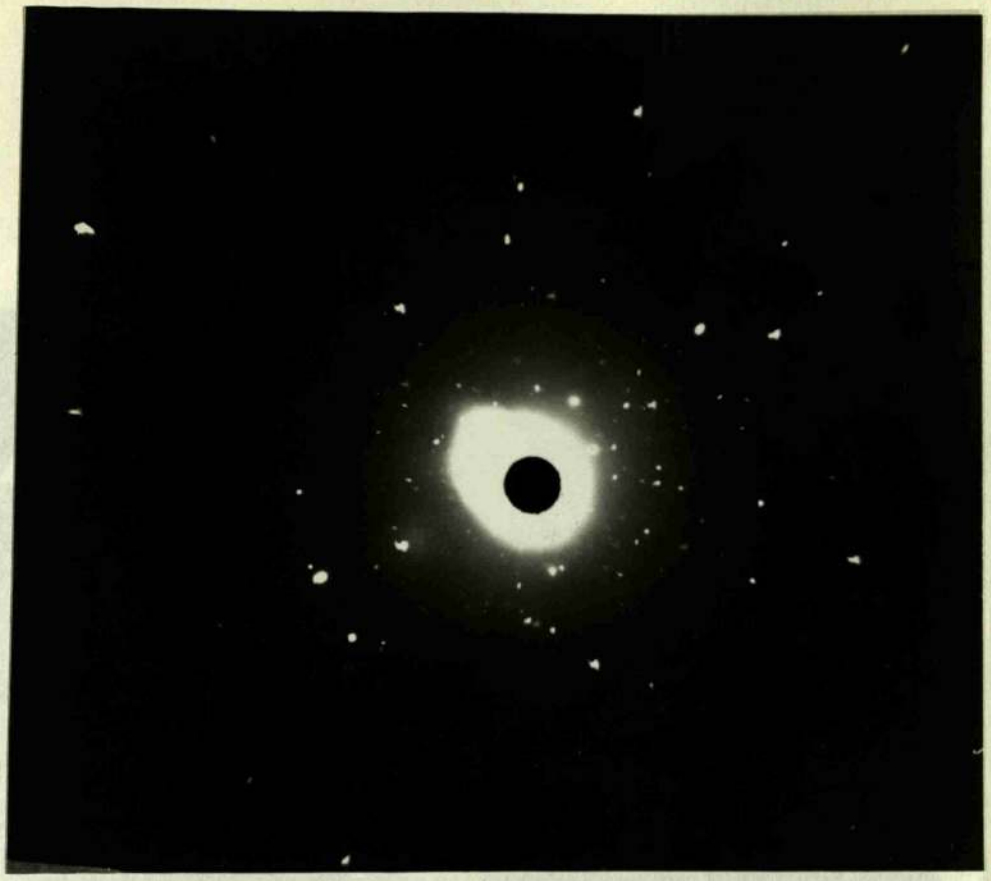

FIG 35

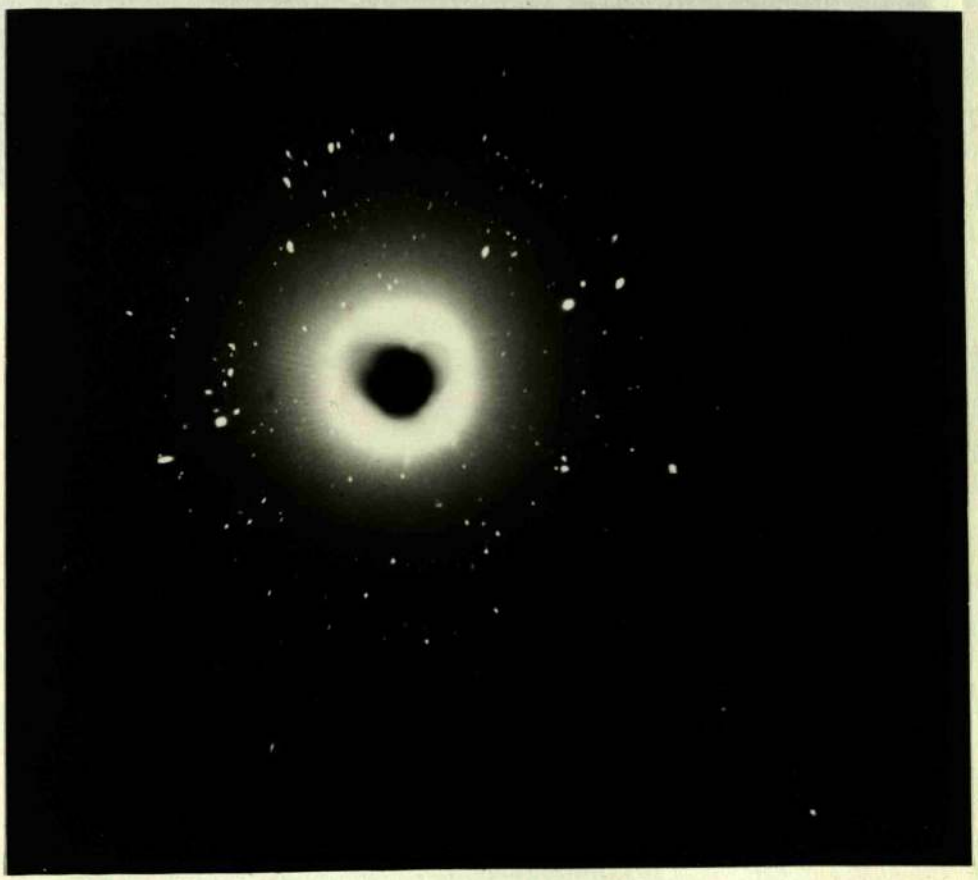

FIG 36

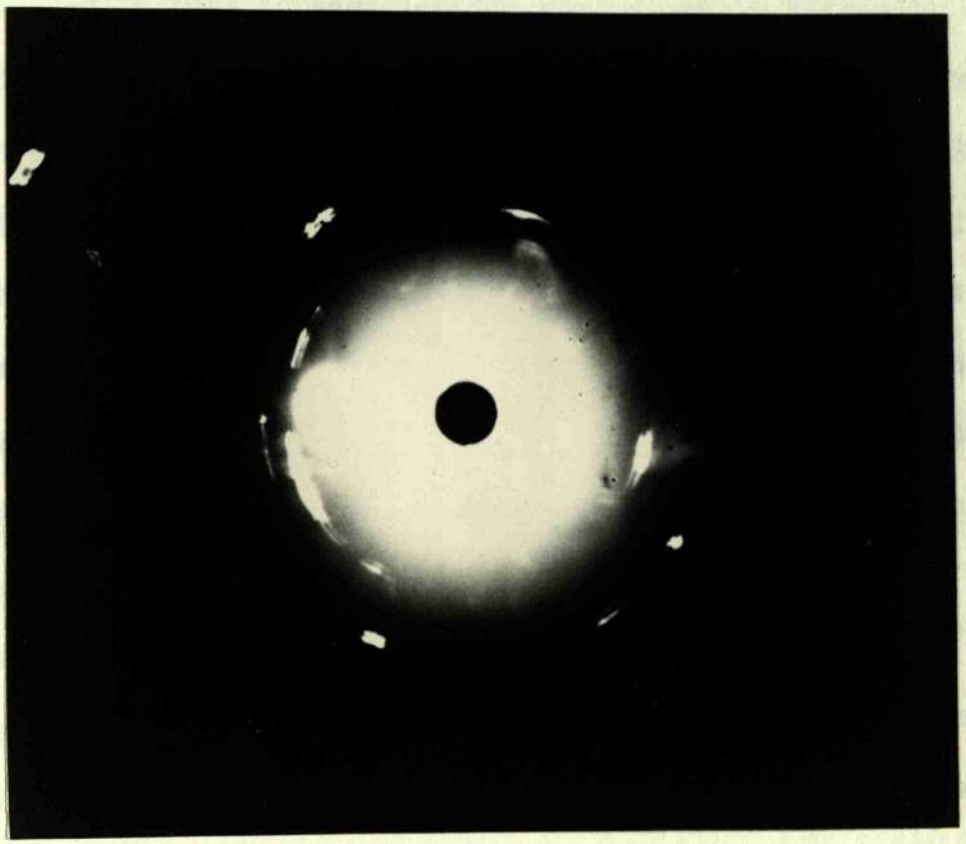

Fig. 37

transcrystalline fracture, with crack initiation starting in regions of slip. This aspect of fatigue surface structure is therefore most important and will now be discussed.

Slip band intensification during cyclic stressing has been observed with the stroboscopic technique resulting in well developed slip bands such as shown in Figs. 7, 15, 16, 17, 22, 29, 30, 32 and 33. Their development has been shown to occur without giving rise to asterism in X-ray back reflection photographs. This means that piled up groups of dislocations are not necessary for the development of coarse slip bands. Broom and Ham[127] have recently shown that coarse slip bands can develop during fatigue of single crystals at room temperature at stresses below those required to give the stage III region of the tensile stress-strain curve. It seems unlikely therefore that the recent theory proposed by Mott, and described earlier, will account for the development of coarse slip bands during fatigue, since this theory depends on annihilation of dislocations by cross slip such as takes place in the stage III region mentioned above. It will now be shown that cross slip may not be essential for the development of coarse slip bands.

Alternative Mechanism for Fatigue Slip Band Formation

In the literature survey it was shown that vacancies appear to be produced in abundance during fatigue. The work of Chapter 4 substantiates this. When slip is operating initially in a fine slip line, vacancies and divacancies will be created in abundance; these will diffuse into the surrounding metal and permit dislocation climb

in adjacent slip planes. If these adjacent slip planes were in a hardened condition they will now be softened by the removal of these dislocations which have climbed out of the plane. The neighbouring slip planes to the original will now be able to operate.. This process could continue until very wide bands are built up.

It is quite reasonable that hardening should occur in regions between the slip bands as shown by Broom and Ham[36,127] while the areas on either side of the operating slip bands will be softened. The concentration of vacancies on either side of the slip band will be high and will enable gross climb of dislocations while between the slip bands the concentration of vacancies will be much smaller, and after room temperature annealing will be sufficient only to either pin or introduce jogs in the dislocations and thus anchor them.

In copper fatigued at higher stresses cross slip may also occur during fatigue as suggested by Mott[15] and further contribute to softening in the immediate vicinity of the slip band, it is not known yet whether this stage III type of dynamic softening occurs during pure fatigue of copper.

In aluminium the high stacking fault energy will give rise to narrow screw dislocations, which will in turn be able to cross slip at much lower stresses than in copper.

The above theory is quite consistent with observations made using X-ray stored energy and hardness measurements. The softening of hard worked metal can also be accounted for by this mechanism quite readily.

a

b

SECTION OF BROAD AND NARROW EXTRUSIONS

FIG 38

SECTION OF BROAD AND NARROW INTRUSIONS

Slip bands have been observed to stop inside grains and away from boundaries, see Figs. (8) and (15). The exact cause of this is not yet known. This effect may be due to either Cottrell-Lomer barriers or to intersection with forest dislocations or some other unknown type of barrier.

The observed holding up of slip bands bear grain boundaries, Fig. 22, and stroboscopic observations, may be expected since back stresses will probably exist due to dislocation interaction with the grain boundary. Subsequent approach to the grain boundary might be enabled by climb of the dislocations by vacancies generated in the slip bands themselves.

The propagation of the slip bands through the grain boundaries may be due to stress concentrations at the end of the slip band which activates Frank-Reid sources in the adjacent grain, slip will then continue as described above. The waxy slip which has been observed in aluminium Figs. (8) and (10) is due to the ready cross slip which can occur in that metal. This in turn is due to the high stacking fault energy and therefore lower extension of the dislocations as already described.

Surface Disturbances of Fatigued Copper and Aluminium

Inspection of Figs. (12), (13), (18) and (24) -(27) shows that surface wrinkling of fatigued copper and aluminiun can be very severe. The present work showsthat extrusions and intrusions may take the forms shown in Figs. 38 a and b, i.e. they may exist in

either broad or narrow forms in the same metal.

In fatigued 99·99% pure aluminium Forsyth[19] observed striations similar to Figs. (7), (12) and (20) only, while in aluminium -4% copper the characteristics were quite different and high narrow extrusions such as shown in Figs.(13) and (26) were observed[28]. The appearance of the fatigue structure on the latter alloy could be made similar to that of the pure metal by fatiguing at -90°C. Forsyth concluded that the broad striations in the pure metal result from the same mechanism as the narrow extrusions he observed with the alloy, the difference arising from the restriction of the mechanism to narrow regions in the alloy; he attributed this restriction to the formation of soft regions in which overageing had taken place[28]. The effect of fatiguing the alloy at low temperatures would thus be to prevent overageing and therefore give the alloy the same fatigue slip band characteristics as the pure metal.

In the present work 0·2% impurity was present in the aluminium. It seems unlikely that this could act in the same way as 4% copper, yet high thin ribbons of material were extruded as shown in Figure (24). No precise explanation can be found for the above sets of observations. In the present case it appears that slip can be localised into narrow regions in one case or into broad regions in the other. The predominating type of region will most likely be influenced by such things as local temperature in slip bands, probability of dislocation climb and cross slip.

The extrusions and intrustions observed in copper in the present work are very similar to those observed by Hull[40], who also showed that these extrusions and intrusions could form at 4°K during fatigue of copper. This shows that their formation depends only on slip and not on such mechanisms as vacancy or interstitial migration. Both Cottrell and Hull[126], and Mott[15] have suggested mechanisms which might account for the formation of extrusions and intrusions; it is however impossible to say at present which, if either, of the proposed models is correct.

After looking at the notch-like structure which can result from deformation by fatigue, it is not surprising that cracks often initiate in slip bands due to stress concentration at these notches. Their propagation is a separate subject.

The great diversity in appearance of various regions shown throughout this work and the intensity of slip in certain regions compared with others must arise from the varying resolved shear stress in differing grains and local inhomogenities of stress inside the grains themselves. The duration of operation of any one slip band will also greatly influence its size.

GENERAL CONCLUSIONS

GENERAL CONCLUSIONS

The following are the general conclusions which may be drawn from the damping recovery results and optical and electron microscope studies applied to transcrystalline failure and from work published during recent years on fatigue.

Transcrystalline Failure

Room Temperature Fatigue

Slip bands develop both in volume and on the surface probably in the manner suggested earlier. These bands will be hindered at grain boundaries for obvious reasons, some however because of considerations such as the relative orientation of two adjacent grains will continue across boundaries.

The large amount of surface wrinkling which has been shown to occur in these bands, by direct observation, will act as stress raisers. These in turn once long enough, say two or three grains long, will permit crack propagation to start as has been suggested by Cottrell and Hull[126] and Mott[15].

The absorption of gases such as oxygen at room temperature will doubtlessly assist in the development of these bands into growing cracks. Room temperature grain fragmentation may also assist by producing additional lattice stresses.

Fatigue at Temperature below room temperature

Damping measurements have shown that vacancies are produced and are mobile at room temperature and therefore must modify the

process of fatigue in that temperature region. As the temperature of fatigue testing is lowered however the softening mechanism due to vacancies will gradually cease and slip bands will tend to be finer and more comparable with pure tensile slip bands. At even lower temperatures complex defects such as divacancies will also be immobilised.

The above must give a two-fold effect; firstly softening of regions surrounding the band will cease and secondly the operating band itself will form rather than will the growth of existing bands continue. The above hardening of the operating slip bands will continue to still lower temperatures where it is likely that interstitials also become frozen into the slip planes.[21] At lower temperatures the effects of grain fragmentation, and possibly also absorbed gases, will gradually disappear.

The gross result of these differences of low temperature fatigue will be an increasing fatigue strength with decreasing temperature. This is in agreement with recent experimental results obtained from fatigue at low temperatures.

Low temperatures will not however suppress dislocation motion and the formation of extrusions, intrusions and general surface wrinkling will continue. In this way stress raisers will always be formed on the surface of fatigued metals although the stress and number of cycles required to cause fracture will naturally increase.

The problems which remain unsolved are the mechanisms of crack propagation once the crack is initiated, and clarifying of the actual dislocation configurations in fatigued metal. Solving the latter problem and probably both would seem to be the lot of the electron microscopist.

Intercrystalline Failure

In this work, intercrystalline failure has been found to be a feature of annealed aluminium fatigued at a high stress level. Little is known theoretically about the behaviour of grain boundaries under cyclic stresses; therefore, an explanation of intercrystalline failure must await further developments in that field.

REFERENCES

1. Ewing, J.A., Humfrey, J.W.C., Phil. Trans. Roy. Soc., 200A, (1903), 241.

2. Beilbey, G.T., Proc. Roy. Soc. A., 79 (1907), 403.

3. Rosenheim, W., Ewing, D., J. Inst.Metals, 8, (1912), 149.

4. Gough, H.J., Hanson, D. Proc. Roy. Soc., 104A, (1923), 538.

5. Wood, W.A., Segall, R.L., Proc. Roy. Soc., 242A, (1957), 180.

6. Orowan, E., Proc. Roy. Soc., 171A, (1939), 79.

7. Rosenheim, W., J. Inst. Metals, 8, (1912), 149.

8. Wadsworth, N.J., Thomson, N., Phil. Mag., 45, (1954), 223.

9. Forsyth, P.J.E., J. Inst. Metals, 82, (1954), 449.

10. Bullen, F.P., Head, A.K., Wood, W.A., Proc. Roy. Soc., 216A, (1953),332.

11. Wood, W.A., Int. Conference on Fatigue of Metals, Session 6, Paper 4.

12. Clarborough, L.M., Hargreaves, M.E., West, G.W., Proc.Roy.Soc., 242A, (1957), 160.

13. Kemsley, D.S., J. Inst. Metals, 87, (1958), 10.

14. Clareborough, L.M.,J. Inst. Metals, 7, (1955), 99.

15. Mott, N.F., Acta. Met., 6, (1958), 195.

16. Seeger, A., Dislocations and Mechanical Properties of Crystals (Wiley and Sons), 1956, p.243.

17. Kemsley, D.S., J. Inst. Metals, 85, (1957), 420.

18. Cottrell, A.H., Vacancies and other point defects in Metals and Alloys, Inst.. of Metals Monograph and Report Series, No. 23, page 1.

19. Broom, T., and Ham, R.K., ibid , page 41.

20. Koehler, J.S., Henderson, J.W., Bredt, J.H., Dislocations and Mechanical Properties of Crystals,(Wiley and Son), (1956), p. 243.

21. McCammon, R.D., Rosenberg, H.M. Proc. Roy. Soc., 242A, (1957), 203.

22. Mason, W.P., Physical Acoustics and the Properties of Solids, 1958, Van Norstrand.

23. Mott, N.F. Dislocations and Mechanical Properties of Crystals (Wiley and Son), 1956, p.458.

24. Seitz, F., Advances in Physics, 1, (1952), 43.

25. Hanstock, R.F., Murray, A., J. Inst.Metals, 72, (1946), 97.

26. Hanstock, R.F., J. Inst. Metals, 83, (1954), 11.

27. Hanstock, R.F. International Conference on Fatigue of Metals London, 1956 Session 5, paper 2.

28. Forsyth, P.J.E., Stubbington, C.A., J. Inst. Metals, 83, (1955), 395.

29. Broom, T., Molimeux, J.H., Whittaker, M. Inst. Metals, 84, (1955-56) 357.

30. Broom, T., Ham, R.K. Proc. Roy. Soc., 242A, (1957), 166.

31. Makin, M.J., Minter, F., U.K.A.E. Res. Est. Rep., M/R2009 1956.

32. Polakowski, N.H., Palchoudhuri, A., Proc. Amer. Soc. Testing Materials, 54, (1954), 701.

33. Ludwick, R., Scheu, R., Z.V.d.I., 67, (1923), 122.

34. Kenyoh, J.N. Proc. Amer. Soc. Testing Materials, 50, (1950), 1073.

35. See reference 18 page 34.

36. Vacancies and Other Point Defects in Metals and Alloys. Inst. Metals Monograph and Report Series No.23 - Discussion p.212.

37. Segall, R.L., Partridge, P.G. Inst. Physics Electron Macrascopy Annual Conference, July,1959.

38. Thomsoh, N., International Conference on Fatigue of Metals, London 1956, Session 6 paper 3.

39. Smith, G.C. Proc. Roy. Soc., 242A, (1957), 189.

40. Hull, D., J. Inst. Metals, 86 (1958), 425.

41. Gough, H.J., Sopwith, D.G., J. Inst. Met., 49, (1932), 93.

42. Farnborough, Metallurgy Department 1959 Newsletter.

43. Cupp, C.R., Progress in Metal Physics No. 4 Pergamon Press 1953.

44. Rhines, F.N., Johnson, W.A., Anderson, W.A., A.I.M.M.E., 147,(1942),205.

45. Meijering, J.M. Druyvesteyn, M.J., Philips Research Reports, 2,(1947), 81.

46.Smith, G.C., Dewhirst, D.W. Trans. Australian Inst. Metals, 3, (1950), 71.

47. Gregory, E. Smith, G.C., J. Inst. Metals, 85, (1956-57), 81.

48. De. Jong, J.J., Ingenieur, 64, (1952), O·92.

49. Martin, J.W., Smith, G.C., J. Inst. Metals, 83, (1954-55), 417.

50. Martin, J.W. Smith, G.C., J. Inst. Metals, 83, (1954-55), 153.

51. Granato, A., Lucke, K., Dislocations and Mechanical Properties of Crystals (Wiley and Sons) 1956, page 425.

52. Forster, F., Z. Metalls., 29, (1937), 109.

53. Zener, C., Elasticity and Anelasticity of Metals, Chicago 1948.

54. Nowick, Progress in Metal Physics, 4, Pergamon Press, 1953.

55. Read, T.A., Phys. Rev., 38, (1940), 371.

56. Weertman, T., Salkovitz, E.I., Acta. Met., 3, (1955), 1.

57. Takahashi, S., J. Phys. Soc. Japan, 11, (1956), 1253.

58. Weinig, S., Machlin, E.S., J. Appl. Phys. 27, (1956), 734.

59. Levy, M., Metzger, M., Phil. Mag., 46, (1955), 1021.

60. Rosewell, A.E., Nowick, A.S., Acta. Met., 5, (1957), 228.

61. Dierckamp, H., Sosin, A., J. Appl. Phys., 27, (1956), 1411.

62. Thomson, D.O., Holmes, D.K., Blewitt, T.H., J. Appl.Phys., 26, (1955), 1188.

63, Thomson, D.O., Holmes, D.K., J. Appl. Phys. 27, (1956), 713.

64. Barnes, R.S., Hancock, N.H., Silk, E.C.H., Phil. Mag., 29 (1958, 519.

65. Read, T.A., Trans. A.I.M.M.E., 143, (1941), 30.

66. Swift, J.H., Richardson, H.E., J. Appl. Phys., 18, (1947), 417.

67. Thomson, D.O., Holmes, D.K., J. Appl. Phys., 30, (1959) 525.

68. Bordoni, P.G., Rec. Sci., 19, (1949), 851.

69. Niblett, D.H., Wilks, J., Phil. Mag., 2, (1957), 1427.

70. Birnbaum, H.K., Levy, M., Acta. Met. 4, (1956), 84.

71. Niblett, D.H. Wilks, J., Proc.Phys. Soc., 73, (1959), 96.

72. Granato, A., Lucke, K., Truell, R. reported in J. Appl. Phys. 27, (1956), 789.

73. Hikato, A., Truell, R., J. Appl. Phys., 28, (1957), 522.

74. Zener, C., Clark, H., Smitch, C.S., Trans., A.I.M.M.E., 147, (1942), 90.

75. Weertmann, J., J. Appl.Phys., 20, (1955), 29.

76. Found, G.H., Trans. A.I.M.M.E., 161, (1945), 120.

77. Lawson, A.W., Phys. Rev., 60, (1941), 330.

78. Nowick, A.S., Symposium on the Plastic Deformation of Crystalline Solids, Pittsburgh (1950), 155.

79. Hasiguti, R.R., Hirai, T., J. Appl. Phys., 18, (1947), 417.

80. Weertmann, J., Koehler, J.S., J. Appl. Phys., 24, (1953), 624.

81. Boulanger, C.R., Acad. Sci. Paris, 226, (1948), 1170.

82. Kosler, W., Z. Arch. Eisenhuttenw, 14, (1940-41), 271.

83. Kosler, W., Z. Metallk. 32, (1940), 282.

84. Darling, A.S., J., Inst. Metals, 24, (1957), 489.

85. Mima, G., Technology Repts. of the Osaka University, 8,(1958),373.

86. Private Communications.

87. Truel, R., Hikata, A., A.S.T.M., Symposium on Non Destructive Testing, 1957.

88. Wert, C.A., J. Appl. Phys., 20, (1949), 29.

89. Birbaum, H.K. Acta. Met., 3, (1955), 297.

90. Beshers, D., J. Appl. Phys., 30, (1959), 252.

91. Forster, F., Korster, W., Z. Metallk., 29, (1937), 116.

92. Koster, W., Rosenthal, K., Z. Metallk., 30, (1938), 345.

93. Fusfeld, H.I. See reference 54.

94. Koster, W., Stalte, E., Z. Metallk., 45, (1954), 356.

95. Granato, A., Hikata, A., Lucke, K., Acta. Met., 6, (1958), 470.

96. Nowick, A.S., Phys. Rev., 80, (1950), 249.

97. Gordon, R.B., Nowick, A.S., Acta. Met., 4, (1956),514.

98. Smith, A.D.N., Phil. Mag., 43, (1952), 1151.

99. Valluri, S.R., National Advisory Committee for Aueronautics Technical Note 4371.

100. Levy, M., Metzger, M., Phil. Mag., (1955), 1021.

101. Read, T.A., Tyndall, E.P.T., J. Appl. Phys., 17, (1946), 713

102. Harper, S., Phys. Rev., 83, (1951), 709.

103. Granato, A., Lucke, K., J. Appl. Phys., 27, (1956), 583.

104. Granato A., Lucke, K., J. Appl. Phys., 27, (1956) 789.

105. Watchman, J.R., Teft, W.E., Rev. Sci. Inst., 27, (1956), 789.

106. See reference 4 page 250.

107. Cottrell, A.H., Report of a Conference of Strength of Solids, Physical Society, London(1948), 30.

108. Koehler, J.S., Imperfections in Nearby Perfect Crystals (Wiley and Sons, New York 1952, p.197).

109. Raleigh, Theory of Sound, Vol. 1, chapter VI, Macmillan and Company 1926.

110. Eshelby, D.J., Rroc. Roy. Soc., 197A, (1949), 396.

111. Leibfreid, G., Z. Physik, 127, (1950), 344.

112. Nabarro, F.R.N., Proc. Roy. Soc., 209A, (1951), 278.

113. Mason, W.P., J. Acoust, Soc., 22, (1955e), 643.

114. Seeger, A., Phil. Mag., 1, (1956), 651.

115. Hikata, A., Truel, R., Granato, A., Chick, B., Lucke, K., J. Appl. Phys., 27, (1956), 396

116. Nowick, A.S., J. Appl. Phys., 25, (1954), 1129.

117. Nowick, A.S.,A.S.M. Seminar 1956 on Creep and Recovery p.146.

118. Bennewitz, K., Rotger, H., Z. f. tech. Phys., 12, (1938),521.

119. Randall, R.H., Rose, F.C., Zener, C., Phys. Rev., 56,(1939),343.

120. Entwhistle, K.M., J. Inst. Metals, 75, (1948-49), 97.

121. Fromer, L., Murray, A., J. Inst. Metals., 70, (1944),1.

122. Huggins, R.G., Acta. Met., 7, (1959), 357.

123. Holden, J., To be published Acta. Metallurgia.

124. Hull, D., Phil. Mag., 3, (1958), 513.

125. Henderson, J.W., Koehler, J.S., Phys. Rev., 104,(1956), 626.

126. Cottrell, A.H., Hull, D., Proc. Roy. Soc., 242A, (1957), 211.

127. Broom, T., Ham, R.K., Proc. Roy. Soc., 251A, (1959), 186.

128. Zener, C., Phys. Rev., 53, (1938), 90.

129. Parasnis, A.S., Mitchell, J.W., Phil. Mag., 4, (1959), 171.

130. Jones, D.A., Mitchell, J.W., Phil. Mag., 3, (1958), 1.

FRACTURE IN METALS

Summary of Thesis presented to the University of Glasgow for the Degree of Doctor of Philosophy - by Sydney O'Hara, B.Sc., A.R.C.S.T.

Damping capacity measurements have been used to investigate the fracture of metals, in particular the existance of cracks in fatigued metal and defects caused by casting and precipitation. The metals used throughout the work were copper and aluminium.

The apparatus constructed gives the damping values of a bar vibrating transversely in the kilo cycle range of frequencies. Experiments were carried out to investigate as fully as possible the effect of variables in technique which might give rise to false damping measurements, the effect of variables in the specimens themselves was also investigated.

The existance of cracks, either created by fatigue or else inherent in the metal is not shown up to any appreciable extent by damping measurements.

The effect of precipitates created by internal oxidation was also investigated since it was thought that these might behave as incipient cracks with respect to damping measurements. Any such effect however was swamped by dislocation damping which in itself gave rise to some very interesting results.

Measurements made on the recovery of damping after fatigue gave a most useful approach to the fracture of metals by fatigue. The results obtained strongly indicate that vacancies modify the process of room temperature fatigue.

The decrease of damping with time observed after fatigue is shown to be due most likely to vacancies migrating to and interacting with dislocations in the metal.

Optical and electron microscope studies were made to amplify the damping recovery measurements. These show that under certain conditions fracture during fatigue of aluminium can be initiated at grain boundaries. The general surface deformation which arises from fatigue was investigated, in particular the formation of extruded and intruded material.

The above experimental work is compared intimately with the great bulk of experimental and theoretical work recently published on the subjects mentioned. A general picture is constructed of the initial stages of fracture during fatigue.